

**FACTORS AFFECT CONCRETE ELECTRICAL  
RESISTIVITY AND ITS MODELLING**

**BY**

**SU WAI HNIN**

**A THESIS SUBMITTED IN PARTIAL FULFILLMENT OF THE  
REQUIREMENTS FOR THE DEGREE OF MASTER OF SCIENCE  
(ENGINEERING AND TECHNOLOGY)  
SIRINDHORN INTERNATIONAL INSTITUTE OF TECHNOLOGY  
THAMMASAT UNIVERSITY  
ACADEMIC YEAR 2017**

**FACTORS AFFECT CONCRETE ELECTRICAL  
RESISTIVITY AND ITS MODELLING**

**BY**

**SU WAI HNIN**



**A THESIS SUBMITTED IN PARTIAL FULFILLMENT OF THE  
REQUIREMENTS FOR THE DEGREE OF MASTER OF SCIENCE  
(ENGINEERING AND TECHNOLOGY)  
SIRINDHORN INTERNATIONAL INSTITUTE OF TECHNOLOGY  
THAMMASAT UNIVERSITY  
ACADEMIC YEAR 2017**

FACTORS AFFECT CONCRETE ELECTRICAL RESISTIVITY AND ITS  
MODELLING

A Thesis Presented

By  
SU WAI HNIN

Submitted to  
Sirindhorn International Institute of Technology  
Thammasat University  
In partial fulfillment of the requirements for the degree of  
MASTER OF SCIENCE (ENGINEERING AND TECHNOLOGY)

Approved as to style and content by

Advisor and Chairperson of Thesis Committee



(Research Asst. Prof. Dr. Pakawat Sancharoen)

Committee Member and  
Chairperson of Examination Committee



(Prof. Dr. Somnuk Tangtermsirikul)

Committee Member



(Dr. Krittiya Kaewmanee)

Committee Member



(Asst. Prof. Dr. Taweechai Sumranwanich)

FEBRUARY 2018

## Acknowledgements

This thesis becomes a reality with the kind support and help of many individuals. I would like to extend my sincere thanks to all of them.

First of all, the author would like to express my deepest thanks and gratitude to Dr. Pakawat Sancharoen, for his valuable advice, suggestion and encouragement during thesis work as an advisor. It is a great honour to work under his supervision.

Author wishes to acknowledge and sincere appreciation to Prof. Dr. Somnuk Tangtermsirikul for his encouragement, creative and comprehensive advice until this research came to existence.

Author also gratefully thanks to her committee members, Dr. Krittiya Kaewmanee to assign the thesis works for her valuable advice and comments, critical reading of this thesis and helped research time.

Moreover, author is appreciated to her external committee members, Dr Taweechai Sumranwanich for his advice, suggestion and offering many valuable suggestions throughout the course of this study.

Thanks are also extended to all of her friends, colleagues and all members of the Faculty of Civil Engineering and Technology, SIIT, lab assistants and all researchers in Construction and Maintenance Technology Research Center (CONTEC) for their cooperation, helping and numerous supporting during this study.

Author special thanks to AUN/SEED-Net and SIIT for supporting a scholarship to study at Sirindhorn International Institute of Technology. And authors acknowledge the Center of Excellence in Material Science, Construction and Maintenance Technology Project, Thammasat University and the National Research University Project, Office of the Higher Education Commission.

Finally, author would like to thank and appreciate NamHeng Ready Mix Concrete Co.,Ltd for their cooperation and participation during my research periods. Whose is not only assisted me financially, but also cooperated and participated their support during my research period.



## **Abstract**

### **FACTORS AFFECT CONCRETE ELECTRICAL RESISTIVITY AND ITS MODELLING**

by

**SU WAI HNIN**

Bachelor of Science in Geology, Dagon University, 2012

Master of Science, Sirindhorn International Institute of Technology, 2018

Concrete electrical resistivity is directly related with designing of cathodic protection system. Electrical resistivity is a fast and simple tested parameter that is also used to evaluate the resistance of concrete against the ingress of ionic species. Electrical resistivity can also be used to estimate the degree of corrosion current.

The aim of this research is to study effects of mix proportion and moisture conditions on electrical resistivity of concrete. The varied parameters in this study were w/b ratio, fly ash content, ratio of paste content of concrete to void content between aggregate ( $\gamma$ ), age of concrete, moisture content, specimen shape, thickness and curing condition.

In this study, electrical resistivity was measured for 20 different concrete mix proportions. Cylinder specimen and four different types of cubic specimen dimensions were prepared for electrical resistivity measurement. Cylindrical specimens were prepared to measure carbonation and rapid chloride penetration test. Before the durability measurement, electrical resistivity was measured for each specimens. Testings are included compressive strength, carbonation depth, rapid chloride penetration test and moisture weight loss test.

Results show that the water to binder ratio and paste content were inversely proportional to the electrical resistivity of concrete. When replacement of fly ash was increased, electrical resistivity of concrete was also significantly increased. It is found that concrete mix proportion strongly related to electrical resistivity.

Correlation between electrical resistivity and other properties such as rapid chloride permeability, compressive strength and moisture content of concrete using results from different mix designs of concrete is conducted. Electrical resistivity and concrete durability properties have a good relationship. Electrical resistivity was increased with the increases of compressive strength. Electrical resistivity is increased, charged passed is significantly reduced. Electrical resistivity increases with an increase of carbonation time. Electrical resistivity increases with the increase of moisture weight loss.

Finally, prediction of electrical resistivity based on mix proportions and other concrete properties were proposed based on the test results in this study. A good correlation is obtained between predicted and tested results. The model simulations showed sufficient accuracy in predicting the test results of concrete specimens at different water/binder ratio, fly ash replacement content, cement paste content, and age of concrete. It is observed that the compressive strength is directly proportional to the electrical resistivity. The model predictions showed reasonable accuracy when compared to the test results.

**Keywords:** Electrical Resistivity, Mix Proportion, Compressive Strength, Rapid Chloride Permeability, Carbonation Depth, Moisture content

## Table of Contents

Chapter	Title	Page
	Signature Page	i
	Acknowledgements	ii
	Abstract	iv
	Table of Contents	v
	List of Figures	vi
	List of Tables	xiv
1	Introduction	1
	1.1 General	1
	1.2 Statement of Problems	3
	1.3 Objectives and Scope of Study	3
2	Literature Review	5
	2.1 General	5
	2.2 Mechanisms of Steel Corrosion in Concrete	5
	2.3 Causes of Corrosion in RC Structures	7
	2.3.1 Carbonation	7
	2.3.2 Chloride	9
	2.4 Factors Affecting Corrosion of Reinforcing Steel in Concrete	11
	2.4.1 Pore Solution of Concrete	11
	2.4.2 Permeability of Concrete	12
	2.4.3 Moisture and Oxygen	13
	2.4.4 Mix Proportion of Concrete	13
	2.4.5 Electrical Resistivity	14
	2.4.6 Thickness of Concrete Cover	15
	2.4.7 Concrete Temperature	15

2.5	Corrosion Protection of Reinforcing Steel	15
2.5.1	Cathodic Protection	15
2.5.1.1	Sacrificial Anode Protection (Galvanic Protection)	15
2.5.1.2	Impressed Current	16
2.5.2	Corrosion Inhibitors	17
2.5.2.1	Anodic Inhibitors (Chemical Passivators)	17
2.5.2.2	Cathodic Inhibitors (Adsorption Inhibitors)	17
2.5.3	Protective Coating	18
2.5.4	Epoxy Coated Reinforcement (ECR)	18
2.6	Concrete Electrical Resistivity	19
2.6.1	Bulk Electrical Resistivity	20
2.6.2	Surface Concrete Electrical Resistivity Test	21
2.6.2.1	Four Point Wenner Probe	22
2.6.2.2	Relationship between Bulk and Surface Resistivity	25
2.7	Factors Affecting the Electrical Resistivity of Concrete	25
2.7.1	Water/Binder Ratio	25
2.7.2	Binder Type	26
2.7.3	Effect of Aggregates	27
2.7.4	Specimen Shape	28
2.7.5	Moisture	31
2.7.6	Sulphates and Chlorides	32
2.7.7	Temperature	33
3	Methodology	35
3.1	General	35
3.2	Materials	35
3.3	Mix Proportions	37
3.4	Specimen Preparation	39
3.5	Methods of Testing	41
3.5.1	Electrical Resistivity of Concrete	41

3.5.1.1	Cubic Specimen	41
3.5.1.2	Cylindrical Specimen	42
3.5.2	Effect of Specimen Thickness	43
3.5.3	Compressive Strength Test of Concrete	44
3.5.4	Rapid Chloride Penetration Test of Concrete	44
3.5.5	Carbonation	45
3.5.6	Weight Loss due to Moisture Loss of Concrete	46
4	Results and Discussion	48
4.1	General	48
4.2	Effect of Mix Proportions on Electrical Resistivity of Concrete	48
4.2.1	Water/Binder ration (w/b)	48
4.2.2	Fly Ash Content	50
4.2.3	Ratio of Paste Content of Concrete to void content between Aggregate (Y)	52
4.2.4	Specimen Length	54
4.2.5	Specimen Shape	55
4.2.6	Specimen Thickness	56
4.2.7	Curing Conditions	57
4.3	Relationship between Electrical Resistivity and Concrete Properties	59
4.3.1	Relationship between Electrical Resistivity and Compressive Strength Test	59
4.3.2	Relationship between Electrical Resistivity and Rapid Chloride Penetration (RCPT) Test	63
4.3.3	Relationship between Electrical Resistivity and Moisture Weight Loss of Concrete	65
4.3.4	Relationship between Electrical Resistivity and Carbonation Depth of Concrete	67
4.4	Prediction Model of Electrical Resistivity	71
4.4.1	Prediction Model of Electrical Resistivity Based on	71

	Mix Proportions	
	4.4.2 Prediction Model of Electrical Resistivity based on Mix Proportions and Hydration Degree	74
	4.4.3 Prediction Model of Electrical Resistivity based on Compressive Strength	76
	4.4.4 Prediction Model of Rapid Chloride Penetration Based on Electrical Resistivity	78
6	Conclusions and Recommendations	80
	5.1 Conclusions	80
	5.2 Recommendations for Future Study	83
	References	84
	Appendices	89
	Appendix A	90
	Appendix B	91
	Appendix C	92

## List of Figures

<b>Figures</b>	<b>Page</b>
1.1 Depssivation of Steel in Concrte	1
1.2 Surface Resistivity Meter (Four Wenner Probe)	3
2.1 Mechanisms of Steel Corrosion in Concrete	6
2.2 Carbonation Process	8
2.3 Steel Corrosion Caused by theIngress of Carbonation	9
2.4 Break Down of Passive Layer	10
2.5 Steel Corrosion Caused by the Chloride	10
2.6 Sacrificial Anodic Protection	16
2.7 Impressed Current-Cathodic Protection	17
2.8 Electrochemical Mechanism of Reinforcement Corrosion	20
2.9 Concrete Bulk Electrical Resistivity Test with Two Electrodes	21
2.10 Schematic of Four-Electrode Resistivity Test	22
2.11 Commercially Available Wenner Probe	23
2.12 Relationship between Bulk and Surface Resistivity for Fly Ash Mix Proportions	25
2.13 Effect of w/c ratio on Concrete Resistivity	26
2.14 Effect of Fly Ash on Electrical Resistivity	27
2.15 Effect of Aggregate Content on Electrical Resistivity	28
2.16 Wenner Probe Placement for Cubic Specimens	29
2.17 Wenner Probe Placement for Cylindrical Specimens	29
2.18 Four Point Electrical Resistivity Measurements on Cubic Specimen	30
2.19 Four Point Electrical Resistivity Measurement on Cylindrical Specimen	30
2.20 Effect of Saturation on Electrical Resistivity of Concrete	31
2.21 Variation of Electrical Resistivity of Concrete with Sulfate Contamination	32
2.22 Electrical Resistivity as a Function of Temperature	33
3.1 Specimen Preparation Procedures for Each Test	41
3.2 Cubic Test Specimen	42
3.3 Measurement Technique for Electrical Resistivity of a Cubic Specimen Using Four Wenner Probe	42

3.4 Cylindrical Test Specimen	43
3.5 Measurement Technique for Electrical Resistivity of a Cylindrical Specimen Using Four Wenner Probe	43
3.6 Procedures of Effect of Specimen Thickness	43
3.7 Procedures of Compressive Strength Test	43
3.8 Procedures of Rapid Chloride Penetration Test	45
3.9 Procedures of Carbonation Test	46
4.1 Effect of w/b ratio on Electrical Resistivity of Concrete	49
4.2 Effect of w/b ratio on Electrical Resistivity of Concrete by percentage Of w/b ratio 0.35	49
4.3 Effect of Fly Ash Content on Electrical Resistivity of Concrete at w/b 0.35	51
4.4 Effect of Fly Ash Content on Electrical Resistivity of Concrete at w/b 0.55	51
4.5 Effect of Different Fly Ash Amount on Electrical Resistivity of Concrete By Percentage of Fly Ash Replacement	52
4.6 Effect of Ratio of Paste Content of Concrete to Void Content between Between Aggregate ( $\Upsilon$ ) on Electrical Resistivity of Concrete	53
4.7 Effect of Ratio of Paste Content of Concrete to Void Content between Aggregate ( $\Upsilon$ ) on Electrical Resistivity of Concrete by Percentage of $\Upsilon=1.3$	53
4.8 Effect of Specimen Length on Electrical Resistivity of Concrete With w/b 0.35	55
4.9 Effect of Specimen Length on Electrical Resistivity of Concrete By Percentage of 15 x 15 x 15 cm Size	55
4.10 Effect of Specimen Shape on Electrical Resistivity of Concrete	56
4.11 Effect of Specimen Thickness on Electrical Resistivity of Concrete	57
4.12 Effect of Curing Condition on Electrical Resistivity of Concrete	58
4.13 Relationship between Electrical Resistivity and Compressive Strength with different w/b ratios at Water-Cured Condition	60
4.14 Relationship between Electrical Resistivity and Compressive Strength With different ratio of Cement Paste Content of Concrete to Void Content between aggregate ( $\Upsilon$ ) at Water-Cured Condition	61
4.15 Relationship between Electrical Resistivity and Compressive Strength With different Fly Ash Content by w/b 0.35 at Water-Cured Condition	61

4.16 Relationship between Electrical Resistivity and Compressive Strength With different Fly Ash Content by w/b 0.55 at Water-Cured Condition	62
4.17 Relationship between Electrical Resistivity and Compressive Strength In Water- Cured Condition	62
4.18 Relationship between Electrical Resistivity and Compressive Strength In Air-Cured Condition	63
4.19 Relationship between Electrical Resistivity and Rapid Chloride Penetration of Concrete	64
4.20 Relationship between Electrical Resistivity and Moisture Weight Loss With different w/b ratios	66
4.21 Relationship between Electrical Resistivity and Moisture Weight Loss With different Fly Ash Content	66
4.22 Relationship between Electrical Resistivity and Moisture Weight Loss With different ratio of Cement Paste Content of Concrete to Void Content between aggregate ( $\gamma$ )	67
4.23 Effect of Carbonation Time on Electrical Resistivity of Concrete With different w/b ratios	68
4.24 Effect of Carbonation Time on Electrical Resistivity of Concrete With different Fly Ash Content at w/b 0.35	69
4.25 Effect of Carbonation Time on Electrical Resistivity of Concrete With different Fly Ash Content at w/b 0.55	69
4.26 Effect of Carbonation Time on Electrical Resistivity of Concrete With different Cement Paste Content at w/b 0.55	70
4.27 Relationship between Electrical Resistivity and Carbonation Coefficient of Concrete with different FA Content (110%, 30%, and 40%)	70
4.28 Comparison between Predicted and Measured Results of Electrical Resistivity of Concrete Based on Mix Proportions	72
4.29 Comparison between Predicted and Measured Results of Electrical Resistivity of Concrete Based on Mix Proportions (different w/b ratios)	73
4.30 Comparison between Predicted and Measured Results of Electrical Resistivity of Concrete Based on Mix Proportions (different FA content with w/b 0.35)	73

4.31 Comparison between Predicted and Measured Results of Electrical Resistivity of Concrete Based on Mix Proportions and Hydration Degree	75
4.32 Comparison between Predicted and Measured Results of Electrical Resistivity of Concrete Based on Mix Proportions and Hydration Degree (different FA content with w/b 0.35)	75
4.33 Comparison between Predicted and Measured Results of Electrical Resistivity of Concrete Based on Mix Proportions and Compressive Strength	77
4.34 Comparison between Predicted and Measured Results of Electrical Resistivity of Concrete Based on Mix Proportions and Compressive Strength (different w/b ratios)	77
4.35 Comparison between Predicted and Measured Results of Electrical Resistivity of Concrete Based on Mix Proportions and Compressive Strength (different FA content at w/b 0.35)	78
4.36 Prediction Model of Rapid Chloride Penetration Based on Electrical Resistivity of Concrete	79

## List of Tables

<b>Tables</b>	<b>Page</b>
2.1 Relationship between Corrosion Rate and Electrical Resistivity of Concrete	14
2.2 Comparison of Chloride penetration level established for standards based On electrical Resistivity (AASHTO) and the amount of Charged Passed (ASTM C1202, 2012)	24
2.3 Electrical Resistivity of Aggregates	27
3.1 Chemical Composition and Physical Properties of Cement and Fly Ash	37
3.2 Mix Proportion of the Tested Concrete	38
3.3 Specimen Dimensions	40
4.1 Electrical Resistivity of Concrete Materials	54
4.2 Relationship between Electrical Resistivity and Rapid Chloride Penetration of Concrete	65

# Chapter 1

## Introduction

### 1.1 General

Reinforced concrete is one of the important composite materials that has been used by the construction industry all over the world. Reinforcing steel corrosion is also an important problem in the construction industry. It is mainly caused by depassivation of steel as shown in Fig. 1.1. It occurs by pH reduction of pore solution of concrete around reinforcing steel from 13 to 9, due to carbonation (Gulikers and Raupach, 2006). Another cause is increasing amount of chloride ions near the steel bars. When the pH level is high, a thin oxide layer forms on the steel surface and prevent iron from dissolving. The passive corrosion rate in reinforced concrete is typically lower than  $0.1\mu\text{m}$  per year. The passive layer breaks down when the alkalinity is decreased or when the chloride concentration in concrete exceeds the critical level.

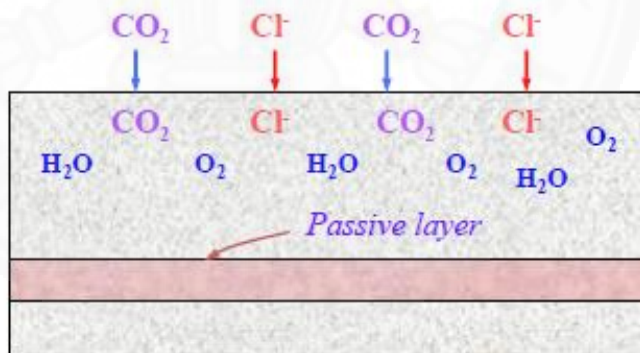


Fig 1.1 Depassivation of steel in concrete.

Corrosion of reinforcing steel is an electrochemical process. Accordingly, concrete electrical resistivity is one of the significant factors controlling this corrosion process. In reinforced concrete structures, concrete electrical resistivity can be used as a tool to evaluate the potential rate of corrosion.

High concrete electrical resistivity will decrease corrosion currents and reduce the corrosion rate. Surface concrete resistivity is used to evaluate the rate which corrosion is occurring in concrete and to assess the capacity of the concrete to prevent corrosion. The microstructure of the cement matrix, pore structure, porosity, and pore size distribution have correlations with electrical resistivity. Concrete electrical resistivity will increase with time due to increased hydration degree of the cement paste of concrete. Normally, electrical resistivity of concrete ranges from 1 to 10,000 k $\Omega$ -cm, depending on the moisture content of the concrete, temperature, and concrete quality (composition, cement type, etc) (Andrade and Andrea, 2010). In concrete, the composite materials that create microstructure and interconnection of pores highly influence the resistivity. Higher resistivity causes lower corrosion current travelling between anodic and cathodic regions in the reinforced concrete structures.

Electrical resistivity is also directly related with cathodic protection system. Parameters such as surface area of reinforcing steel, coating effectiveness, current density, and resistivity are needed to design sacrificial anode protection system. When the fresh concrete sets and hardens, discontinuity of the capillary pore space leads to an increase in its electrical resistivity. Electrical resistivity is transmitted by dissolved charged ions flowing into the concrete pore solution and a good indicator of concrete pore structures. Concrete resistivity is directly related to the corrosion process by representing the flow of current which passes between anode and cathode (Gowers and Millard, 1999).

Electrical resistivity is a fast and simple test that is also used to compute the resistance of concrete against the ingress of ionic species. The most common non-destructive method for measuring surface concrete electrical resistivity is the four point Wenner probe method as shown in Fig. 1.2. It can be used to estimate the likelihood of corrosion, correlate the chloride permeability, and determine the section requirements for cathodic protection systems, etc.



Fig 1.2 Surface resistivity meter (four Wenner probe)

### 1.2 Statement of problems

Civil engineers face the huge drawback of the reinforcing steel corrosion of concrete structures. It is very expensive to maintain and rehabilitate the reinforced concrete structures which are damaged by steel corrosion. Electrical resistivity is one of the methods used to estimate the severity of corrosion. Surface concrete resistivity is used to assess the capacity of the concrete to allow corrosion to occur and evaluate the rate at which corrosion is occurring in concrete. Therefore, the measurement of resistivity of concrete and investigating the relationships between resistivity and other parameters of concrete could provide useful information to reduce or minimize the corrosion of reinforcing steel. Moreover, electrical resistivity is an important parameter for design of sacrificial anode protection system.

### 1.3 Objectives and Scope of study

The main objective of this research is to study the factors affecting concrete electrical resistivity such as water to binder ratio (w/b), fly ash content, ratio of paste content of concrete to void content between aggregate ( $\gamma$ ), time, moisture content, specimen shape, thickness, and curing condition. Also correlations between electrical resistivity and factors such as rapid chloride permeability, compressive strength and moisture content of concrete using results from different mix designs of concrete are

conducted. And then objective is to predict electrical resistivity of concrete based on mix proportions and the tested parameters.



## Chapter 2

### Literature Reviews

#### 2.1 General

This chapter presents literature reviews for this study. Topics in this chapter are focused on the fundamentals of steel corrosion in concrete, the causes of corrosion in RC structures, the factors affecting corrosion of reinforcing steel in concrete, corrosion protection of reinforcing steel, and methodology of surface electrical resistivity. Literature reviews are presented in the following sections.

#### 2.2 Mechanisms of steel corrosion in concrete

Corrosion of reinforcing steel and other embedded steel inside concrete causes deterioration of the concrete structures by the mechanisms shown in Fig. 2.1. Concrete provides an alkaline environment where the pH value normally ranges from 12 to above 13. It mainly causes passivation of steel, however, reduction of pore solution pH or chloride content increasing causes depassivation.

Steel corrosion is an electrochemical process. Four components must be present i.e anode, cathode, metallic path, and electrolyte. An electrochemical cell is set up, when a difference in electrical potential presents along the steel in concrete. It forms anodic and cathodic regions, connected by the electrolyte in the pore solution of the hardened cement paste.

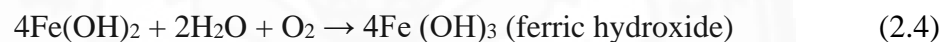
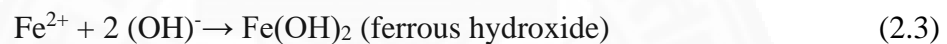
The positive charge, ferrous ions ( $\text{Fe}^{2+}$ ), at the anode dissolves into solution of the concrete while the negative charge, free electrons ( $e^-$ ) travel mostly through the steel. This is called the anodic reaction in concrete which is shown in the following equation 2.1.



Then the released of electrons from an anodic reaction combines with water and oxygen to form hydroxyl ions (OH)<sup>-</sup>. This may occur at the location where concrete is not depassivated. This reaction is called the cathodic reaction in concrete which is shown in the following equation 2.2.



Hydroxyl ion (OH)<sup>-</sup> pass through the electrolyte and combine with the ferrous ions to produce ferric hydroxide, Fe(OH)<sub>2</sub>, which is transformed by further oxidation to ferric hydroxide, Fe(OH)<sub>3</sub>, and hydrated ferric oxide, Fe<sub>2</sub>O<sub>3</sub>.H<sub>2</sub>O which are called rust as shown in equation 2.3 -2.5.



When steel corrodes, the volume of rust is between two to ten times of the original steel. This expansion results in tensile stresses which leads to the cracking, delamination, and spalling of the concrete.

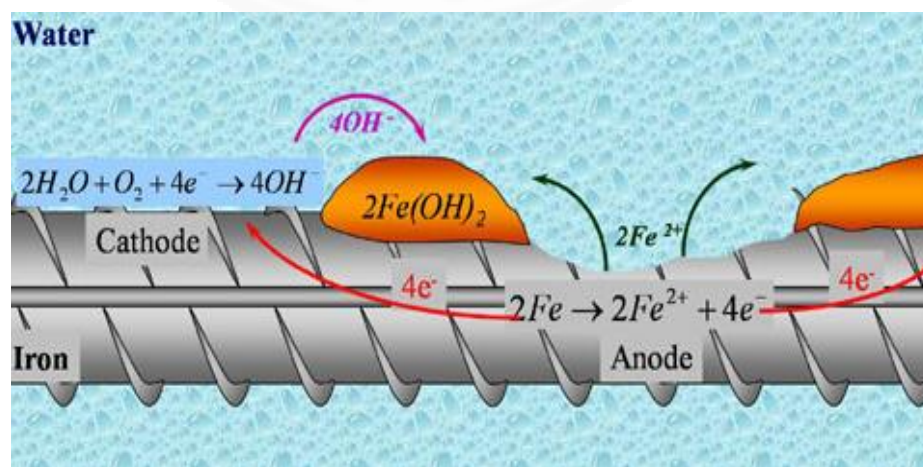


Fig 2.1 Mechanisms of steel corrosion in concrete (<http://www.cement.org>)

## 2.3 Causes of corrosion in RC structures

Concrete as an electrolyte is high in alkaline (pH 12 to above 13). At the high pH, a thin oxide layer forms on the steel and forbids iron from dissolving. The passive layer breaks down either with the reduction of the alkalinity of concrete or with the increase of the chloride concentration at steel surface to a critical level. There are two major causes of electrochemical corrosion which are carbonation and chloride penetration.

### 2.3.1 Carbonation

In corrosion process, carbonation is mostly recognized as a significant factor. In concrete, cement starts to hydrate, and reaction of cement and water in the concrete produces calcium hydroxide as shown in Fig. 2.2. It is important to maintain the high alkalinity of the concrete (pH more than 12.6) to passivate the steel and to protect the reinforcement from corrosion. In high alkali environment, steel corrosion can not process even when water penetrates to the reinforcement through concrete. Carbonation happens when atmospheric carbon dioxide (CO<sub>2</sub>) penetrate the concrete and reacts with calcium hydroxide (Ca(OH)<sub>2</sub>) to form carbonates. The reaction can be described as shown in equation 2.6. Steel corrosion caused by the ingress of carbonation as shown in Fig. 2.3.



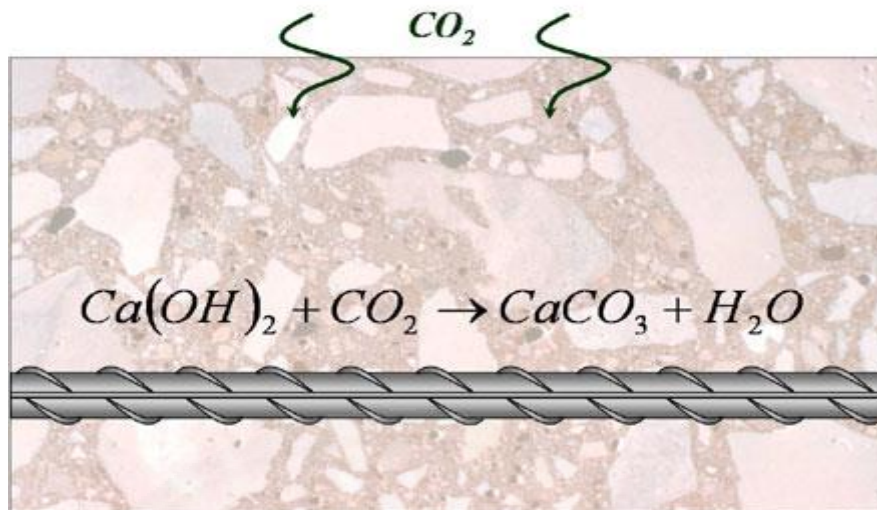


Fig 2.2 Carbonation Process (<http://www.cement.org>)

Normally, Carbonation is a slow process. The rate of which is determined by the amount of carbon dioxide that can penetrate into the concrete. Claisse, El-Sayad, and Shaaban (1999) reported that carbonation may proceed at a rate of 1mm to 5 mm per year depending on the porosity and permeability of concrete. Generally, the rate of carbonation is increased by high water to cement ratio, low cement content, short curing, low strength, and highly permeable or porous paste in concrete. The relative humidity is a major factor for carbonation of the concrete. Basheer et al. (2001) observed that the highest carbonation occurred at 55% relative humidity and carbonation depth decreased when RH increased from 55% to 75%. Carbonation destroys the passive film of the reinforcement although it does not significantly affect the rate of corrosion.



Fig 2.3 Steel corrosion caused by the ingress of carbonation  
(<https://hongten91.files.wordpress.com/2014/12/con1.jpg?w=794>)

### 2.3.2 Chloride

Chloride can come from many ways in the concrete. They can be brought into the concrete structure by the use of deliberate admixtures, or chloride contaminated mixing water or aggregates. The main cause of chloride induced corrosion is the diffusion of chlorides because of the direct exposure to the marine environment and due to the deicing salts and chemicals used.

Similar to the carbonation process, chloride attack does not directly damage the reinforcing steel, except causing the protective film of iron oxide to break down and develop the rate of corrosion. The passive layer can be destroyed by chloride and corrosion is initiated. Chloride ions activate the surface of the steel to form an anode. The reactions are as shown below.



Chloride ions are not consumed in the process but collaborate in breaking down the oxide passivation layer on the steel and then permit the corrosion process to move quickly. This process is shown in Figure 2.4 (Broomfield, 2006). The chloride ions are rejuvenated so that the rust contains no chloride, although iron chloride is formed at the

intermediate stage. The factors influencing the level of chloride threshold are the type of cement, type of mineral admixture, water/cement ratio, curing, moisture content, oxygen availability, and type of steel, surface roughness and surface condition. The main cause of chloride induced corrosion is diffusion of chlorides especially in marine environment, uses of deicing salts and chemicals. Steel corrosion caused by the chloride as shown in Fig. 2.5.

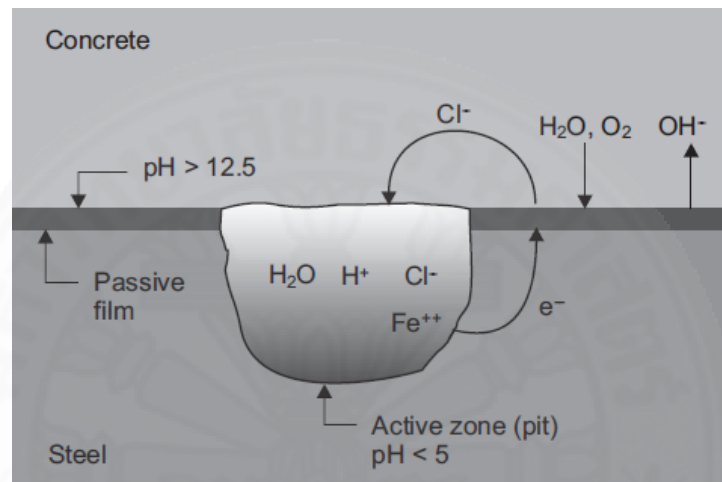


Fig. 2.4 Break down of passive layer (<http://www.sxd.danang.gov.vn/documents>)



Fig. 2.5 Steel corrosion caused by the chloride  
([https://eduardodseng.files.wordpress.com/2013/12/concrete\\_spalling.jpg](https://eduardodseng.files.wordpress.com/2013/12/concrete_spalling.jpg))

## **2.4 Factors Affecting Corrosion of Reinforcing Steel in Concrete**

The behavior of reinforcing steel corrosion in concrete does not only depend on steel, but also the properties of interfacial zone of concrete. That is mainly influenced by composition of concrete pore solution and steel properties especially chemically. Deterioration of the cover concrete from external environmental factors may accelerate the ingress of aggressive agents, causing the pore solution in contact with the steel to be more corrosive. Broomfield (2006) showed that chloride ions and carbon dioxide play an important roles in corrosion of reinforcing steel in corrosion structures. Besides these two factors, temperature, moisture and other factors also affect the corrosion of steel in concrete.

### **2.4.1 Pore solution of concrete**

The concrete pore solution is physically present in the pores of the concrete which is an electrolyte, due to the capillary force supplied by menisci and the adsorption. Under certain conditions, corrosion damage at the steel surface can occur when it reacts with the steel reinforcement. Various ions are contained in the pore solution, such as sodium, potassium, calcium, hydroxyl, sulphate, and sulphite, etc. The pore solution composition varies with cement and age of concrete. Burchler , Elsner , and Bohni, (1996) proved that the water to cement ratio can affect compositions of pore solution, but after 30 days of curing, the hydration would not directly affect the chemical composition of pore solution of hardened cement paste. Diamond (1981) found that different types of cement lead to different pore solution composition, and that it become constant after certain period for completing hydration.

The corrosion may be initiated when an exact chloride amount is present in the pore solution, even when its pH value is high. The pH value of the new concrete is about 13.5, and if there is no chloride, thereis no corrosion problem in a young reinforced concrete structure. However, the pH value cannot always be kept so high. Atmospheric carbon dioxide dissolved in the pore solution can reduce the pH value by reacting with the calcium hydroxide to form calcium carbonate. The pore solution of

the passive film on the steel reinforcement will no longer be stable, and when the pH value is lower than 9, rapid corrosion will happen on the surface of the steel.

Steel reinforcement corrosion in concrete is related with the pore solution ingress by chloride or de-alkalised by carbon dioxide. Therefore, there are two major conditions of the pore solution such as the chloride pollution and carbon dioxide de-alkalisation from a corrosion point of view. Both of them are directly answerable for the deterioration of reinforced concrete structures.

Haque and Kayyali (1995) found that the  $\text{OH}^-$  level in the pore solution relied on the concentration of the added NaCl in the concrete. By adding higher amount of chloride ions, the  $\text{OH}^-$  concentration in the pore solution also increased, but after a certain amount of chloride was added, the hydroxyl concentration decreased with the increase of added chloride. Tuutti (1982) showed that chloride ions would be discharged from cement and aggregate into the pore solution with lower pH value.

#### **2.4.2 Permeability of Concrete**

More corrosion damage in the steel is caused by higher porosity and larger pore size of concrete. Resistivity of concrete can be partly attributed to the permeability as well, so the permeability of concrete also influence the ion flowing process in the cover concrete. If the concrete is low in permeability, the aggressive species will be difficult to ingress to the reinforcement, and reinforcement corrosion possibility may be low.

The permeability of concrete is mainly influenced by concrete porosity and its pore size distribution, which are mostly dependent on the w/b ratio of the concrete. The permeability of concrete increases with high w/b ratio. Then cement hydration also affect porosity and permeability. Fly ash also has a significant influence on the chloride diffusion than that of the oxygen diffusion of concrete. Permeability of concrete cover can be low by using lower w/b ratio, better compaction, fly ash, etc. That may develop resistance of reinforced concrete corrosion.

### 2.4.3 Moisture and Oxygen

González, Miranda, and Feliu (2004) found that the steel corrosion rate in concrete is influenced by the moisture content. There is no corrosion in reinforcing steel in concrete, if there is no water available in concrete. Thus, moisture content is a significant factor in the steel corrosion problems. The concrete electrical resistivity is affected by moisture that can control the galvanic corrosion rate. Nevertheless, anodic and cathodic reactions had reverse effect on moisture increasing. When the humidity is increased, the rate of anodic reaction is increased and the rate of cathodic reaction is reduced (Ahmad, 2003). Corrosion is caused by presence of moisture and oxygen. Moisture fulfils the electrolytic demand of the corrosion cell. Moisture and oxygen together support the formation of more  $\text{OH}^-$  thereby producing more rust component, i.e,  $\text{Fe}(\text{OH})_2$ . Cathodic reactions are caused by oxygen. If there is no enough oxygen, even in a depassivation condition, corrosion will not propagate because of the cathodic polarization.

### 2.4.4 Mix proportion of concrete

Water to cement ratio (w/b) has a very significant influence on the porosity of concrete. Higher w/b ratio causes higher porosity concrete which is easily penetrated by aggressive species. Silva (2013) reported that the w/b ratio has higher influence on corrosion rate than the binder type. Moreover, aggregates usually influence reinforcement corrosion in many cases. Blended cements such as blast furnace slag, fly ash or silica fume can improve durability in marine environment and cause longer service life of concrete structures when compared with concrete containing only Ordinary Portland cement.

Fly ash blended cement is also one of the cements with improved durability performance. Saleem et al. (1996) reported that corrosion initiation time of steel reinforcement in blended cement concrete with 30% fly ash replacement was about twice longer than that in the plain cement concrete. The  $\text{OH}^-$  concentration in pore solution of the fly ash replaced cement concrete was lower than the cement concrete.

Moreover, the unbound chlorides in pore solution could decrease with the partial replacement of cement by fly ash. Fly ash blending refined the distribution of pore size, reduced the average pore radius from 240 to 166 Å, reduced the permeability, and the chloride diffusivity. The electrical resistivity of concrete was increased nearly 2.2 times with the fly ash replacement.

#### 2.4.5 Electrical resistivity

McCarter, Ezirim, and Emerson (1992) found that the electrical resistivity of hardened cement paste, mortar and concrete is a significant factor to the corrosion of reinforcement in concrete. The mortar and concrete resistivity is determined by microstructure of cement paste (pore volume, distribution of the pore radius), moisture and soluble salt content, and temperature. Normally, electrical resistivity of concrete ranges from 1 to 10,000 kΩ-cm depending on the moisture content of concrete, temperature, and concrete quality (composition, cement type, etc.) (Andrade and Andrea, 2010). High concentration of chloride and a relatively higher level of moisture, usually corresponds to a low resistivity. The relationship between the corrosion rate and electrical resistivity of concrete was reported by many previous studies which can be summarized in Table 2.1.

Table 2.1 Relationship between corrosion rate and electrical resistivity of concrete (Broomfield, 2006)

Corrosion rate	Concrete electrical resistivity $\rho$ (kΩ-cm)
Low corrosion rate	>100
Low to moderate corrosion rate	50 - 100
High corrosion rate	10 - 50
Very High corrosion rate	<10

#### **2.4.6 Thickness of concrete cover**

The thickness of cover concrete influences the period for aggressive agents to ingress to steel rebar in concrete. Basically increasing the thickness of the concrete cover can improve the service life of reinforced concrete structures (Liang, Wang, and Liang, 1999). For most structures, the normal thickness of concrete cover is around 50mm. However, not all structures strictly follow the designed cover thickness.

#### **2.4.7 Concrete temperature**

The corrosion rate of reinforcement is also influenced by concrete temperature. All the corrosion processes such as electrochemical reactions (anodic and cathodic), ingress of corrosive agents to steel surface, collection of corrosion agents on the steel surface or leaving from the interface of steel/concrete, and ionic flow over concrete can be altered by the concrete temperature. Increasing the concrete temperature results in increasing rates of all the above mentioned processes, subsequently increasing the corrosion rate.

### **2.5 Corrosion Protection of Reinforcing Steel**

Corrosion protection is the process to prevent reinforcing steels from corrosion by using different methods which are described as follows.

#### **2.5.1 Cathodic Protection**

Cathodic protection is an electrical method of inhibiting corrosion on metallic structures in electrolytes (for example, soil or water). It is used as cathode in the electrolytic cell, in a decreasing or prohibition of corrosion. Corrosion does not occur since there is no space for anodic on metal. There are two methods of applying cathodic protection to metallic structures which are mentioned below.

### 2.5.1.1 Sacrificial Anodic Protection (Galvanic Protection)

This method is mainly used for ships, offshore oil and gas production platforms etc. The more reactive metal is applied to become immunity region on reinforcing steel and vary the electrode potential. Zn, Al, and Mg are commonly used as sacrificial anodes. It produces the anodic dissolution current with more negative potential. Therefore, cathodic curve intersection shifts to the immunity region that is a more negative potential. At this region, the corrosion rate of steel is insignificant. Sacrificial anodic protection system as shown in Fig. 2.6.

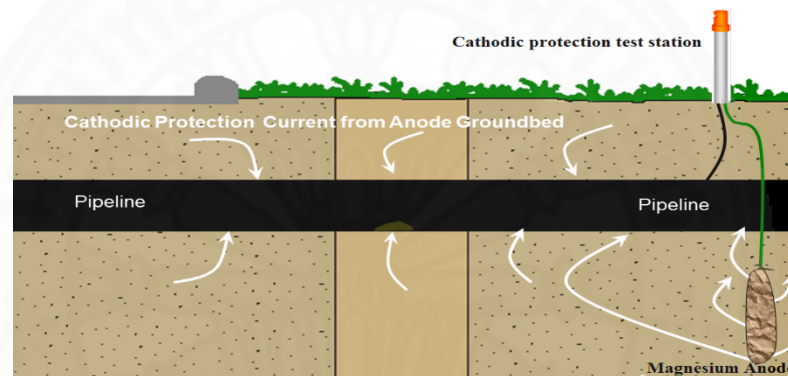


Fig 2.6 Sacrificial anodic protection (<https://www.google.co.th/cathodic-protection-systems.php>)

### 2.5.1.2 Impressed Current

This method is usually applied for the prevention of pipelines and the bodies of ships in sea water. The metal surface is applied by the DC electrical circuit. The negative and positive terminals of the current basis are connected to the metal needing protection and an auxiliary anode, respectively. The electric current flow charges the electron structure and shifts the potential of electrode into the negative direction as shown in Fig. 2.7. It supports till it reaches the immunity region. The current flows from anode to cathode. Hence, it protects corrosion of metal surface.

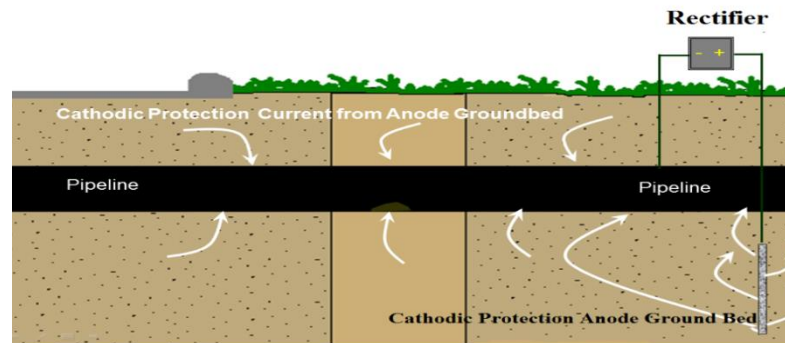


Fig 2.7 Impressed Current –Cathodic protection system  
 (<https://www.google.co.th/cathodic-protection-systems.php>)

## 2.5.2 Corrosion Inhibitors

The rate of corrosion is decreased by using two main types of inhibitors which are organic or inorganic substances. Usually inhibitors are used in small quantities to the corrosive medium. They are categorized into anodic inhibitors and cathodic inhibitors as described below.

### 2.5.2.1 Anodic inhibitors (chemical passivators)

It reduces the corrosion of metals by producing an additional soluble compound with newly made metal cations. This compound will then consume the surface of corroding metal and forming a passive film or barrier. Anodic inhibitors are used to repair;

- (1) crack of the oxide film through the metal surface
- (2) pitting corrosion
- (3) porous oxide film produced on the metal surface.

### 2.5.2.2 Cathodic inhibitors (adsorption inhibitors)

These are further classified into two types in an electrochemical corrosion depending on the nature of the cathodic reaction.

- (1) In an acidic solution: the principal cathodic reaction is the free of hydrogen gas, in which the corrosion can be controlled by reducing the diffusion of  $H^+$  ions through the cathode.
- (2) In a neutral solution: the cathodic reaction is the adsorption of oxygen or production of hydroxyl ions, in a neutral solution. Therefore, the corrosion is controlled either by retarding its diffusion or by removing oxygen from the corroding medium to the cathodic area. By adding the inhibitors like Mg, Zn or Ni salts, diffusion of oxygen can be controlled.

### **2.5.3 Protective Coating**

Coating method is used on protected steel surface or concrete surface. The coating surface protects members from risky factors in the environment such as moisture, attacking chemical and gases around the members. Coating has many methods which depend on materials and coating techniques. There are two main materials for coating such as metallic and non-metallic coatings. The metallic coating is the thin film formed on protected metal which is more stable than it. So stable film has effect on increasing corrosion resistance of the protected steel. This coating methods involves the coating with organic chemical coating. Liquid organic coating is used to coat surface of protected steel by painting, roller or spraying. The liquid coating consists of resin which is the coat base, organic soluble and color

### **2.5.4 Epoxy Coated Reinforcement (ECR)**

Many researchers have tried to determine the usefulness of ECR in preventing corrosion. Kobayashi and Takewaka (1984) proved that the corrosion prevention contributed by epoxy with an approximately 0.2  $\mu m$  coating thickness was better than that contributed by galvanized steel. Weyers et al. (1997) investigated the performance of ECR in three 17-year old bridge decks in Virginia. They found that the ECR would debond at high humidity and chloride contents with a faster rate. They reported that for 95% of the bridge decks in Virginia, before the chloride arrived the epoxy coating

would debond from the steel, thus, contribute no additional service life. Epoxy coating is intended to prevent steel from corrosion by prohibiting access of chlorides, oxygen, and moisture to steel surface. To minimize the corrosion current flow that the high electrical resistance of epoxy coating provides electrical insulation. The capability of an epoxy coating to prohibit corrosion is mostly depends on its surface defects and adhesion to the underlying steel.

## 2.6 Concrete Electrical Resistivity

Electrical resistivity of concrete is mainly influenced by the microstructure of cement matrix, pore structure, porosity, and pore size distribution. These parameters are controlled by the degree of hydration of cement paste in concrete. Others significant parameters are concrete temperature, relative humidity, ions concentration and the mobility in the pore solution. Resistivity is a measure of the mobility of the ions or an electric current of a material. The conductivity ( $\sigma$ ) is inversely proportional with resistivity. The range spanned by resistivity is one of the greatest of any material property. Resistivity of oven dried concrete is  $10^7$  k- $\Omega$ cm and saturated concrete is  $10^2$  k- $\Omega$ cm (D. A. Whiting and Nagi, 2003).

Steel is protected against corrosion by a thin iron- oxide layer (passive film) in high alkaline environment of the concrete pore solution. But the presence of a sufficient chloride amount or carbonated, the passive film is not stable. Then corrosion may occur.

The steel corrosion propagation is an electrochemical reaction that consists of four different steps as shown in Figure 2.8. Each process represents the current flow in the cell. Accordingly the corrosion current will be controlled by the highest resistance, the resistances are connected in series. The resistance of current flow through the steel will be lower when compared to that of other three processes. The resistance of concrete and cathode may be high because there is a passive film. The passive film will increase resistivity, but for metal and anode, the resistance may be very small because there is no film. If the resistance is very high, it can suppress the corrosion current. Accordingly, corrosion rate is limited by the cathodic, anodic or concrete resistance ( $R_{con}$ ), which

mainly depends on environmental or material properties (González et al., 2004). Corrosion process and concrete resistivity can have a direct relationship because the current flows between anode and cathode regions as shown in Fig. 2.8. Absence of chlorides or carbonation of concrete results in higher anodic resistance ( $R_a$ ) which prevents corrosion onset. In a submerged structure, cathodic reaction will be slow because of limited oxygen, even a sufficient chloride amount is present. In very dry environments, the corrosion rate will be inhibited by the high concrete resistance.

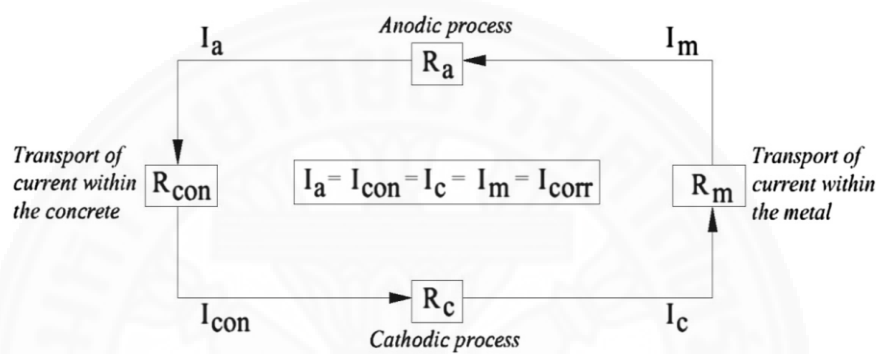


Fig 2.8 Electrochemical mechanism of reinforcement corrosion (Bertolini, Elsener, Pedeferri, and Polder, 2004)

In Fig. 2.8,  $R_a$  is anodic resistivity;  $R_c$  is cathodic resistivity;  $R_{con}$  is concrete resistivity;  $R_m$  is metal resistivity;  $I_a$  is anodic current;  $I_{con}$  is concrete current;  $I_c$  is cathodic current; and  $I_m$  is metal current.

### 2.6.1 Bulk Electrical Resistivity test

The test method is based on applying a potential difference to the specimen, thus supplying a current flow through the specimen. The potential difference and resulting current can be applied to obtain the electrical resistance. The geometrical factor in this method can be obtained by the following equation:

$$P = RI \text{ ( Ohm's Law)} \quad (2.10)$$

$$R = \rho \frac{L}{A} \rightarrow \rho = \frac{P}{I} \left( \frac{A}{L} \right) \quad (2.11)$$

$$\rho = \frac{\pi d^2}{4L} \times \frac{P}{I} \quad (2.12)$$

Where  $\rho$  is resistivity ( $\Omega$ -cm),  $d$  is section diameter (cm),  $L$  is the length of the cylinder (cm),  $I$  is the current passed through the specimens (A), and  $P$  is the voltage drop (V).

This nondestructive test takes only few seconds. However, the application of this test method for field evaluation is very limited and complicated by the need for effective and uniform contacts between the end electrodes and concrete specimen end surfaces, so flat cylinder end surface, flexible electrodes, and resistance free connections between electrodes and concrete are required (Morris, Moreno, and Sagüés, 1996).

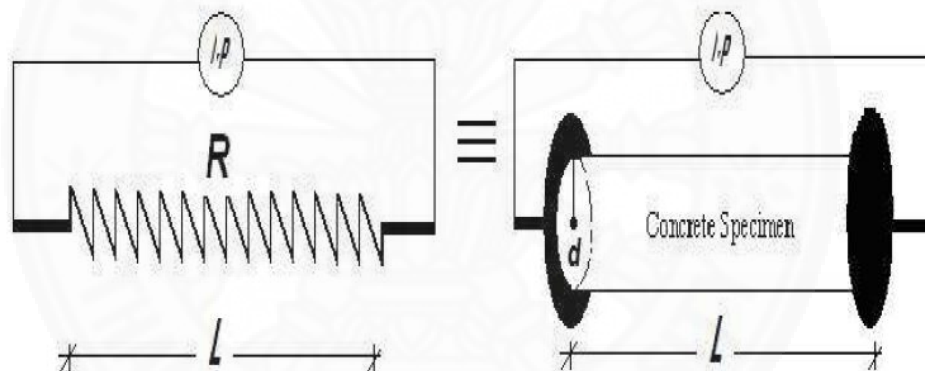


Fig. 2.9 Concrete Bulk electrical resistivity test with two electrodes (Morris et al., 1996).

### 2.6.2 Surface concrete electrical resistivity measurement

Concrete electrical resistivity is a volumetric property that indicates ability of transporting electrical charges through a material. Most concrete resistivity tests require the application of a current and measuring the resulting voltage. The resistivity ( $\rho$ ) is as shown in equation (2.13)

$$\rho = \frac{kV}{I} \quad (2.13)$$

Where  $\rho$  is the resistivity ( $\Omega\text{-cm}$ );  $I$  is the alternating current [A];  $V$  is the potential difference [V];  $k$  is a factor which depends on the size and shape of the specimen and the distance of the probes.

### 2.6.2.1 Four point Wenner probe

The most widespread method for the measurement of surface concrete electrical resistivity is the non-destructive four point Wenner probe method. The Wenner probe was selected as a standard concrete resistivity test in Europe, based on its efficiency and ease of use (Tang, 2005). It is designed specifically to correspond to the AASHTO TP 95-11 standard for “Surface Resistivity Indication of Concrete’s Ability to Resist Chloride Ion Penetration.”

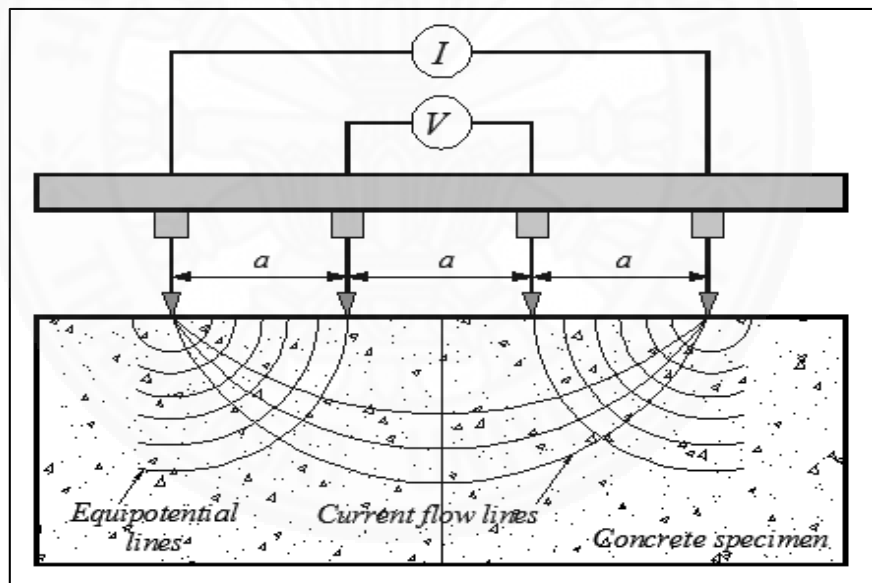


Figure 2.10 Schematic of four – electrode resistivity test

A current is applied to the two outer probes, and the potential difference is supported between the two inner probes (Resipod, 2016). The current is carried by ions in the pore liquid. The resistivity is calculated as shown in equation 2.15.

$$k = 2\pi a \quad (2.14)$$

$$\rho = \frac{2\pi aV}{I} \quad (2.15)$$

Where,  $\rho$  is the resistivity ( $\Omega$ -cm);  $a$  is the distance between inner electrodes (cm);  $I$  is the alternating current supplied through outer probes [A];  $V$  is the potential difference between inner probes [V].

Commercially available four point Wenner Probes automatically calculate the resistivity and display the reading as shown in Fig. 2.11.

Many researchers have categorized electrical resistivity as an indicator of chloride penetration resistance and quality assurance of concrete and a prominent parameter in the determination of concrete durability (Kessler, Powers, Vivas, Paredes, and Virmani, 2008). Presently in the USA, concrete resistivity is substituted by the Rapid Chloride Penetrability Test (RCPT) as a quality control parameter for construction and to evaluate concrete permeability (Kessler et al., 2008). Table 2.2 shows the comparison of chloride penetrability levels established in some standards based on electrical resistivity and the amount of charges passed in RCPT.



Figure 2.11 Commercially available Wenner probe

Table. 2.2 Comparison of chloride penetrability levels established in standards based on electrical resistivity (AASHTO TP95) and the amount of charges passed (ASTM C1202, 2012) (D. A. Whiting & Nagi, 2003)

<b>ASTM C1202/ AASHTO T277</b>		<b>AASHTO TP95</b>
<b>Chloride ion penetrability</b>	<b>RCP Test (Coulombs)</b>	<b>Electrical resistivity test (kΩ-cm)</b>
High	>4,000	<12
Moderate	2,000-4,000	12-21
Low	1,000-2,000	21-37
Very Low	100-1,000	37-254
Negligible	<100	> 254

#### **2.6.2.2 Relationship between Bulk and Surface Electrical Resistivity**

Fig. 2.12 shows the relationship between bulk and surface resistivities of different concrete mix proportions. It can be concluded that the relationship between the bulk and surface electrical resistivities of concrete is shown as linear.

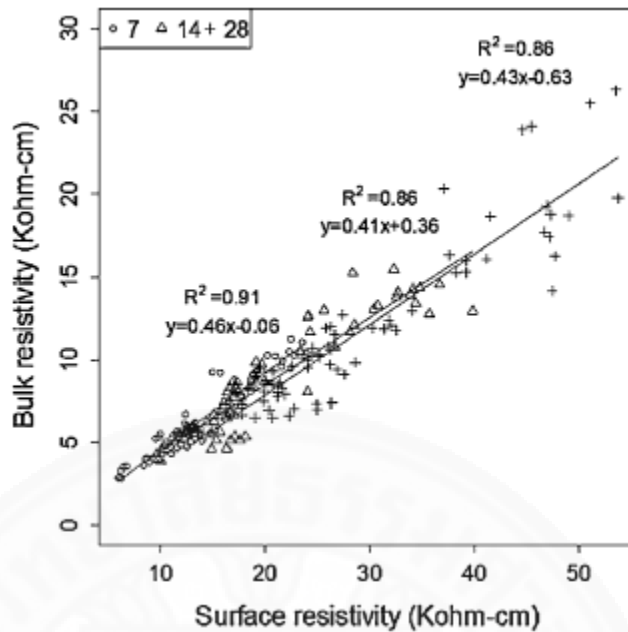


Fig. 2.12 Relationship between bulk and surface resistivity for fly ash mix proportions (Ghosh & Tran, 2015)

## 2.7 Factors Affecting the Electrical Resistivity of Concrete

Factors of concrete and its environment tend to lead to variability in the test results of concrete electrical resistivity. These include water/binder ratio, binder type and specimen shape, moisture and temperature and curing condition. However, other concrete parameters such as aggregates have a low influence on the variability of resistivity results, readings is taken over the concrete specimen and an average reading recorded (Morris et al., 1996).

### 2.7.1 Water to binder ratio

The resistivity is dependent on the concrete mix proportions and water to binder ratio of the concrete. Low w/b ratio shows higher resistivity than those with high w/b ratio. This is because the amount of interconnected pores decreases as the w/b ratio decreases (Addis, 2008). The w/b ratio plays an important role in shaping the microstructure of cement paste and the ionic concentration of its pore solution. Fig.

2.13 shows an example of results indicating effect of w/b on concrete electrical resistivity.

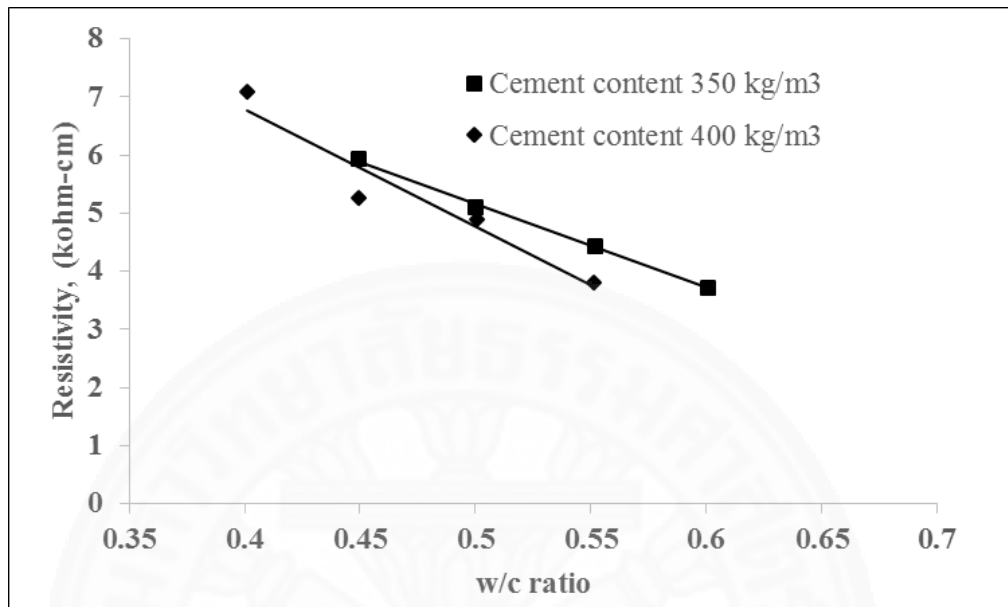


Figure 2.13 Effect of w/c ratio on concrete electrical resistivity (Huges, 1985)

### 2.7.2 Binder type

Binder type and content substantially influence the concrete resistivity (Hornbostel, Larsen, and Geiker, 2013). Binder type has higher influence on concrete resistivity than cover depth or w/b ratio. The most common supplementary cementing materials (SCMs) are fly ash, silica fume, and ground granulated blast furnace slag. When Fly Ash was added to the mix, the long-term increase in concrete resistivity was seven times higher than that measured at 28 days (Cabrera and Claisse, 1990). Increasing the percentage of silica fume showed a large initial increase in resistivity which tapered off and matched that of 100 % PC in the long-term. Because of the effect of their pozzolanic reaction and their physical properties. Mostly, SCMs cause finer pores and lower ionic concentration in the pores, which results in higher electrical resistivity when compared to the Ordinary Portland cement concrete (OPC) as shown in Fig. 2.14.

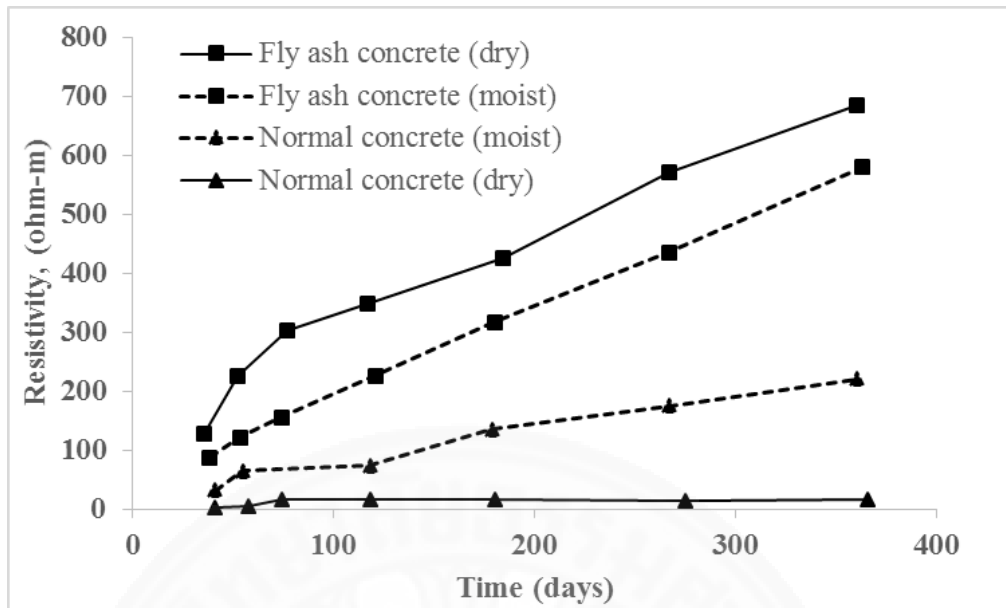


Figure 2.14 Effect of fly ash on electrical resistivity (Cabrera et al., 1994)

### 2.7.3 Effect of aggregates

The electrical resistivity of aggregate is higher than that of the cement paste. Monfore (1900) tested the electrical resistivity of many different aggregates generally used for concrete. The resistivity of marble and granite are mainly infinite as compared to the resistivity of cement paste as shown in Table 2.3.

Table 2.3 Electrical Resistivity of Aggregates (Monfore, 1900)

Type	Absorption (% by weight)	Resistivity (ohm.cm)
Sandstone	9.2	18,000
Limestone	6.0	30,000
Marble	0.9	290,000
Granite	0.34	880,000

Although the resistivity of concrete is significantly influenced by the cement paste, different aggregate types and content. The electrical resistivity increases as aggregate content increases. It was also found that the bigger the aggregate, the higher

the resistivity. Higher porosity presents in the interfacial zone between aggregates and cement paste. The interfacial zone increases its total volume with smaller aggregates due to a larger aggregate surface area. R.W. (1985) measured electrical resistivity of concrete with different amount of aggregate contents rendering the results shown in Figure 2.15.

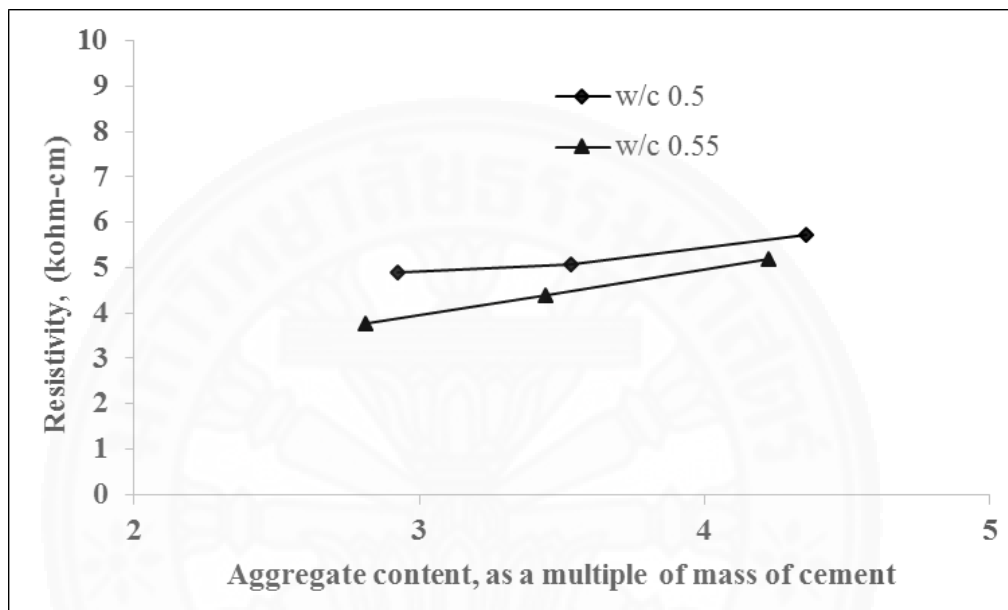


Fig. 2.15 Effect of aggregate content on electrical resistivity (Hughes 1985)

#### 2.7.4 Specimen Shape

Figs 2.17 and 2.18 show the placement of the Wenner probe on concrete specimens. Specimen geometry also plays important role on the measured results of electrical resistivity of concrete. Sengul and Gjrv (2009) demonstrated in Fig. 2.18 and 2.19 the electrical resistivity measurements with time performed on cylindrical (1, 3, 8, 15, 22, 29, and 91 days) and cubes (1, 3, 8, 29, and 91 days) specimens with the different curing conditions. Based on their results, the resistivity increases with time because as the hydration reactions proceed the concrete microstructure becomes denser. It was observed that the cubic specimens show higher electrical resistivity when compared with cylindrical specimens.

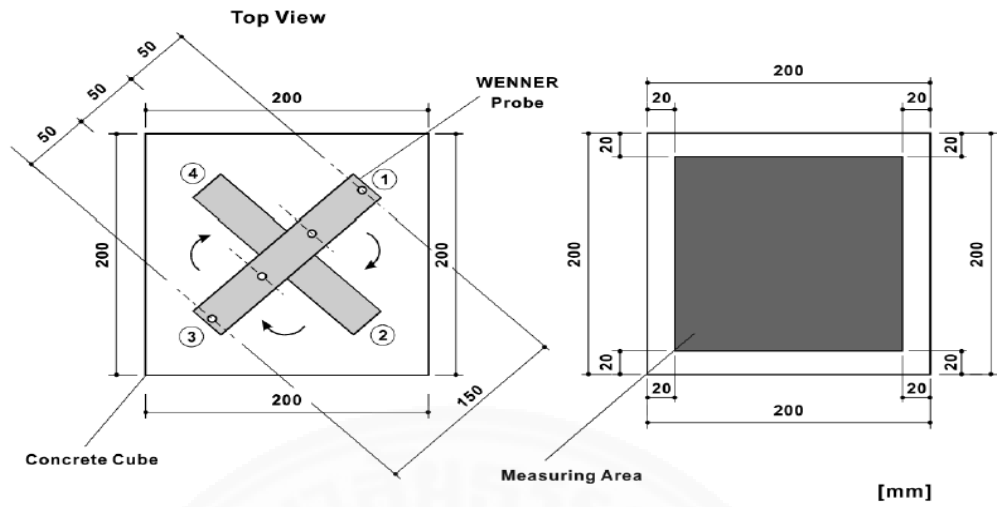


Fig 2.16 Wenner probe placement for cubic specimens (DURACRETE, 1999)

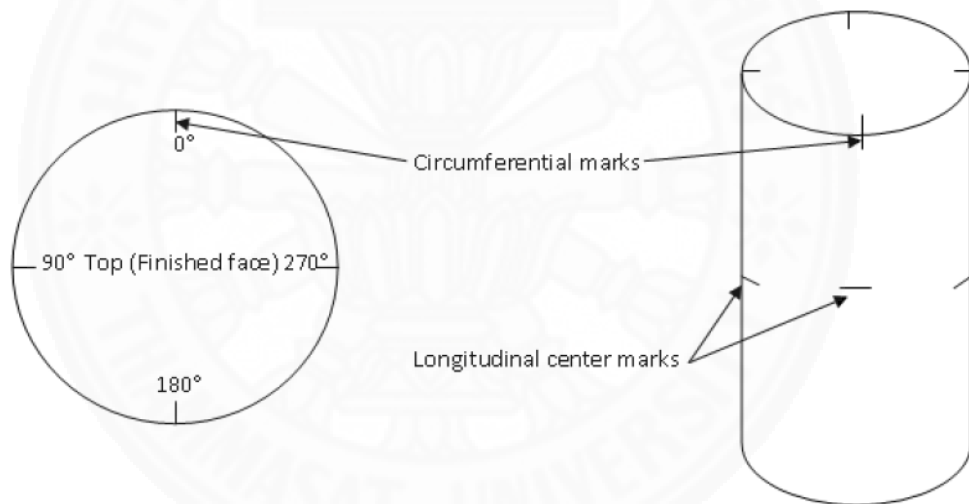


Fig 2.17 Wenner probe placement for cylindrical specimens (FDOT, 2004)

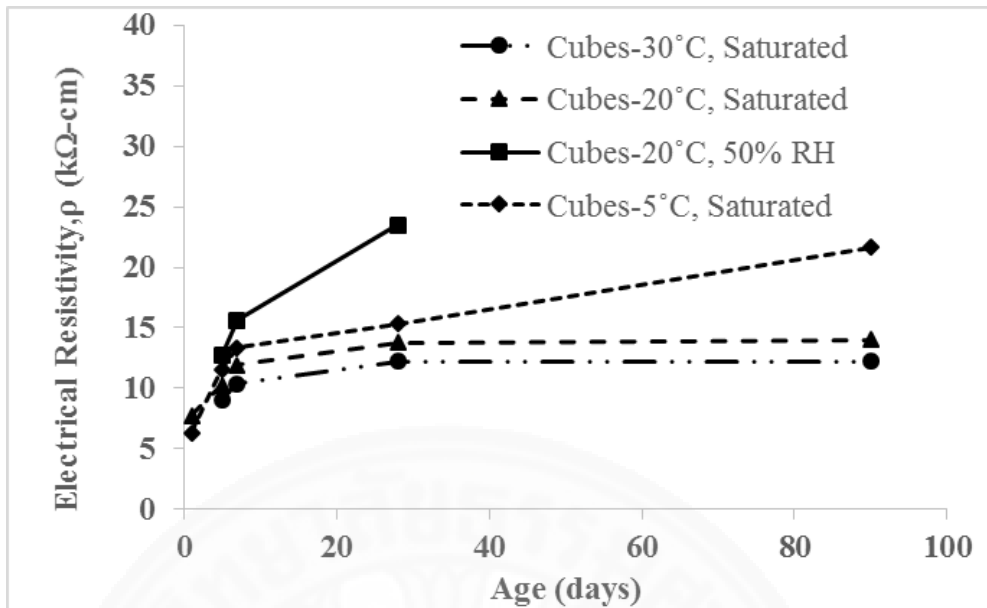


Figure 2.18 Four point electrical resistivity measurements on cubic specimens (P. C. Silva, Ferreira, and Figueiras, 2011)

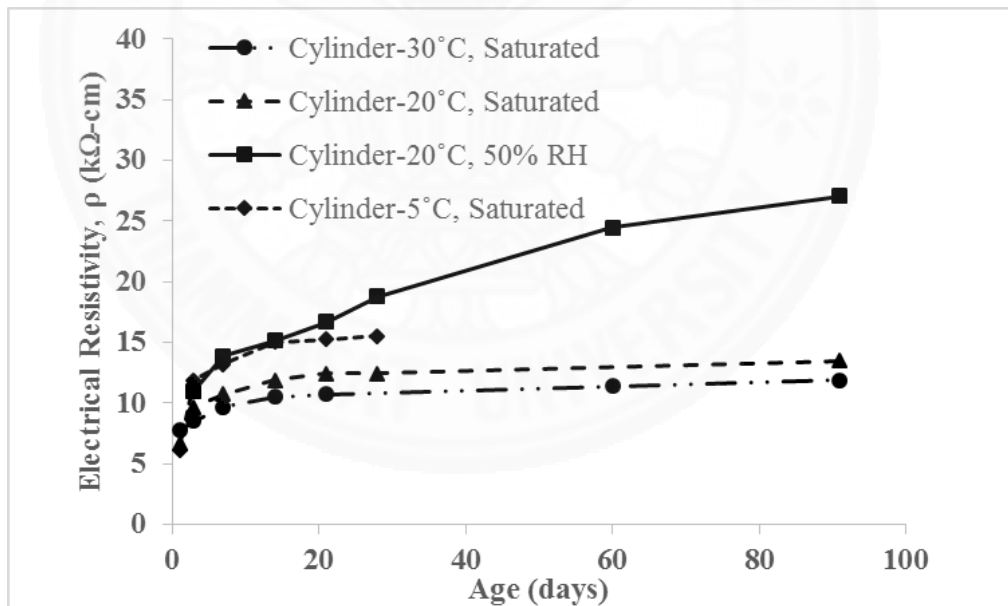


Figure 2.19 Four point electrical resistivity measurements on cylindrical specimen (P. C. Silva et al., 2011)

### 2.7.5 Moisture

Among the factors affecting on electrical resistivity, moisture content is the most significant factor. There is less pore water to carry the current when moisture content decreases. So, the electrical resistivity will increase. It is also related to the pore structure of the cement paste, as the current is carried by pore water. Powers (1958) defined a difference between pores, classifying them into three types: the air voids which are the ones that enter in the paste during the mixing of fresh concrete, the capillary pores and the gel pores in which the total evaporable water is held.

Hunkeler (1996) determined that the conductivity of concrete is essentially zero at a relative humidity of 40% and although at this condition there is still water in the gel pores, it is not conductive as it is bonded to the surface of the cement paste. The effect of degree of saturation on concrete electrical resistivity is shown in Fig. 2.20. The resistivity was measured in concretes that were dried from 100% to 20% saturation. The resistivity was measured in four different saturation levels as can be seen in Fig. 2.20.

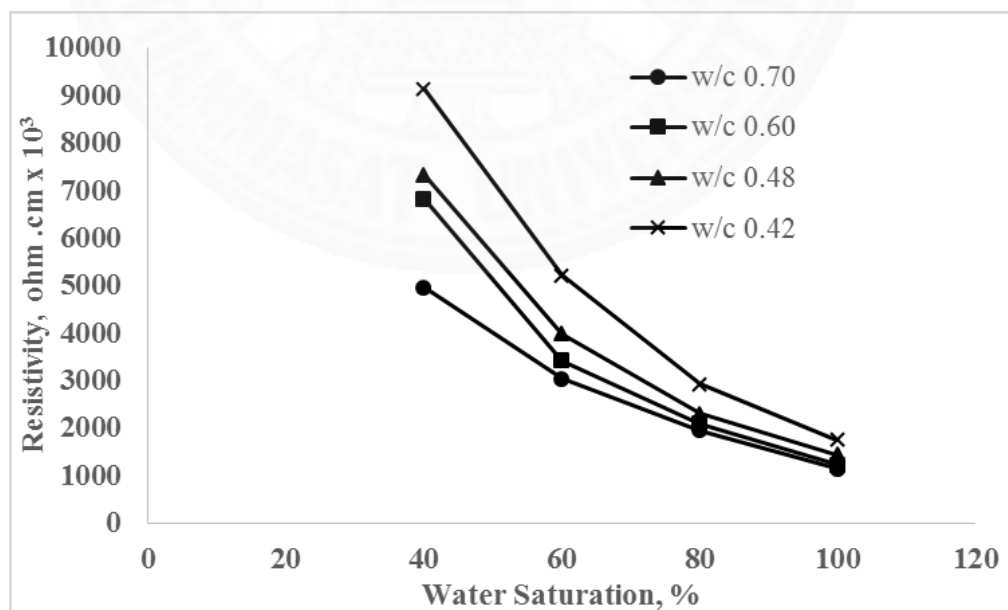


Figure 2.20 Effect of saturation on electrical resistivity of concrete (Gjorv et al 1977)

When specimens are exposed to wet cycle periods of 1 and 2 weeks, they have better electrical connection and therefore lower concrete electrical resistivity values. Conversely, when exposed to dry cycle periods, the electrical connectivity is lost and the concrete resistivity is high (Smith et al. 2004). Therefore, concrete electrical resistivity highly depends on moisture content of concrete.

Moreover, concrete resistivity measured during rainy season is likely to be lower than in dry season. This is because high pore saturation makes the flow of ions easier and consequently the resistivity is less. An increased number of pores and a higher water cement ratio also decrease the resistivity (Polder, 2001) .

#### 2.7.4 Sulfates and Chlorides

Concentrations of sulfate and chloride also affect on concrete resistivity (Saleem et al., 1996). When the chloride content increased the electrical resistivity also decreased (Saleem, Rashad, and El-Sabbagh, 2010) as shown in Fig. 2.21. Specimens contaminated with different sulfate and chloride concentrations showed a decrease in resistivity as their concentrations were increased.

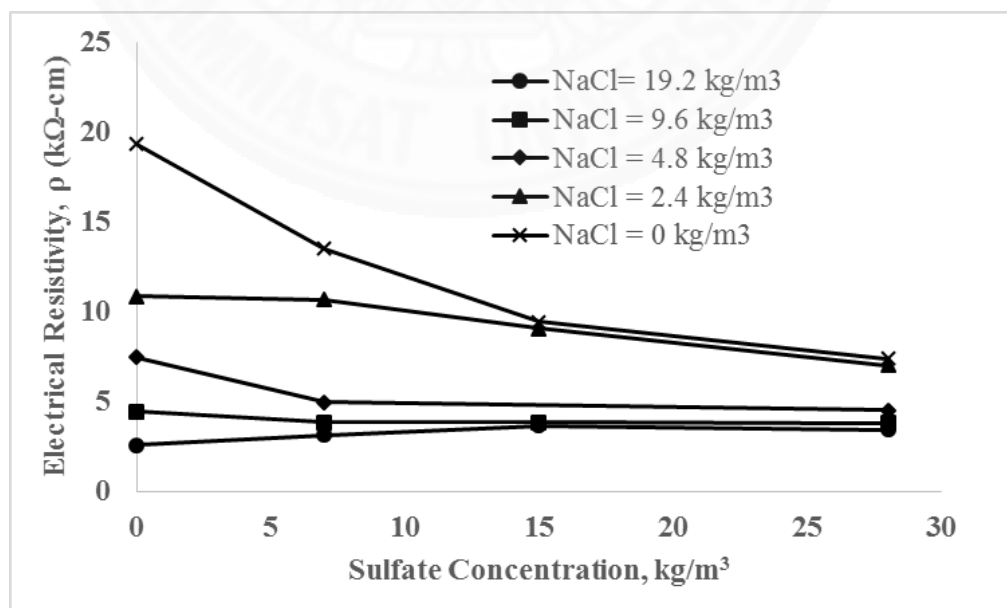


Fig 2.21 Variation of electrical resistivity of concrete with sulphate contamination (Saleem et al., 1996).

### 2.7.5 Temperature

In most electrochemical processes, the external and internal temperatures affect the concrete electrical resistivity. The effect of temperature is the same as that mentioned for moisture. The resistivity decreases as the temperature increases (Silva et al., 2011). Temperature effects depend on the behavior of the electrolyte: as the temperature rises, the viscosity of the fluids (pore water) decreases facilitating the ion mobility. The current is carried by these ions and thus, the resistivity decreases (McNeil, 1980).

Hope, Ip, and Manning (1985) measured the effect of temperature on electrical resistivity of concrete with different w/c ratios. Initially concretes were cured at 21°C and over 54 days in the water. Then, specimens were placed over a saturated salt solution at 75% RH for 14 days. The results are shown in Fig 2.22.

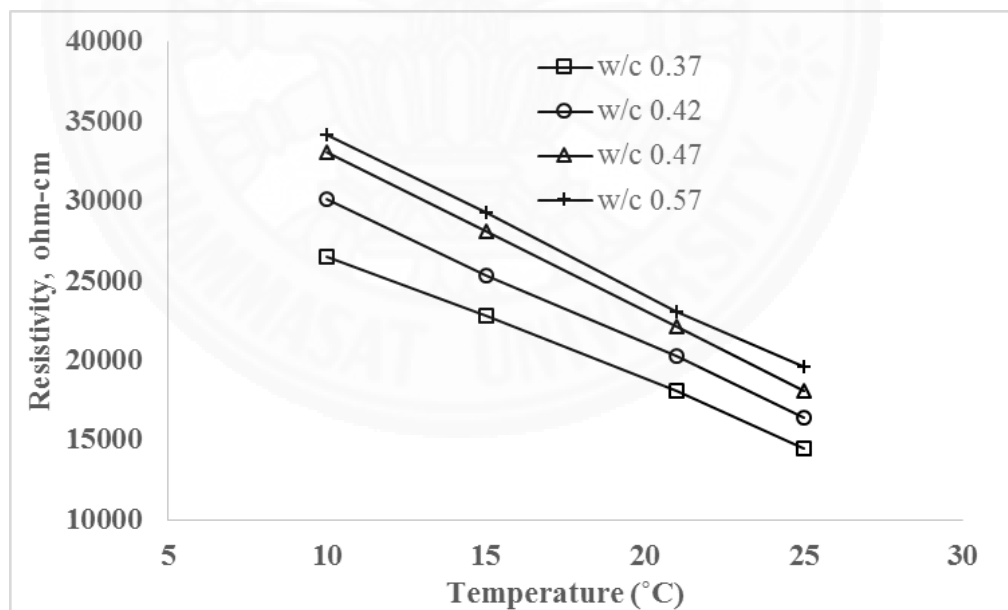


Fig 2.22 Electrical resistivity as a function of temperature (Riding et al., 2008)

McCarter, Ezirim, and Emerson (1996) reported a more comprehensive method of accounting for electrical resistivity at different temperatures by means of the Arrhenius equation as mentioned in equation 2.16.

$$\rho_e(T) = \rho_0 \cdot e^{A\left(\frac{1}{T} - \frac{1}{T_0}\right)} \quad (2.16)$$

Where  $\rho_e(T)$  and  $\rho_0$  ( $\Omega\text{m}$ ) are the resistivities at ambient temperature  $T$  and measured temperature  $T_0$  [K],  $A$  is the activation energy [K],  $T$  is the time at first measurement of the resistivity (years), and  $T_0$  is the time of the final measurement of resistivity (years).

The Arrhenius equation was proven experimentally to be an accurate presentation of the relationship between concrete resistivity and temperature using an activation energy of 3270 K (Osterminski, Schießl, Volkwein, & Mayer, 2006). Prior to this, (DURACRETE, 1999) had also advocated for the use of the Arrhenius equation for concrete resistivity measurements.

## **Chapter 3**

### **Methodology**

#### **3.1 General**

The purpose of this study is to investigate the effects of various parameters including mix proportion and conditions of the natural environments on surface electrical resistivity measurement of concrete. Moreover, durability tests such as rapid chloride permeability and moisture weight loss are studied. All of experimental details are described in this chapter.

#### **3.2 Materials**

##### **3.2.1 Ordinary Portland cement (OPC)**

In this experimental study, Ordinary Portland Cement Type I was used for all mixtures. The cement was in Thailand by Siam Cement Group Public Company Limited (Elephant Brand) according to TIS 15. Table 3.1 shows its chemical compositions and physical properties.

##### **3.2.2 Fly Ash**

Coal fly ash type 2b, according to TIS2135, from Mae-Moh power plant in Thailand, was used as a cement replacement material in some mixtures. Chemical compositions and physical properties are shown in Table 3.1.

##### **3.2.3 Aggregates**

Natural river sand, passing sieve No.4 (4.75-mm openings) was used as a fine aggregate for all mixes. Specific gravity and water absorption were 2.62 and 1.16%, respectively. Crushed limestone with a maximum size of 19 mm was used as coarse aggregate. It retained on sieve No.4 (4.75-mm openings) and cleaned before used.

Specific gravity in accordance with ASTM C127 was 2.8 and water absorption was 0.32%.

### **3.2.4 Water**

Ordinary tap water was used for all concrete specimens.

### **3.2.5 Admixture**

Mighty X, Naphthalene based, according to ASTM C1582 type F, from Kao Corporation, Thailand, was used as a high-range water reducing admixture.

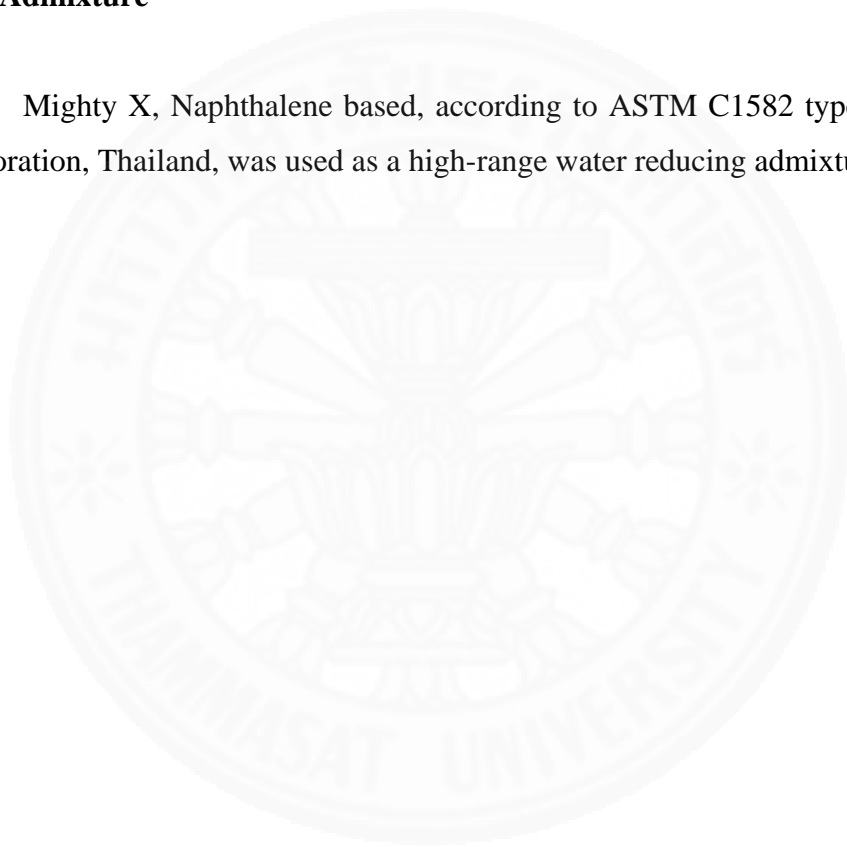


Table 3.1 Chemical compositions and physical properties of cement and fly ash.

Chemical compositions (%)	Cement	Fly ash
Silicon dioxide (%)	19.7	25.22
Aluminum oxide (%)	5.19	13.88
Iron oxide (%)	3.34	17.39
Calcium oxide (%)	64.80	26.25
Magnesium oxide (%)	1.20	2.38
Sulfur trioxide (%)	2.54	9.44
Insoluble residue(%)	0.13	-
Sodium oxide (%)	0.16	1.4
Potassium oxide (%)	0.44	1.92
Titanium dioxide (%)	0.25	-
Phosphorus pentaoxide (%)	0.11	-
Free Lime (%)	0.87	3.06
Gypsum Content (%)	5.6	-
<b>Physical Properties</b>		
Specific gravity	3.15	2.54
Loss of ignition (%)	2.10	0.56
Blaine fineness (cm <sup>2</sup> /g)	3350	2722
Water requirement (%)	100	95.6

### 3.3 Mix proportions

In this study, electrical resistivity was measured on 20 different concrete mix proportions, as shown in Table 3.2. Ordinary Portland cement (type I) was used as a binder. Fly ash is also used to partially replace cement in concrete at the levels of 0, 10, 30, and 40% by weight of binder. Water to binder ratios were varied of 0.35, 0.45, 0.55, and 0.65. Ratio of paste volume of concrete to void content between aggregate ( $Y$ ) was varied at 1.3 and 1.4.

Table 3.2 Mix proportions of the tested concrete

Designation	Y	w/b	Unit Content (kg/m <sup>3</sup> )						Sl (cm)
			OPC	FA	Water	Sand	Gravel	SP	
0.35 OPC	1.3	0.35	433	0	149	771	1138	2.16	1.5
0.35 FA 10		0.35	385	43	148	771	1138	2.14	6.5
0.35 FA 30		0.35	293	126	144	771	1138	2.093	8.6
0.35 FA 40		0.35	248	166	43	771	1138	2.07	8.9
0.45 OPC		0.45	377	0	168	771	1138	1.88	6.2
0.55 OPC		0.55	333	0	183	771	1138	0	10.3
0.55 FA 10		0.55	297	33	182	771	1138	0	11.7
0.55 FA 30		0.55	227	97	179	771	1138	0	15.2
0.55 FA 40		0.55	193	129	177	771	1138	0	16.5
0.65 OPC		0.65	299	0	194	771	1138	0	16
0.35 OPC	1.4	0.35	467	0	159	746	1101	2.34	3.5
0.35 FA 10		0.35	416	46	159	746	1101	2.31	8.6
0.35 FA 30		0.35	316	136	155	746	1101	2.26	10.1
0.35 FA 40		0.35	268	179	154	746	1101	2.24	11.2
0.45 OPC		0.45	407	0	181	746	1101	2.03	7.8
0.55 OPC		0.55	360	0	198	746	1101	0	12.5
0.55 FA 10		0.55	321	36	196	746	1101	0	13
0.55 FA 30		0.55	245	105	193	746	1101	0	13.8
0.55 FA 40		0.55	208	139	191	746	1101	0	17
0.65 OPC		0.65	322	0	210	746	1101	0	22

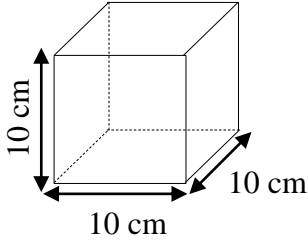
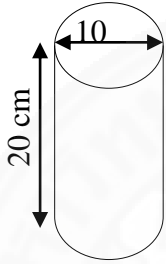
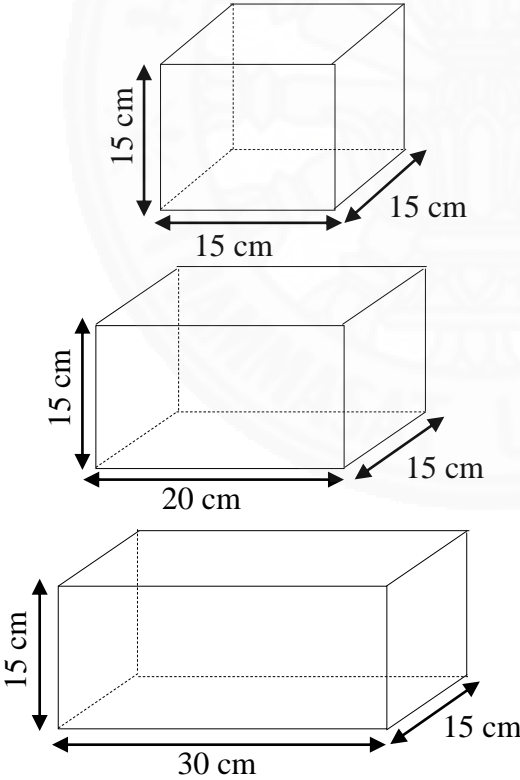
Remark: w/b is the water to binder ratio, Y is volume ratio of paste content to void content between aggregate in concrete, OPC is ordinary Portland cement, FA is fly ash, SP is superplasticizer, and Sl is slump of fresh concrete (cm).

### 3.4 Specimen Preparation

As shown in Table 3.3, four different types of cube and prism specimen dimensions (10 x 10 x 10 cm), (15 x 15 x 15 cm), (20 x 15 x 15 cm), and (30 x 15 x 15 cm) were prepared for electrical resistivity measurement. Cylindrical specimens  $\phi(10 \times 20 \text{ cm})$  were prepared to measure carbonation and rapid chloride penetration. The 38mm (1.5 inch) model of respirod was used in this experiments.

Before the durability measurement, electrical resistivity was measured for each specimen. At 1 day after casting, each specimen was demolded and cured in water. The four Wenner probe test, requiring wetting or saturating of the concrete before measurements, were undertaken in the laboratory. In addition, the tips or probes of the electrode were also moistened in water to improve the electrical connection. The size spacing between the probe is 3.8 cm. Electrical resistivity was measured every four days from the age of 1 day to 28 days. After 28 days, measurements were taken every week until 91 days. After 91 days, specimens were kept in a control room in which the temperature and humidity were controlled at  $28 \pm 1^\circ\text{C}$  and  $70 \pm 5\%$ , respectively and measured electrical resistivity every week until 182 days. Afterwards the specimens were cured in the water bath to measure long term electrical resistivity. Cubic and prism specimens (15 x 15 x 15 cm), (20 x 15 x 15 cm), and (30 x 15 x 15 cm) were prepared to test the specimen size effect on electrical resistivity. One concrete mix proportion was prepared to test the effect of size of specimens. Measurement techniques of electrical resistivity was conducted following the procedures as mentioned above. These three different size of specimens were cured only in water. The specimen preparation procedures for each test are shown in Figure 3.1 and Table 3.3.

Table 3.3 Specimen dimensions in this study for all testings of concrete (not in scale)

Test Specimen	Laboratory Testing
 <p>A 3D perspective drawing of a cube. The front horizontal edge is labeled '10 cm', the depth edge is labeled '10 cm', and the vertical edge is labeled '10 cm'.</p>	<ul style="list-style-type: none"> <li>➤ Electrical resistivity test (four Wenner probe method)</li> <li>➤ Compressive strength test</li> <li>➤ Moisture Weight loss</li> </ul>
 <p>A 3D perspective drawing of a cylinder. The diameter of the top circular face is labeled '10', and the height of the cylinder is labeled '20 cm'.</p>	<ul style="list-style-type: none"> <li>➤ Electrical resistivity test (four Wenner probe method)</li> <li>➤ Rapid chloride permeability test</li> <li>➤ Carbonation test</li> </ul>
 <p>Three 3D perspective drawings of rectangular prisms. The first is a cube with all edges labeled '15 cm'. The second has a front edge of '20 cm', a depth edge of '15 cm', and a vertical edge of '15 cm'. The third has a front edge of '30 cm', a depth edge of '15 cm', and a vertical edge of '15 cm'.</p>	<ul style="list-style-type: none"> <li>➤ Electrical resistivity test (four Wenner probe method)</li> </ul>

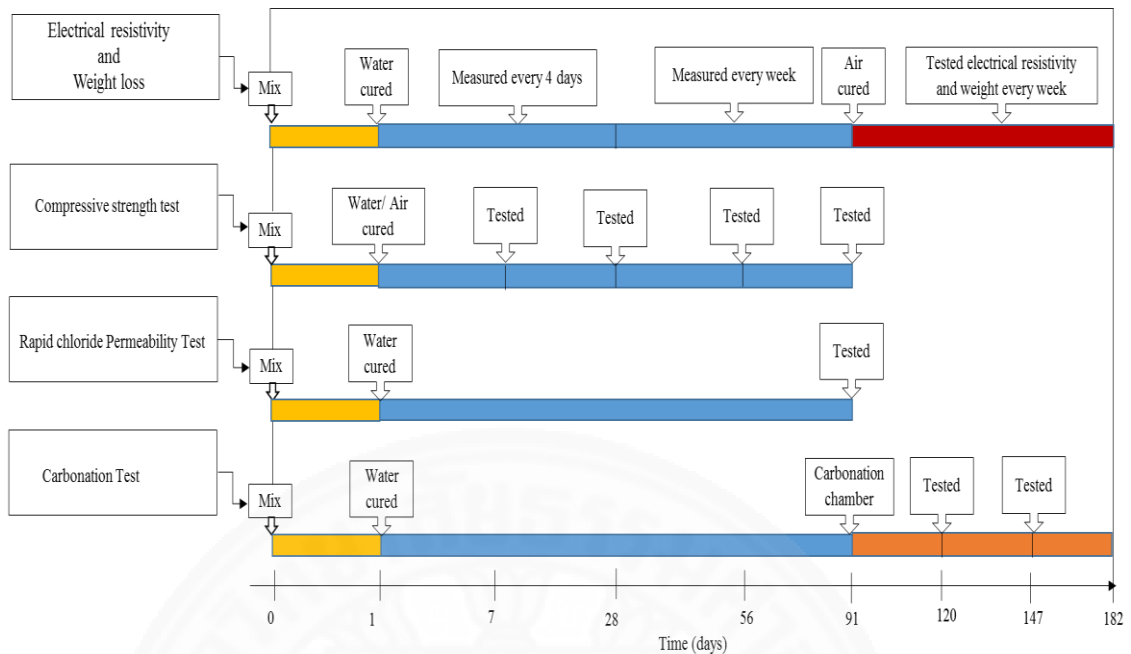


Figure 3.1: Specimen preparation procedures for each test (not in scale)

### 3.5 Methods of Testing

#### 3.5.1 Electrical Resistivity of Concrete

Three concrete specimens were removed from the water and extra surface moisture was wiped off. When measuring all the points, the probes were made in contact with the concrete and waited for three to five seconds until readings were obtained. Average resistivity for the set of sample was then derived from the three specimens.

##### 3.5.1.1 Cubic specimen

Specimen thickness and edge also affect the electrical resistivity of concrete. For each cubic specimen, resistivity measurement was performed on bottom surface of the specimen and two diagonal measurements perpendicular to each other were conducted. To get a good indication of concrete resistivity, five measurements were taken for their average as shown in Fig 3.2. The measurement using the Wenner probe is shown in Fig. 3.3. In this study, a set of PVC pipe was used as an insulator bottom of

the specimen to disconnect the specimen from floor. The resistivity value of PVC is  $10^{14}$ - $10^{15}$  ( $\Omega$ -cm).

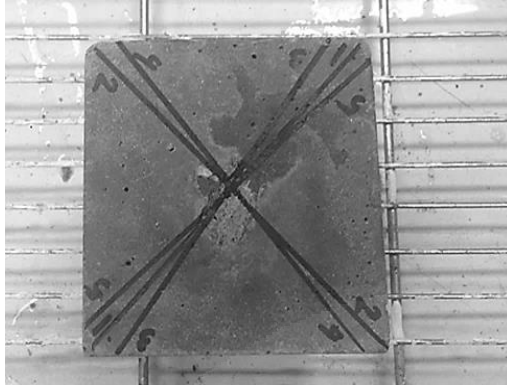


Figure 3.2: Cubic specimen



Figure 3.3: Measurement technique for electrical resistivity of a cubic specimen using a four Wenner probe

### 3.5.1.2 Cylindrical specimen

The test procedure was in accordance with AASHTO TP-95. Immediately after deomolding, four permanent lines along the longitudinal axis of each specimen were drawn on the circumference face of the specimen at 0, 90, 180, and 270 degree of the circular cross section. Then the Wenner array probe was placed longitudinally along the length of the specimen at the 0 degree line. The probe must be centered along the height on the side of the specimen (ASTM C-192). Three times repetitions of the measurement were obtained at 90, 180, and 270 degree lines, respectively as shown in Figures 3.4 and 3.5. a set of PVC pipe was used as an insulator as in the case of cubic and prism specimens.



Figure 3.4: Cylindrical specimen



Figure 3.5: Measurement technique for electrical resistivity of a cylindrical specimen using a four Wenner probe

### 3.5.2 Effect of specimen thickness

After 270 days of saturation, some of the concrete specimens (10 x 10 x 10) cm were cut and electrical resistivity measurements were done with different thickness as shown in Figure 3.6 (a)-(c). Electrical resistivity measurement was followed as cubic specimen of electrical resistivity measurement. Specimens were cut from bottom surface to vary the height to be 10 cm to 4 cm.

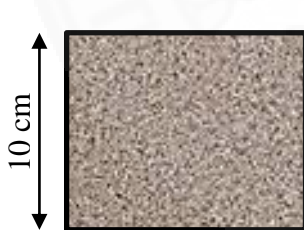


Figure 3.6 (a):  
Before specimen  
cutting

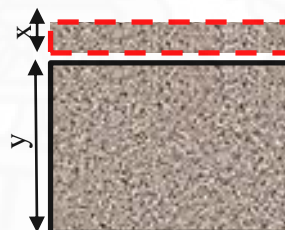


Figure 3.6 (b): Cut  
off thickness from  
0 to 6 cm

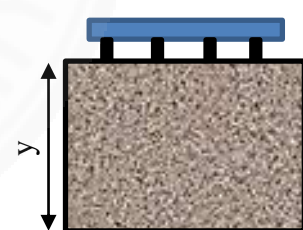


Figure 3.6 (c): Specimen  
after cutting for electrical  
resistivity measurement

Fig 3.6 Procedures of effect of specimen thickness

Where,  $x$  is the cut off thickness (0 to 6) cm and  $y$  is the height after specimen cutting (10 to 4) cm for electrical resistivity measurement.

### 3.5.3 Compressive Strength Test of Concrete

The test procedure was in accordance with BS 1881-116. Cubic specimens of (100 x 100 x 100 mm) were cast and demolded at 24 hours after casting. Specimens were cured in water and air conditions. Three specimens were tested for obtaining their average at the ages of 7, 14, 28, 56, and 91 days as shown in Figure 3.7 (a) – (c).

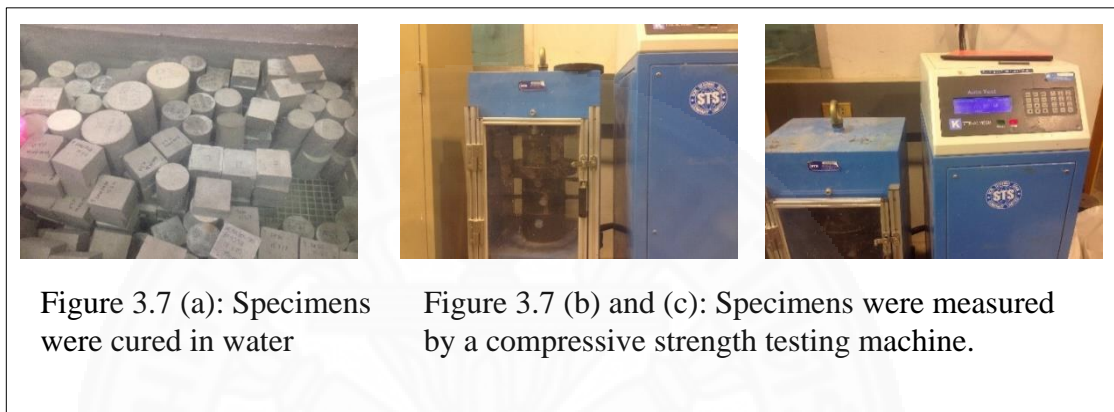


Figure 3.7 (a): Specimens were cured in water

Figure 3.7 (b) and (c): Specimens were measured by a compressive strength testing machine.

Fig 3.7 (a)-(c): Procedures of compressive strength test

### 3.5.4 Rapid Chloride Penetration Test of Concrete

For rapid chloride penetration of water-saturated concrete, 100 x 200 mm cylindrical specimens were tested after 91 days of curing in accordance with ASTM C1202, 2012. Three 50 mm thick disc samples were cut from a specimen and were placed in a vacuum chamber for 3 hours as shown in Figure 3.8 (a) and (b). Then the samples were immersed in water and vacuum saturated for 1 hour and allowed to soak in the water for 18 hours as shown in Figure 3.8 (c). Then each sample was placed between two cells of 0.3N NaOH and 3% NaCl. The system was tested by applying potential difference of 60 V for 6 hours of direct current as shown in Figure 3.8 (d). After that, samples were removed from the cells and the charge passed between the samples were calculated.

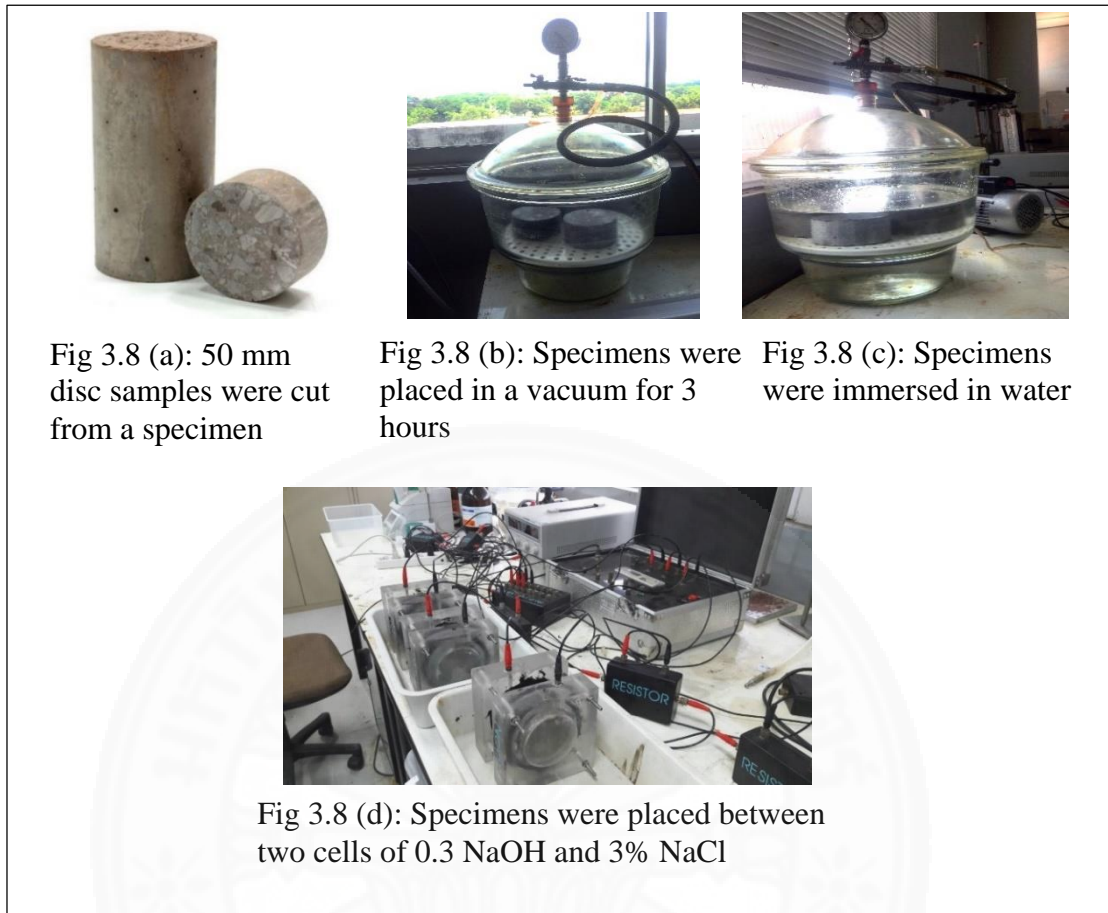


Fig 3.8 (a) - (d) Procedures of rapid chloride penetration test

### 3.5.5 Carbonation

Carbonation of cylindrical concrete specimens with size 100 x 200 mm were tested after 91 days of curing. All specimens were stored in a carbonation chamber of which the relative humidity and temperature were set at 40°C and 55 ± 5%, respectively as shown in Figure 3.9 (a) and (b). The carbon dioxide concentration in the chamber was 4% (40,000 ppm). The specimens were split for measuring the carbonation depth at 28 and 56 days of exposure to carbon dioxide as shown in Figure 3.9 (c). The depth of carbonation was determined 3 times from each sides and totally 12 times per specimen by spraying a solution of 1% phenolphthalein in 70% ethyl alcohol and water as shown in Figure 3.9 (d). Carbonation coefficient was calculated as shown in equation 3.1.

$$k = \frac{X_c}{\sqrt{t}} \quad (3.1)$$

Where K is the corresponding carbonation coefficient (mm/month<sup>0.5</sup>), X<sub>c</sub> is the tested carbonation depth (mm), and t is the period of specimen in the carbonation chamber (month).

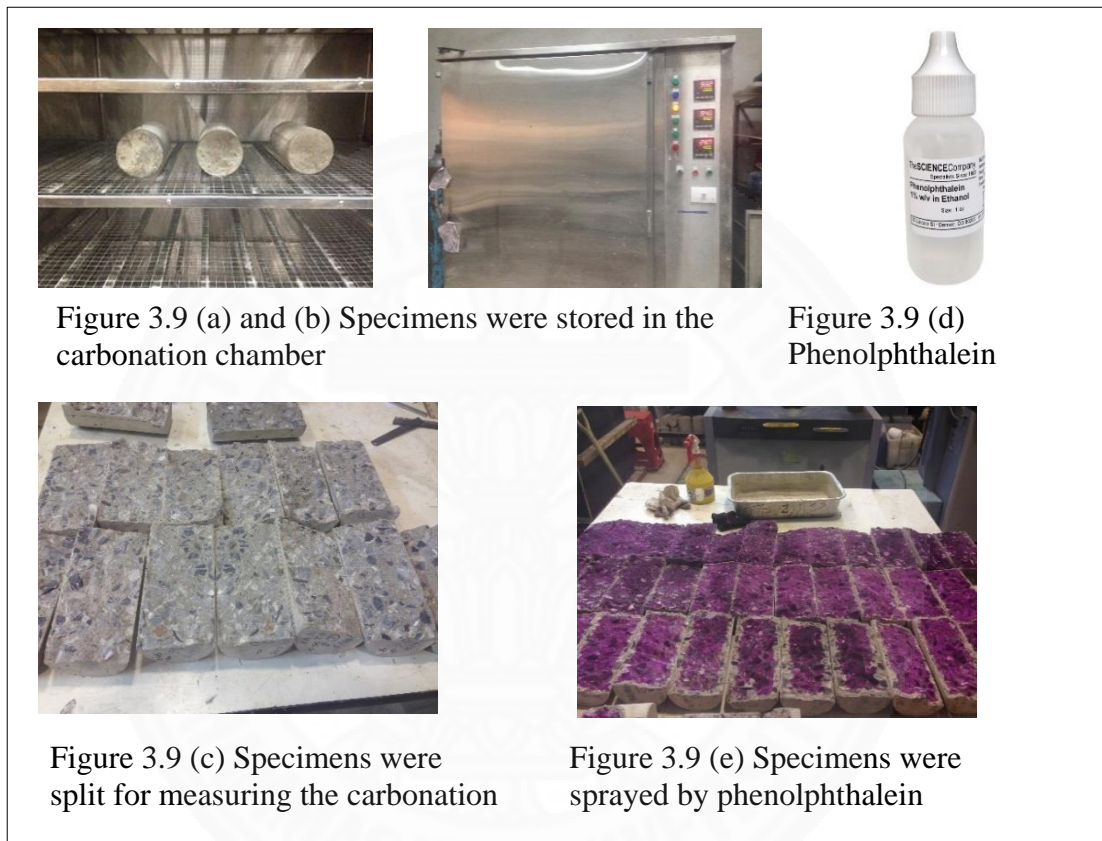


Fig 3.9 (a)-(e) Procedures of carbonation test

### 3.5.6 Weight Loss due to Moisture Loss of Concrete

Concrete specimens were kept in the air after 91 days of water curing. The weight of each specimen was measured every week until 183 days. An equation is used for calculating moisture weight loss as shown in equation 3.2. Measurements were taken up to 182 days.

$$wl(t) = \frac{W_s - W_{d(t)}}{W_s} \times 100 \% \quad (3.2)$$

Where,  $wl(t)$  is moisture weight loss of the specimen (%),  $Ws$  is fully saturated weight of specimen at the age of 91 days (g),  $Wd(t)$  is weight in the air of specimen after 91 days to 182 days (g).



## **Chapter 4**

### **Results and Discussion**

#### **4.1 General**

This chapter presents the results of laboratory experiments carried out in this study. The influences of various parameters affecting electrical resistivity of concrete mixtures are discussed. The relationship between electrical resistivity and durability test results such as rapid chloride permeability and moisture content are also discussed. Moreover, prediction equations of electrical resistivity are presented based on mix proportions and durability parameters.

#### **4.2. Effect of mix proportions on electrical resistivity of concrete**

##### **4.2.1. Water/binder ratio (w/b)**

Fig. 4.1 shows the effect of water to binder ratio on electrical resistivity of concrete. As shown in Fig. 4.1 electrical resistivity is increased with age of concrete because of the densification due to cement hydration especially in the first 28 days. According to the results, low water to binder ratio concrete shows higher electrical resistivity than those with higher water to binder ratios. This is because amount of interconnected pores decrease as the w/b ratio decreases (Addis, 2008). The resistivity values at w/b 0.55 and 0.65 are not noticeably different, but it becomes significant for w/b 0.45. As shown in Fig. 4.2 the electrical resistivity of specimens with higher w/b ratios (0.45, 0.55, and 0.65) decrease 40, 50, and 55 %, respectively when compared to the specimen with the lowest w/b ratio (0.35) at 91 days.

When w/b ratio was decreased, pore structure is denser, leading to increase electrical resistivity. Specimens were kept from 91 to 182 days in control room in which the temperature and humidity were controlled at  $28 \pm 1^\circ\text{C}$  and  $70 \pm 5\%$ , respectively. After 182 days, specimens were cured in water again. As the wetting followed the

drying in the control room, very small pores may not be fully saturated. This may be one of the reasons causing increase of electrical resistivity after 182 days. In long term, electrical resistivity still shows increasing trend even at the age of 270 days.

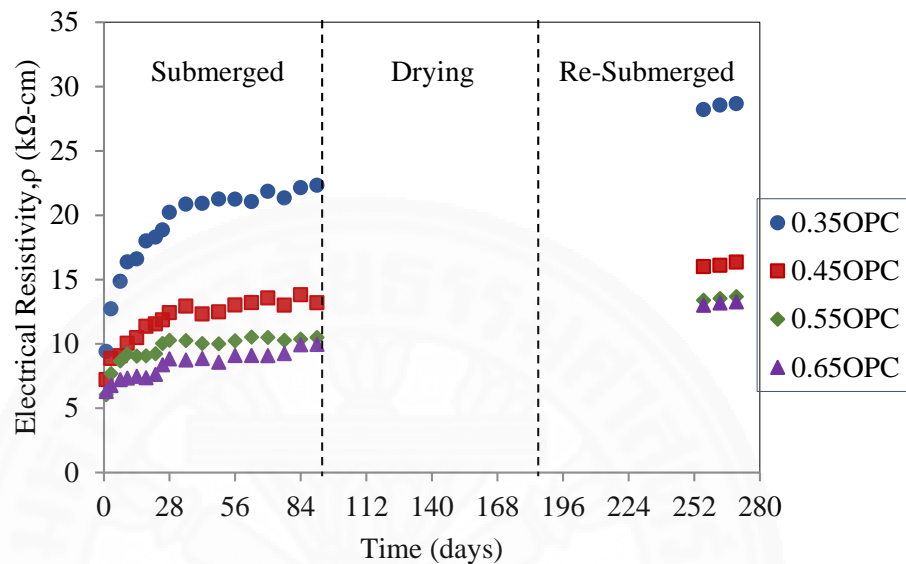


Fig 4.1 Effect of w/b ratio on electrical resistivity of concrete.

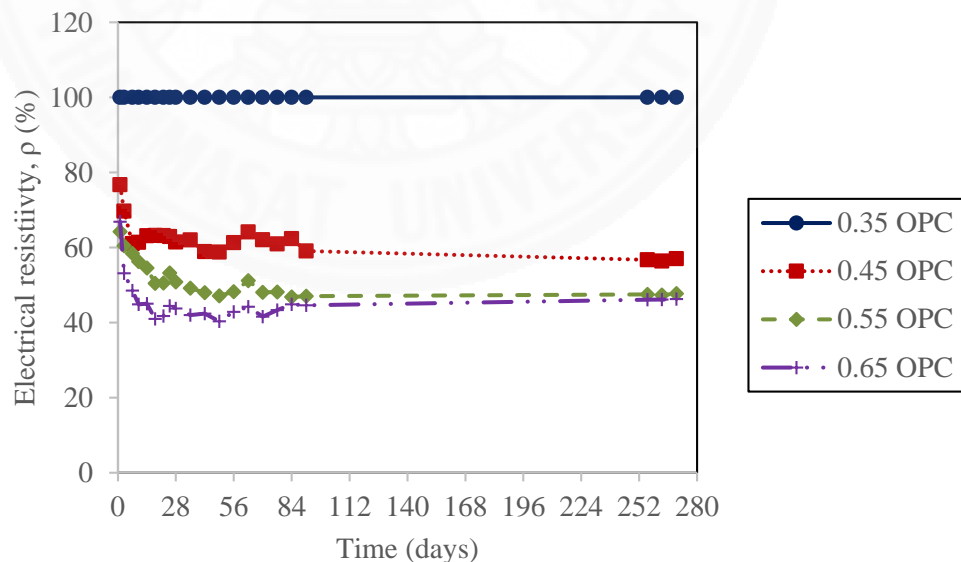


Fig 4.2 Effect of w/b ratio on electrical resistivity of concrete by percentage of w/b

0.35

#### 4.2.2 Fly ash content

Figs. 4.3 and 4.4 show the effect of different replacements of fly ash on the electrical resistivity of concrete specimens with w/b 0.35 and 0.55, respectively. As shown in Figs. 4.3 and 4.4, before 14 days, resistivity of fly ash concrete is very small when compared to OPC concrete because pozzolanic reaction is very slow at early age. After 14 days electrical resistivity of fly ash concrete sharply increased, especially in case of concrete with 30% and 40% fly ash replacements. The rate of electrical resistivity increase with time is higher for fly ash concrete. As shown in Fig. 4.3, at very low w/b, pores are already disconnected and pore structure is dense, so the effect of fly ash replacement of 10% is not significant. Concrete with 10% fly ash replacement was not significantly different in term of resistivity when compared to OPC. When 30% of fly ash was replaced, the concentration of hydroxyl ions was reduced, and pore distribution was finer than OPC concrete, so electrical resistivity rate obviously increased. Moreover, the resistivity value of fly ash is higher than OPC as shown in Table 4.1. As shown in Fig. 4.4 for w/b 0.55, even 10% at significantly increased the resistivity. As shown in Fig. 4.5, electrical resistivity of fly ash 10, 30, 40% increase 20, 190, 330 % respectively, when compared to fly ash 0 % replacement (OPC) at 91 days.

Fly ash content has substantial influence on the concrete resistivity. Effect of fly ash on electrical resistivity is mainly due to the changes in the pore structure of concrete. The use of fly ash can reduce pore structure of concrete through its both physical and chemical effects during the freshly mixed and subsequent hydrating states due to the pozzolanic reaction. The effects of different pore solution chemistry and refinement of pore structure on electrical resistivity were also discussed by D. Whiting et al., 1993.

Fly ash causes finer pores and lower ionic concentration in the pores, which leads to a higher electrical resistivity than OPC concrete (Monfore, 1900). In long term, resistivity values of fly ash concrete showed significantly increasing tendency when compared to that of OPC concrete. This is because of the pozzolanic reactivity of fly

ash which is still active in long term. Therefore corrosion current flow in fly ash concrete is expected to be reduced.

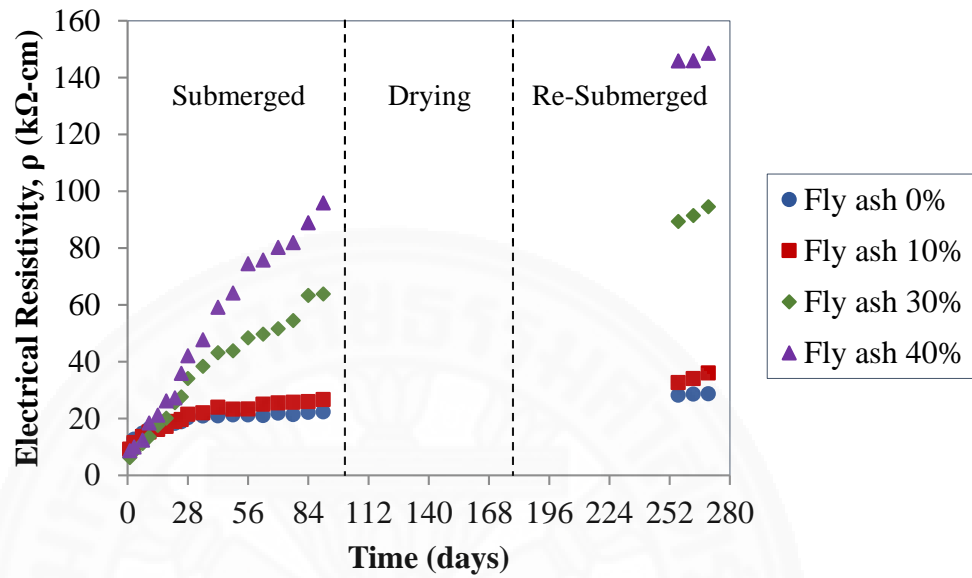


Fig 4.3 Effect of fly ash content on electrical resistivity of concrete with w/b 0.35.

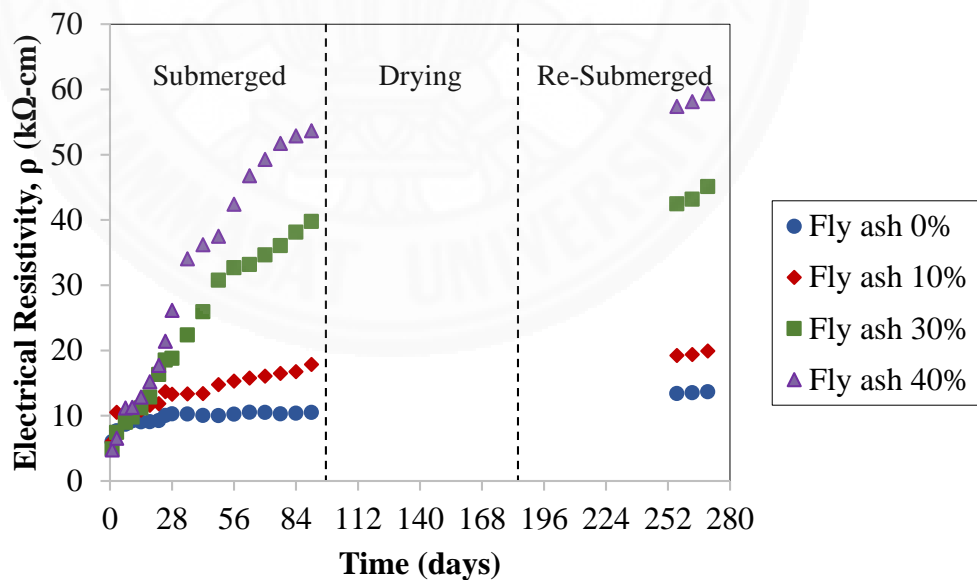


Fig 4.4 Effect of fly ash content on electrical resistivity of concrete with w/b 0.55.

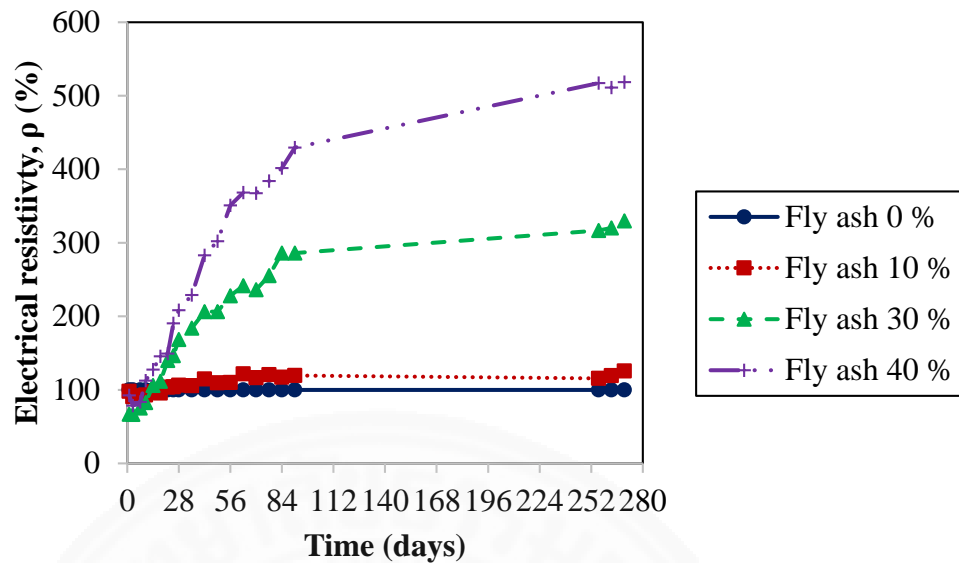


Fig 4.5 Effect of different fly ash amount on electrical resistivity of concrete relative to fly ash replacement 0% at w/b 0.35

#### 4.2.3 Ratio of paste content of concrete to void content between aggregate ( $\Upsilon$ )

Fig. 4.6 shows effect of ratio of paste content of concrete to void content between aggregate ( $\Upsilon$ ) on electrical resistivity of concrete. Low  $\Upsilon$  concrete has higher electrical resistivity than high  $\Upsilon$  concrete because the larger amount of aggregate and lower cement paste content increases the electrical resistivity as shown in Fig. 4.6. As shown in Fig. 4.7, electrical resistivity of high  $\Upsilon$  (1.4) decreases approximately 10 percent when compared to that of low  $\Upsilon$  (1.3) in case of concrete with w/b 0.35 at 91 days.

Electrical resistivity is also affected by cement paste content, aggregate type and content. The resistivity of cement paste is lower than that of the aggregates in concrete. The more cement paste in concrete, the lower the value of resistivity. Increasing in aggregate content and reduction in cement paste for a given volume results in higher resistivity values because of replacing of the porous hardened cement paste with denser aggregates. In addition, the electrical resistivity value of the aggregate is higher than that of cement paste as shown in Table 4.1.

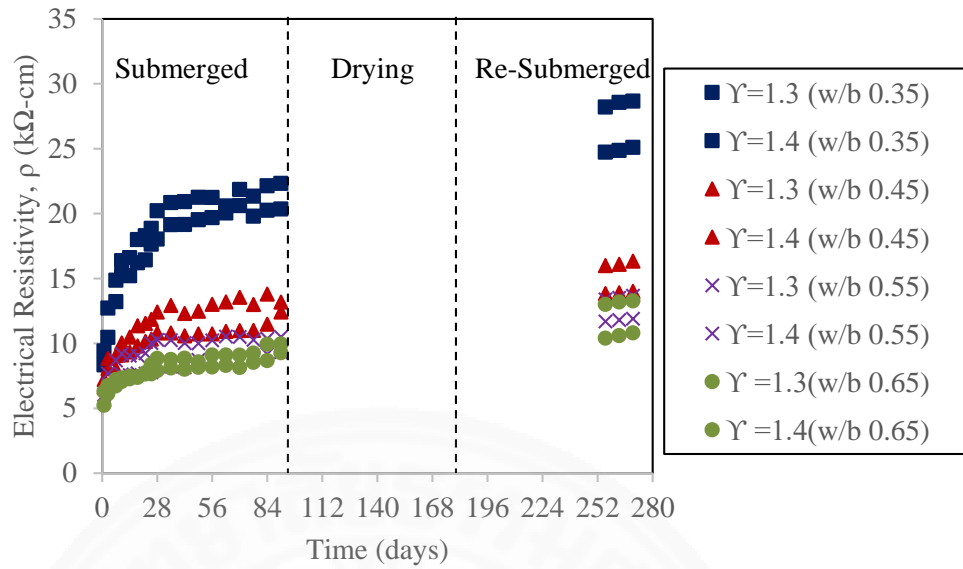


Fig 4.6 Effect of ratio of paste content of concrete to void content between aggregate ( $\gamma$ ) on electrical resistivity of concrete

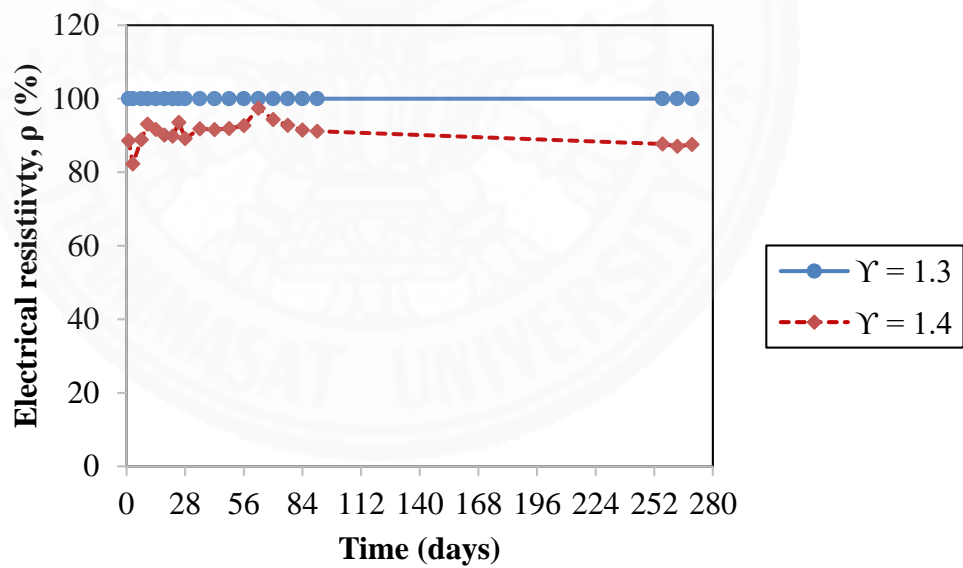


Fig. 4.7 Effect of ratio of paste content of concrete to void content between aggregate ( $\gamma$ ) on electrical resistivity of concrete by percentage of  $\gamma=1.3$  at w/b 0.35

Table 4.1 Electrical resistivity of concrete raw materials

Concrete Materials	Electrical Resistivity, $\rho$ ( $k\Omega$ -cm)	References
Cement	$1 \times 10^3 - 4 \times 10^3$	Woelfl et al., 1979
Fly Ash	$10^3$ - $10^{11}$ (In lab)	White, 1953
Fly Ash	$10^5$ - $10^8$ (In Field)	White, 1953
Cement paste	1 – 1.3	Ramacandran et al., 2001
Limestone	$5 \times 10^3 - 10^8$	Reynolds, 1997
Sand	$5 \times 10^2 - 10^4$	Reynolds, 1997
Water	2 - $2 \times 10^2$	Helmenstine, 2017
Air	$1.3 \times 10^{15} - 3.3 \times 10^{15}$	Helmenstine, 2017

#### 4.2.4 Specimen Length

Fig. 4.8 presents effect of three different prism specimen length electrical resistivity of concrete with w/b 0.35. Based on the results, short specimen length increased the measured values of electrical resistivity. If the length of the concrete is longer, the current is less constricted to flow into a field pattern that may be the one reason of the longer length of concrete electrical resistivity is decreased. Fig 4.9 shows that the electrical resistivities of specimens with the length of (20 x 15 x 15) cm and (30 x 15 x 15) cm decrease 6 and 7 %, respectively when compared to that of (15 x 15 x 15) cm specimen length.

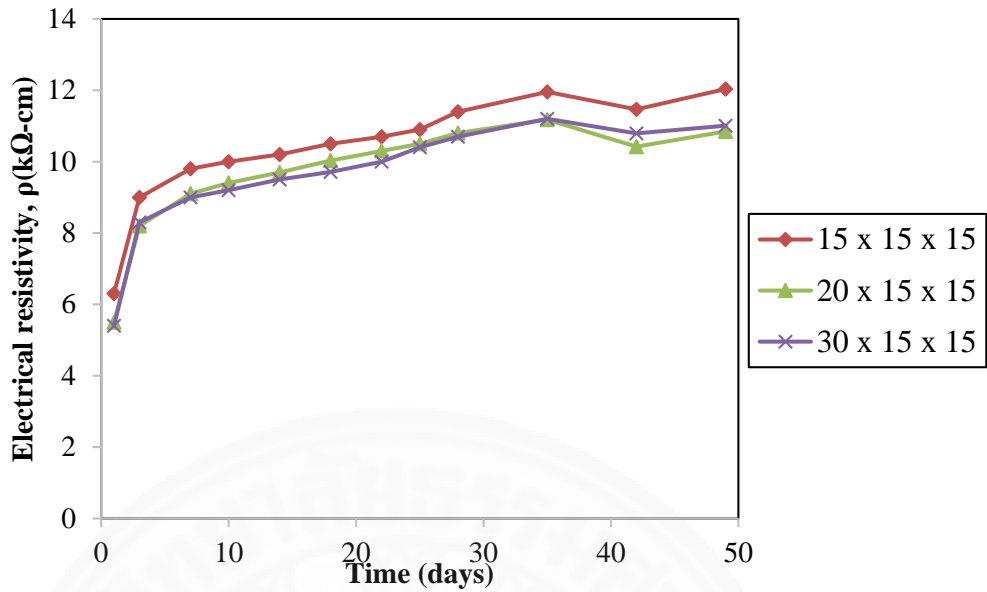


Fig 4.8 Effect of specimen length on electrical resistivity of concrete with w/b 0.35.

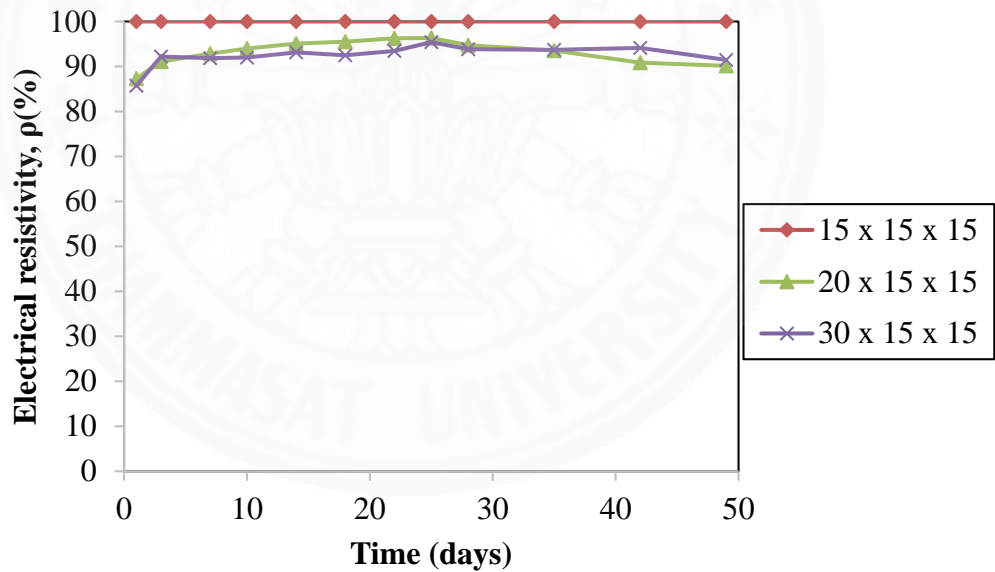


Fig 4.9 Effect of specimen length on electrical resistivity of concrete by percent of 15 x 15 x 15 cm size

#### 4.2.5 Specimen shape

Two types of concrete specimen shape were tested in this research:  $\phi$  100 x 200 mm concrete cylinder and 100 x 100 x 100 mm concrete cubes. Fig. 4.10 illustrates the

electrical resistivity measurements of cubic and cylinder specimens with different w/b ratios. As shown in Fig. 4.10, electrical resistivity values of the cubic specimens are higher than that of the cylindrical specimens. Electrical resistivity depends on the area based on equation 4.1. Electrical resistivity and area of specimen are directly proportional to each other. In this study, area of cubic specimen is higher than cylindrical specimen. That may be the main reason electrical resistivity of cubic specimen is higher than cylindrical specimen.

$$\rho = R \cdot \frac{A}{L} \quad (4.1)$$

When  $\rho$  is resistivity (k $\Omega$ -cm), R is resistance of concrete (k $\Omega$ ), A is the cross sectional area of the specimen (cm<sup>2</sup>), and L is the length of the specimen (cm).

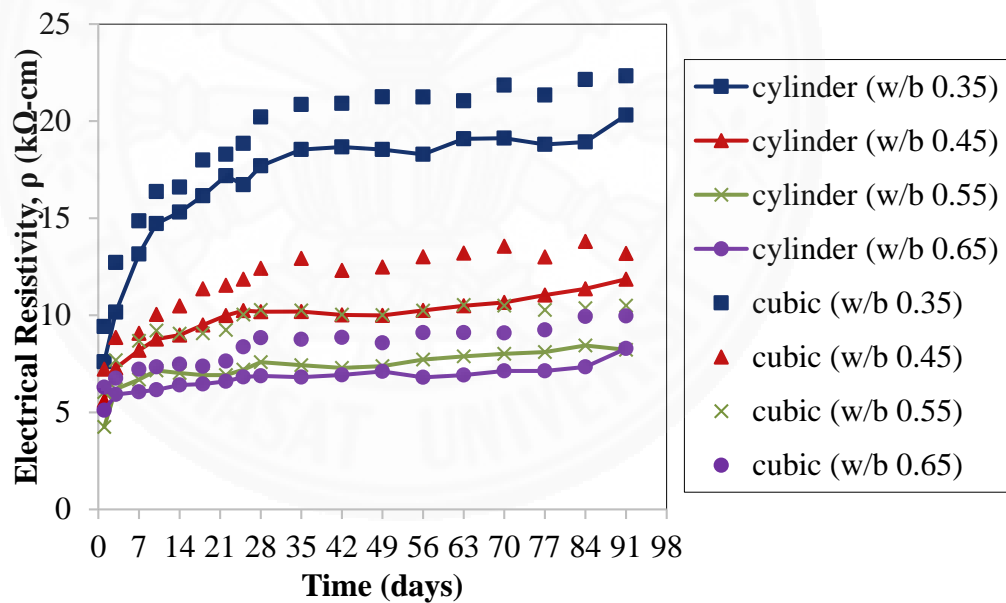


Fig 4.10 Effect of specimen shape on electrical resistivity of concrete

#### 4.2.6 Specimen thickness

Fig. 4.11 presents the effect of specimen thickness on electrical resistivity of specimens with different concrete mix proportions. Testing procedure was mentioned in chapter 3, subheading 3.5.2. As shown in Fig. 4.11, 10 cm thickness of the specimen

results in slightly higher electrical resistivity than other thinner specimens except for very thin specimens (4-5 cm). That may be partly due to the effect of mold surface on pore structure of concrete. From 6-9 cm, electrical resistivities are almost the same. In specimens with 40% fly ash replacement and w/b 0.55, thickness from 6-10 cm show only slightly differences of the resistivity. For specimens with small thickness electrical resistivity increases instantly. Gowers and Millard (1999) found that a significant error occurs if resistivity measurements are taken on a thin concrete section or near to an edge. If the dimensions of a concrete element are relatively small, the current is constricted to flow into a different field pattern that will result in an over estimation of the evaluation of electrical resistivity of concrete. The size of the concrete structure with respect to the electrode spacing has a significant effect on electrical resistivity measurements. Electrical resistivity readings will be more accurate for structures with relatively large dimensions and measurement made from the edge.

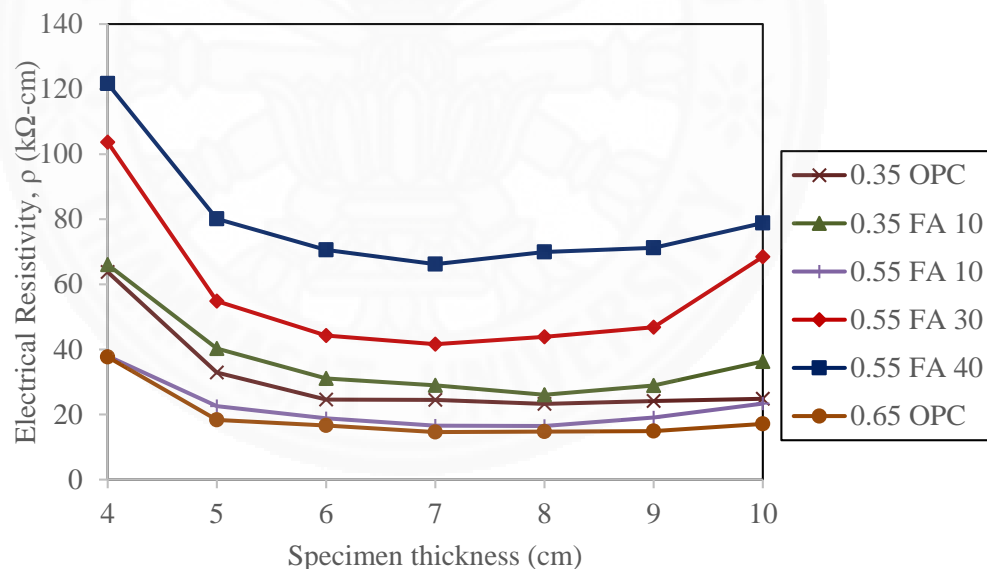


Fig 4.11 Effect of specimen thickness on electrical resistivity of concrete

#### 4.2.7 Curing condition

Fig. 4.12 shows effect of curing condition on the electrical resistivity of concrete. As shown in Fig. 4.12, air cured concrete has higher electrical resistivity than

water cured concrete. This is because the resistivity values of air which is  $1.3 \times 10^{15}$  to  $3.30 \times 10^{15}$  ( $k\Omega\text{-cm}$ ) is higher than that of the water which is 2 to  $2 \times 10^2$  ( $k\Omega\text{-cm}$ ). Based on the test results, in air dry condition, the air-cured concrete has approximately 70% higher resistivity than water cured at 91 days.

With the progress of cement hydration, water permeability values decrease rapidly because the gross volume of gel increases, so the gel gradually fills some of the original water filled spaces (Neville, 2011).

Electrical resistivity of concrete largely depends on the properties of microstructure, such as pore size distribution and the shape of the interconnections, conductivity of pore fluid, degree of saturation, and temperature. Change in the degree of saturation varies the amount of fluid in the pore network. In concrete, the current is carried by ions dissolved in the pore liquid. Resistivity is increased at lower w/b ratio and longer curing periods in constant moisture content. Electrical resistivity largely depends on the moisture content of concrete.

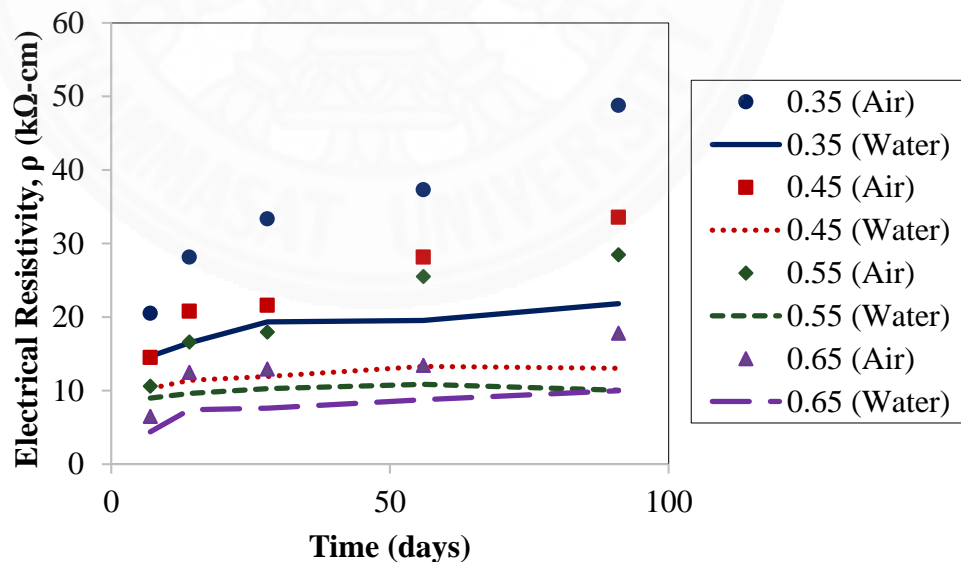


Fig 4.12 Effect of curing condition on electrical resistivity of concrete.

### **4.3 Relationship between Electrical Resistivity and Concrete Properties**

#### **4.3.1 Relationship between Electrical Resistivity and Compressive Strength Test**

As shown in Fig. 4.13, both electrical resistivity and compressive strength of concrete increase with lower w/b ratio and age of concrete as a result of decreasing of pore space and increasing amount of hydration products. Electrical resistivity increased with the increases of compressive strength. Concrete with higher w/b ratio has lower strength and electrical resistivity due to larger amount of saturated capillary pores in the paste. The larger quantity of capillary pores results in lower density and lower strength of the paste. As shown in Fig. 4.14, higher paste content have larger amount of pore that leads to decrease of both electrical resistivity and compressive strength in case of high cement paste content concrete.

As shown in Fig. 4.15, 40 % fly ash replacement increase when compared to that of OPC concrete, the compressive strength by 8% where the electrical resistivity was increased by up to 75% at 91 days. As shown in Fig. 4.15, at very low w/b, pores are already disconnected so the effect of fly ash replacement of 10% is not significant on both electrical resistivity and compressive strength. On the other hand, 10% replacement fly ash more significantly increases electrical resistivity at higher w/b ratio 0.55. Fig. 4.16 shows that 40% fly ash replacement increases when compared to that of OPC concrete, the compressive strength by 20% where the electrical resistivity was increased by up to 85% at 91 days. For fly ash concrete, strength at early ages is generally lower than that of the cement only concrete but higher in long term. Therefore, the relation with age in fly ash concrete is different from that of the OPC concrete.

A good correlation of electrical resistivity and compressive strength of concrete in water-cured condition was observed as shown in Fig. 4.17. The curing condition also plays an important role in the electrical resistivity, since the mobility of ions in the pores solution is largely affected. Both electrical resistivity and compressive strength are influenced by the concrete porosity.

Based on the results as shown in Fig. 4.18, air cured specimen showed higher electrical resistivity than that of water- cured specimen, even though the strength was lower at the same testing age. As shown in Figure 4.18, correlation between electrical resistivity and compressive strength of concrete in air-cured condition is obtained. However, the correlation for the air-cured condition is more scattered than that of the water-cured condition. This may due to difficulties of measuring the electrical resistivity of dry specimen.

Moisture needs to be provided before measuring the electrical resistivity. It can be seen in Fig. 4.17 and 4.18 that the relations were not linear because the surface resistivity is more influenced by the pore system than compressive strength. The concrete electrical resistivity highly depends on the moisture content. Increasing of moisture content will result in decreasing the electrical resistivity. Higher compressive strength of concrete is due to the increased of cement hydration that supports the growth of (C-S-H) gels. For hydration to proceed, (C-S-H) gels must be saturated with water. Therefore, compressive strength of water cured is higher than air-cured concrete.

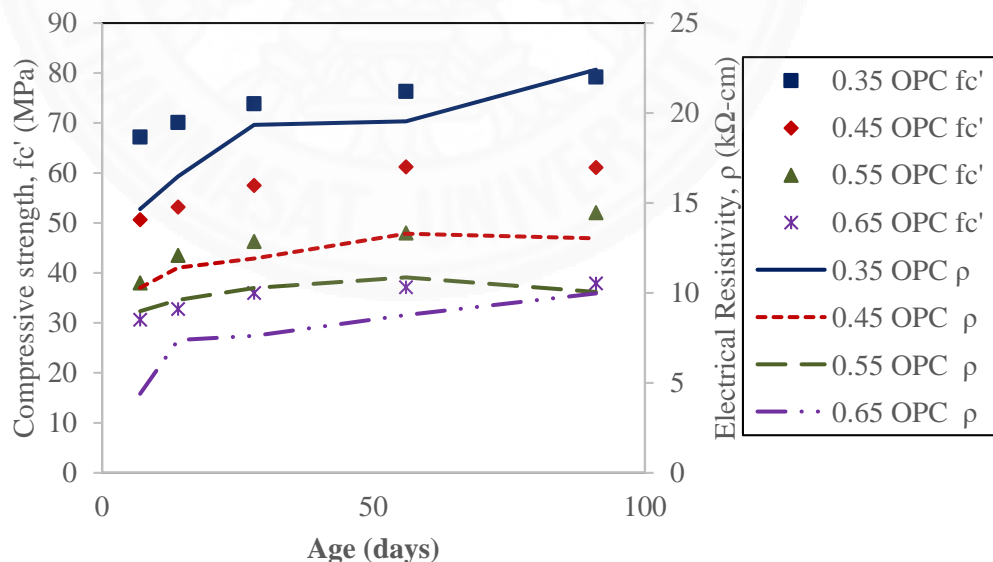


Fig 4.13 Relationship between electrical resistivity and compressive strength with different w/b ratios at water cured condition.

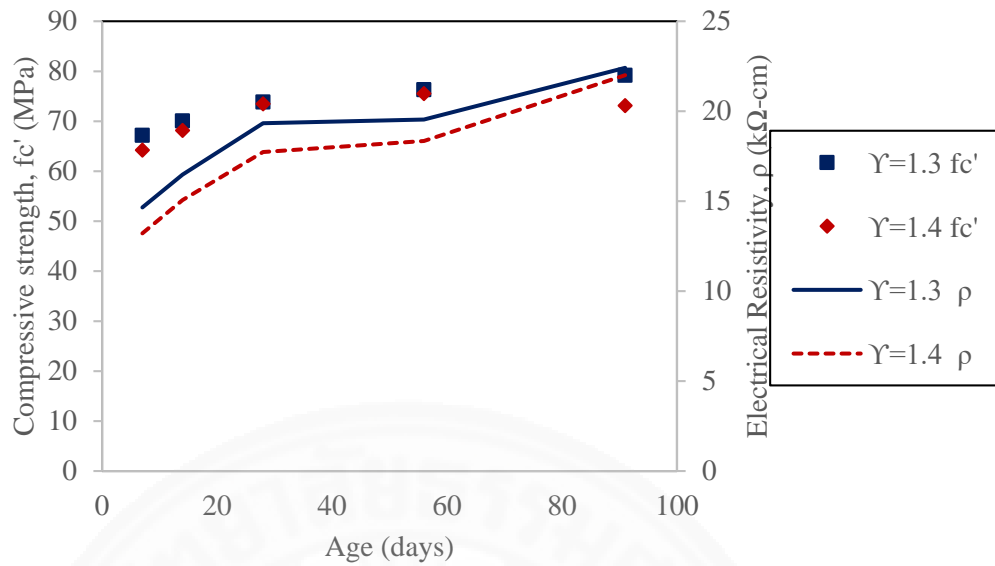


Fig 4.14 Relationship between electrical resistivity and compressive strength with different ratio of cement paste content of concrete to void content between aggregate at water cured condition.

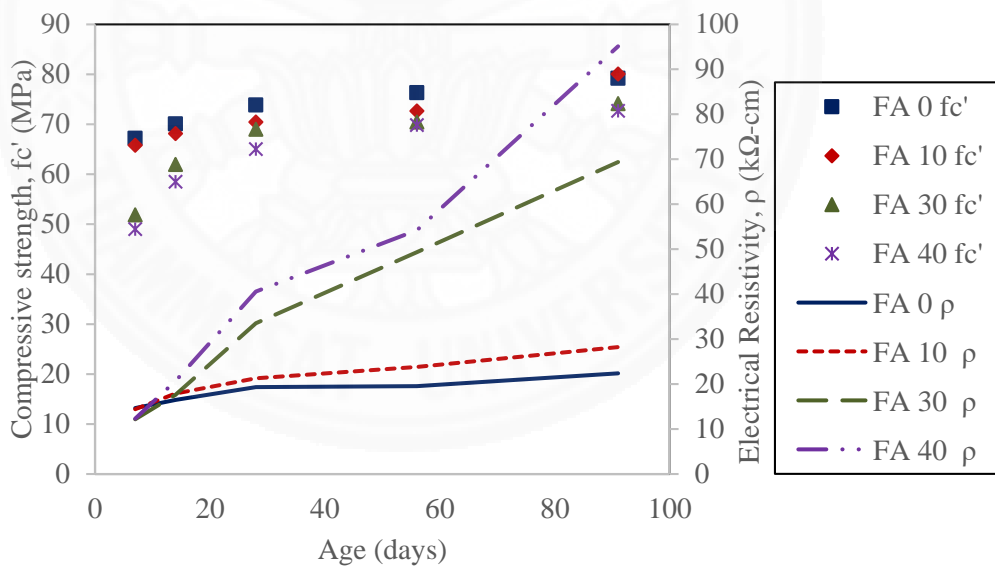


Fig 4.15 Relationship between electrical resistivity and compressive strength with different fly ash content by w/b 0.35 at water cured condition.

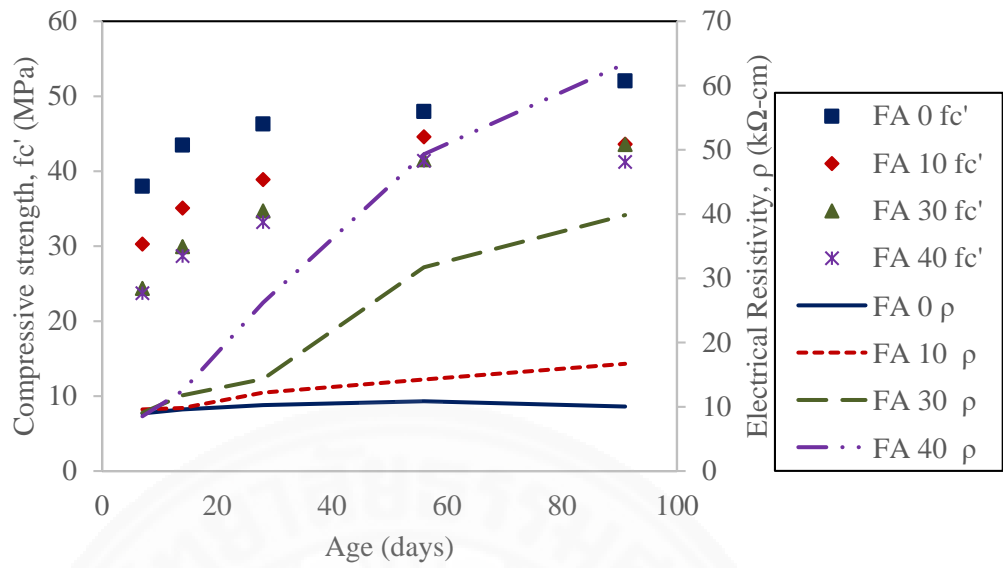


Fig 4.16 Relationship between electrical resistivity and compressive strength with different fly ash content by w/b 0.55 at water cured condition.

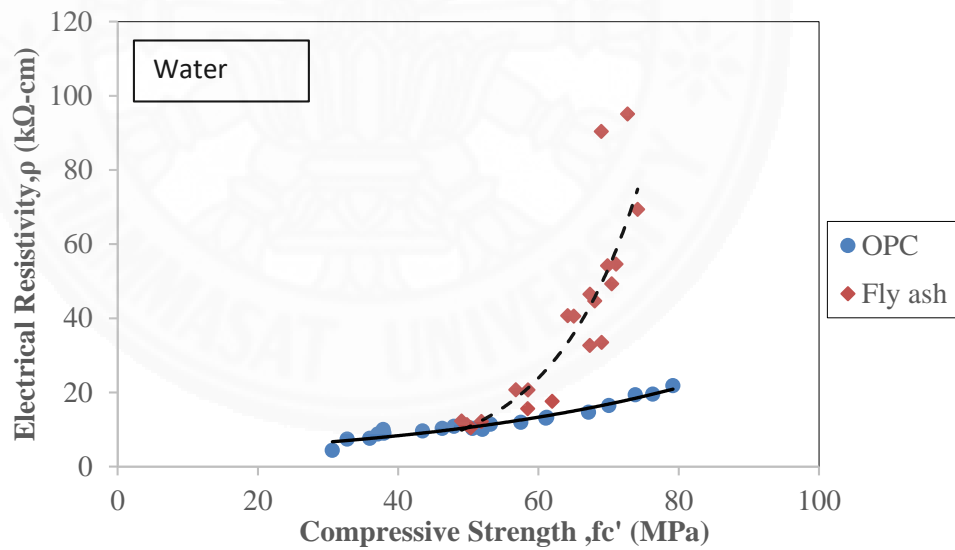


Fig 4.17 Relationship between electrical resistivity and compressive strength in water cured condition.

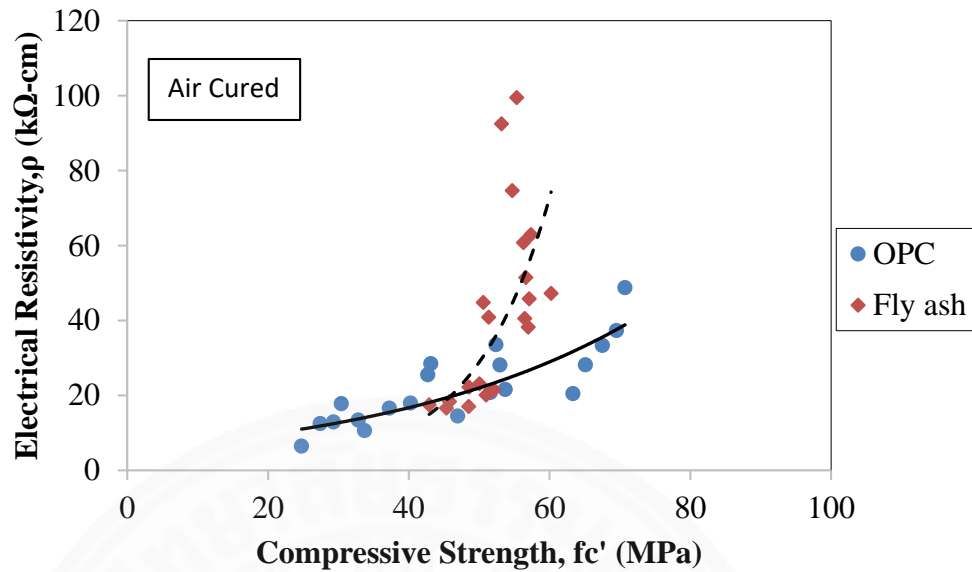


Fig 4.18 Relationship between electrical resistivity and compressive strength in air cured condition.

#### 4.3.2 Relationship between Electrical Resistivity and Rapid Chloride Penetration (RCPT) of concrete

Fig. 4.19 shows the relationship between electrical resistivity and rapid chloride penetration of concrete. Fig 4.19 presents results from all concrete mix proportions at the age of 91 days. Resistivity is mainly related to rapid chloride penetration by the densification of pore structure.

When electrical resistivity is increased, charge passed is significantly reduced. The amount of charge passed is mainly controlled by pore structure, similarly to the electrical resistivity. Both w/b ratio reduction and fly ash replacement can be considered as resulting to a refinement of pore structure. Electrical resistivity test is easy to use especially on site, fast and an accurately repeatable test of which a strong correlation with rapid chloride permeability can be obtained. Table 4.2 shows the relationship between electrical resistivity and rapid chloride penetration of concrete obtained by (Rupnow & Icenogle, 2012) and this study. It was observed that other results underestimate RCPT of concrete in Thailand. When compared the values of electrical resistivity with authors results and AASHTO TP 95, authors's electrical resistivity

values are lower than AASHTO. AASHTO tested included field and laboratory prepared samples. Therefore, the effect of local materials properties should be considered.

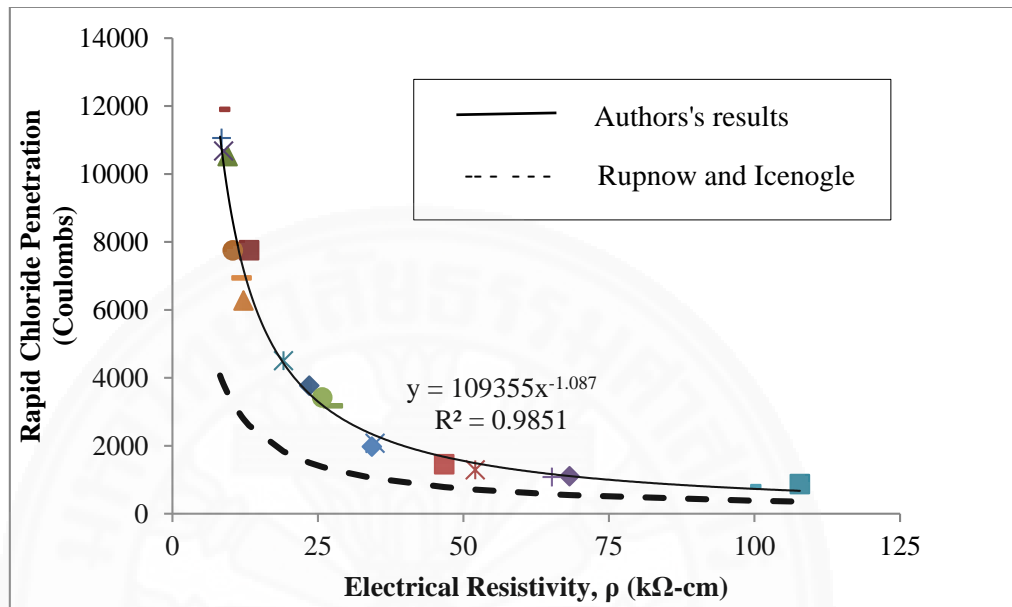


Fig 4.19 Relationship between electrical resistivity and rapid chloride permeability of concrete

Table 4.2 Relationship between electrical resistivity and rapid chloride penetration of concrete

ASTM C1202/ AASHTO T277		AASHTO TP95	Rupnow and Icenogle	Author's result
	RCP Test Charge passed (coulombs)	Electrical resistivity Test ( $k\Omega\text{-cm}$ )	Electrical resistivity Test ( $k\Omega\text{-cm}$ )	Electrical resistivity Test ( $k\Omega\text{-cm}$ )
High	>4,000	<12	-	<20
Moderate	2,000- 4,000	12-21	10-25	20-35
Low	1,000- 2,000	21 -37	25-40	35-55
Very Low	100- 1,000	37-254	40-80	55-110
Negligible	<100	>254	-	-

#### 4.3.3 Relationship between Electrical Resistivity and Moisture Weight Loss of Concrete

Figs. 4.20 – 4.22 show the relationship between electrical resistivity and moisture weight loss of concrete with different concrete mix proportion. As shown in Figs. 4.20-4.22, electrical resistivity and moisture weight loss are directly proportional to each other. Although electrical resistivity of concrete increases in low w/b ratios, moisture weight loss decrease as shown in Fig. 4.20. Moisture content is one of the most significant factors affecting on the electrical resistivity of concrete. This is because the pore water carries a substantial proportion of electrical current passing through concrete. Evidently, higher moisture content causes easier electrical flow and hence, the electrical resistivity reduces. As shown in Fig. 4.21, weight loss is lower when replacing higher fly ash content because pore is very dense in fly ash. But increasing in electrical resistivity that is due to the less amount of pore water to carry the current, when the moisture content of concrete decreases. Electrical resistivity of concrete

increases in low cement paste content but moisture weight loss is not significantly affected as shown in Fig. 4.22.

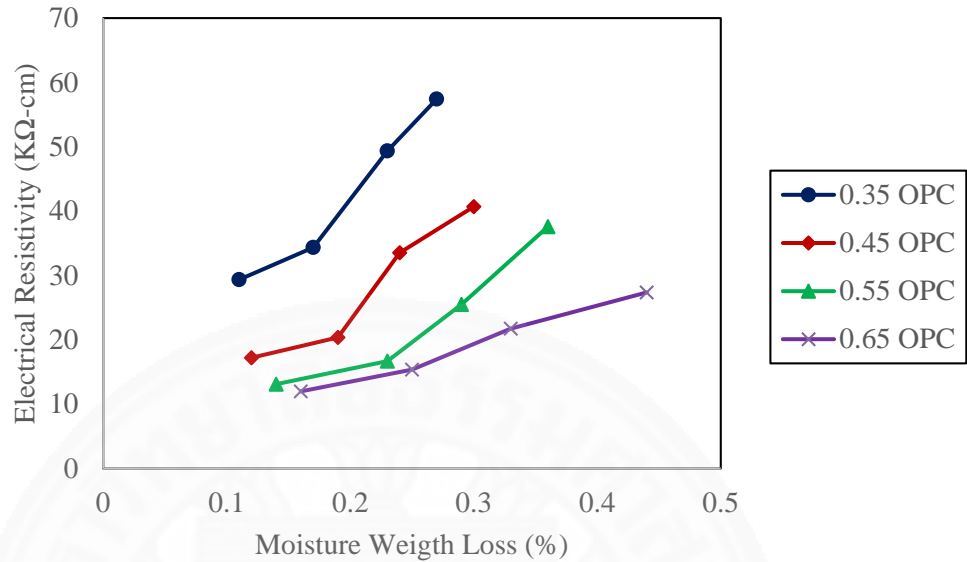


Fig 4.20 Relationship between electrical resistivity and moisture weight loss with different w/b ratios.

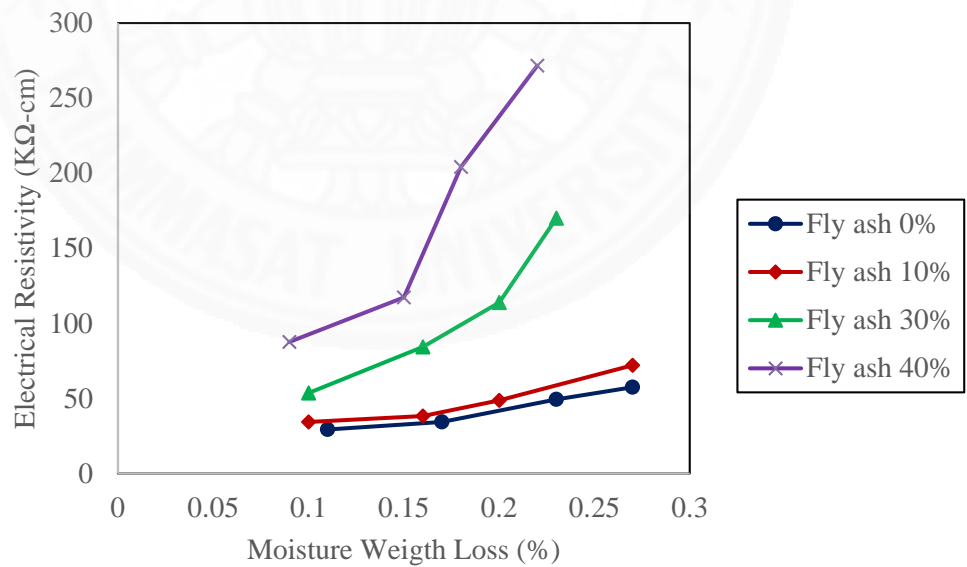


Fig 4.21 Relationship between electrical resistivity and moisture weight loss with different fly ash content at w/b 0.35

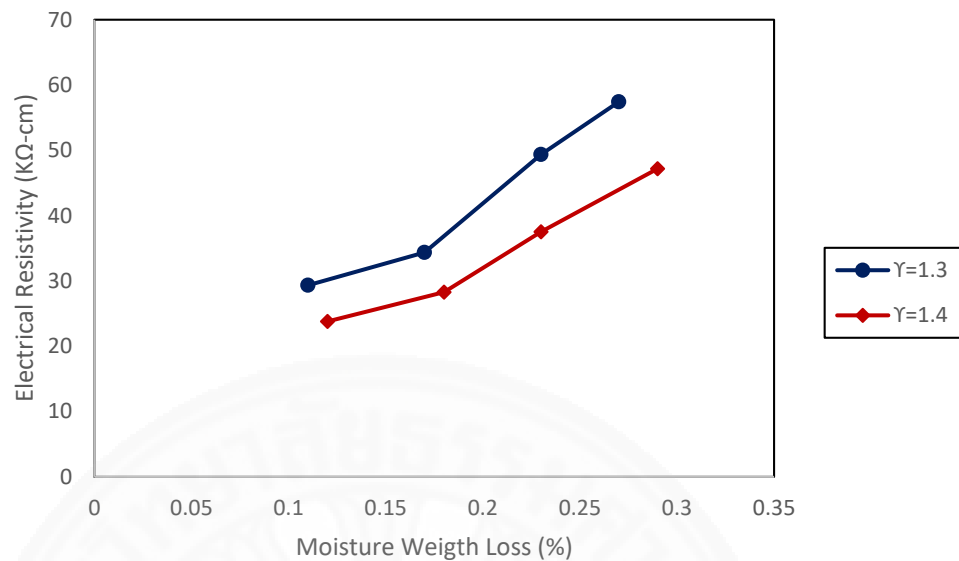


Fig 4.22 Relationship between electrical resistivity and moisture weight loss of concrete with different ratios of cement paste content of concrete to void content between aggregate at w/b 0.35.

#### 4.3.4 Relationship between Electrical Resistivity and Carbonation Depth of Concrete

Specimens were tested for electrical resistivity then kept in carbonation chamber for 1 and 2 months. Fig. 4.23 points out that lower w/b ratios causes lower carbonation depth because of the pore structure densification that causes increasing electrical resistivity. Concrete electrical resistivity increases with the increase of carbonation time. Figs. 4.24 and 4.25 demonstrate that the increase of fly ash content, the carbonation depth increases. When the large amount of fly ash content is used, the effect of the consumption of calcium hydroxide (CH), by pozzolanic reaction of fly ash and decrease cement content reduce the alkalinity of the concrete. Fly ash delays the hydration and increases the total porosity of the concrete at the same w/b ratio. Fly ash can significantly reduce porosity of the concrete and increasing the electrical resistivity of carbonated concrete by pozzolanic reaction and pore refinery property. As shown in Fig. 4.26, carbonation depth increased by lower volume of cement paste or aggregate. But volume of cement paste or aggregate slightly affects the carbonation resistance of

concrete. Fig. 4.27 shows relationship between electrical resistivity and carbonation coefficient of concrete with different FA content (10%, 30%, 40%). When concrete is denser, electrical resistivity is higher. In this study, carbonation coefficient is higher as fly ash content increases. Based on this result electrical resistivity is not appropriate to evaluate carbonation resistance.

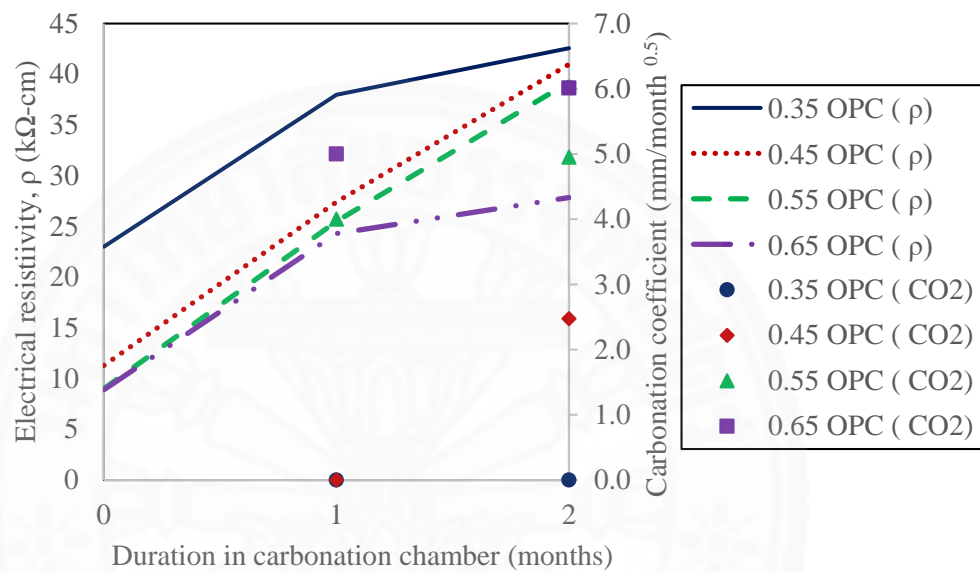


Fig 4.23 Effect of carbonation time on electrical resistivity of concrete with different w/b ratios

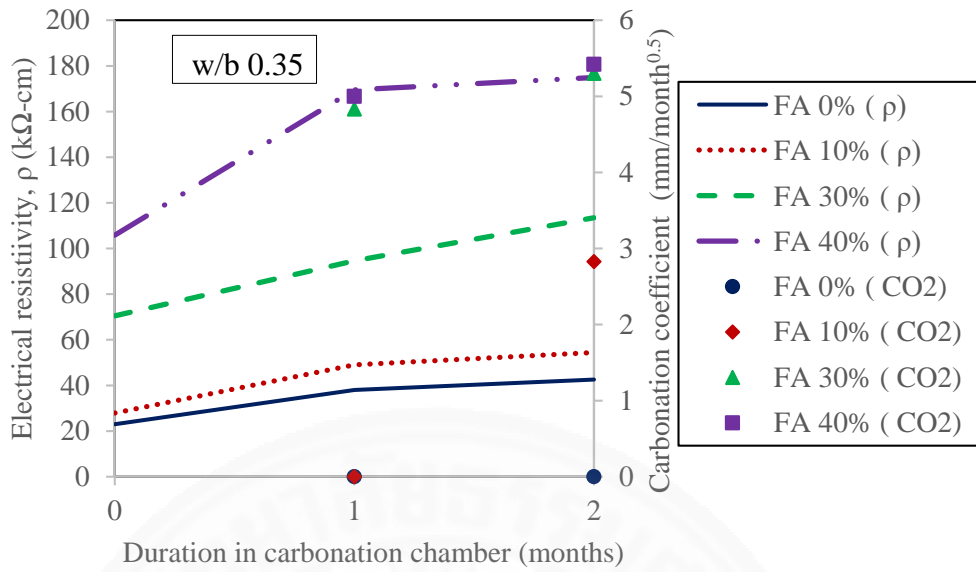


Fig 4.24 Effect of carbonation time on electrical resistivity of concrete with different fly ash content at w/b 0.35

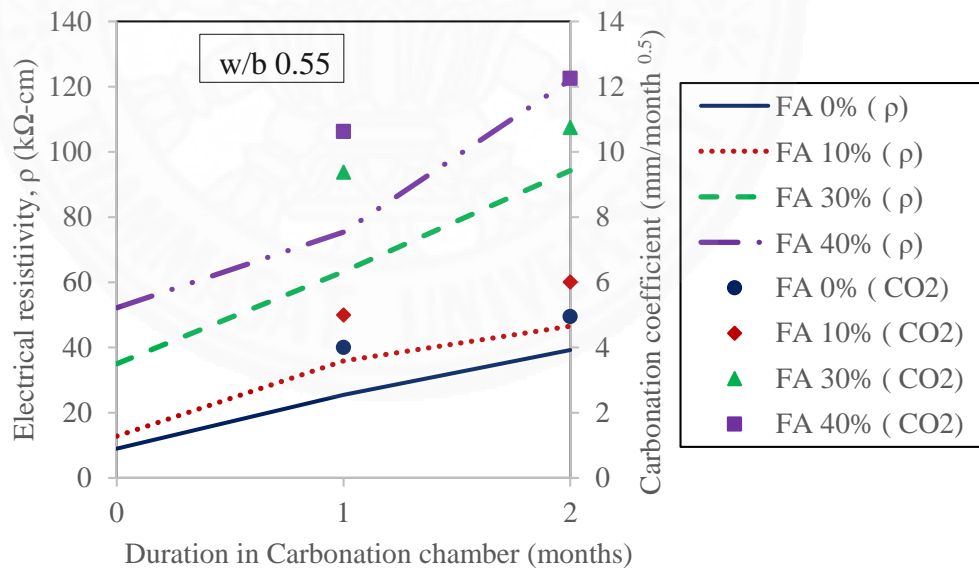


Fig 4.25 Effect of carbonation time on electrical resistivity of concrete with different fly ash content at w/b 0.55

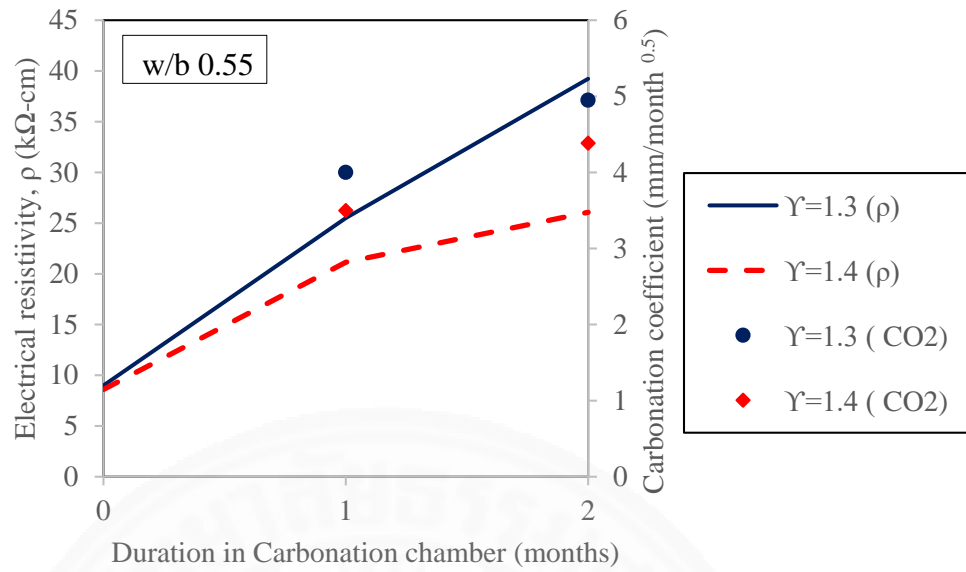


Fig 4.26 Effect of carbonation time on electrical resistivity of concrete with different cement paste content at w/b 0.55

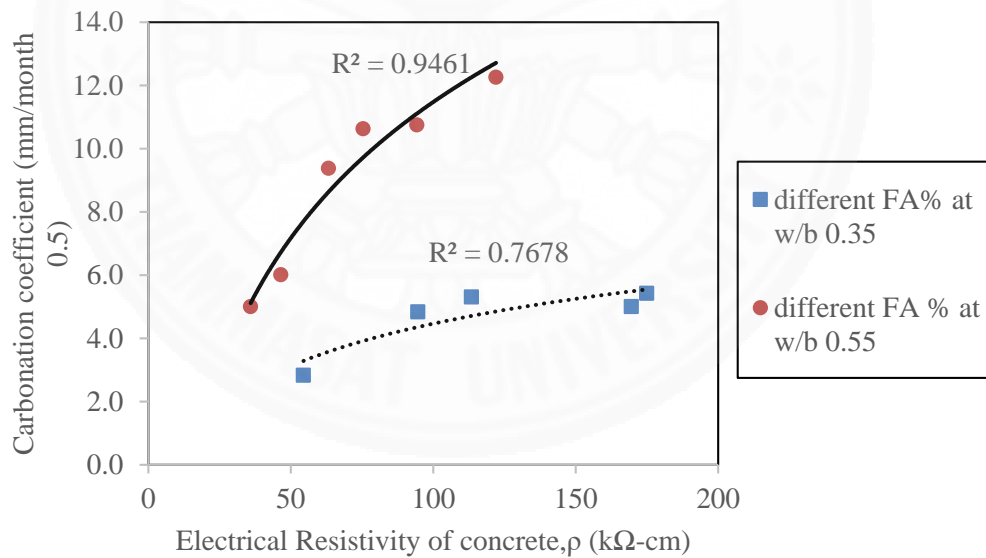


Fig. 4.27 Relationship between electrical resistivity and carbonation coefficient of concrete with different FA content (10%, 30%, 40%)

#### **4.4 Prediction Model of the Electrical Resistivity**

In this section, four different model to predict electrical resistivity of concrete. Authors are proposed equations (4.2) and (4.3) to predict the electrical for new construction based on concrete mix proportion under good curing condition. The proposed model equation (4.4) to predict electrical resistivity in case of curing problem affecting hydration degree of concrete. If have compressive strength results, equation (4.5) can be used to predict electrical resistivity in case compressive strength of concrete is known. The details of each model is explained below.

##### **4.4.1 Prediction Model of Electrical Resistivity based on mix proportions**

The electrical resistivity of concrete was modeled as a function of concrete mix proportions based on the test results in this study by the equations (4.2) and (4.3). The prediction equation for low w/b ratios ranging from 0.35 to 0.45 is shown in Equation (4.2). That for the water to binder ratio ranging from 0.45 to 0.65 is shown in Equation (4.3). This model is proposed to predict electrical resistivity if already have mix proportion. Water to binder ratio, fly ash content, cement paste content and age are considered as parameters to predict the electrical resistivity as shown in Equations (4.2) and (4.3).

The comparison between tested and predicted results is shown in Figs. 4.28 – 4.30. As shown in Fig. 4.28, early age electrical resistivity of fly ash concrete is very small when compared to OPC concrete because pozzolanic reaction is very slow. It is seen from Fig. 4.28 that low electrical resistivity values are not quite well predicted but the prediction for electrical resistivity of concrete can be made with a possible error of  $\pm 20\%$ .

As shown in Figs. 4.29 and 4.30, electrical resistivity of concrete increases with age. Increase in w/b leads to an increase in porosity of concrete, and higher w/b is associated with larger pore size in cement paste. When replacement of fly ash is increased, electrical resistivity of concrete is also increased. Water to binder ratio and

paste content are inversely proportional to the electrical resistivity of concrete. As shown in Fig. 4.28, comparison of tested and predicted values of electrical resistivity are in good accuracy with  $R^2=0.9776$ . Equations (4.2) and (4.3) may be used to predict the electrical for new construction.

$$(w/b < 0.45) \rho = \{29.1594 + [23.729 + (fa^{1.5254})] * \frac{[0.0004*(t^{0.9035})]}{[(\frac{w}{b})^{3.0734}]+(\gamma*(-16.3335))}\} \quad (4.2)$$

$$(w/b \geq 0.45) \rho = \{38.6768 + [141.6688 + (fa^{1.9143})] * \frac{[-4.2243+(t^{0.7287})]}{[(\frac{w}{b})^{-5.6273}]+(\gamma*(-18.2861))}\} \quad (4.3)$$

Where,  $\rho$  is electrical resistivity of concrete ( $k\Omega\text{-cm}$ ),  $fa$  is fly ash content (%),  $t$  is age of concrete (days),  $w/b$  is water to binder ratio, and  $\gamma$  is ratio of paste content of concrete to void content between aggregate.

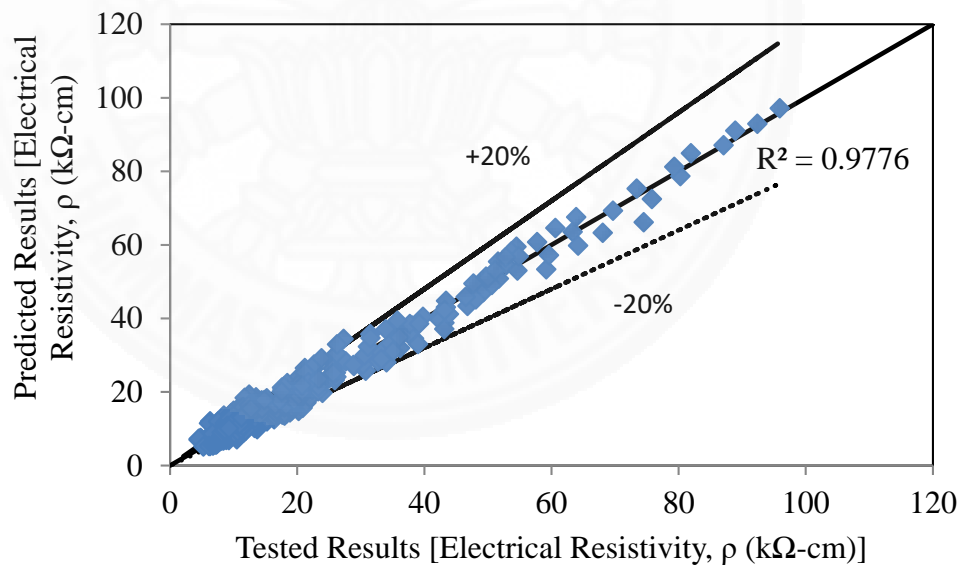


Fig 4.28 Comparison between predicted and measured results of electrical resistivity of concrete based on mix proportions

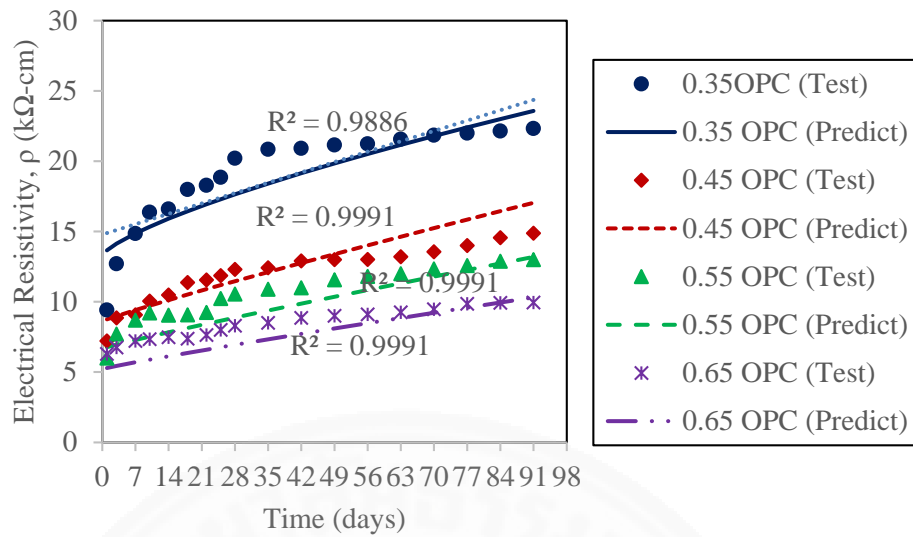


Fig 4.29 Comparison between predicted and tested results of electrical resistivity based on mix proportions (different w/b ratios)

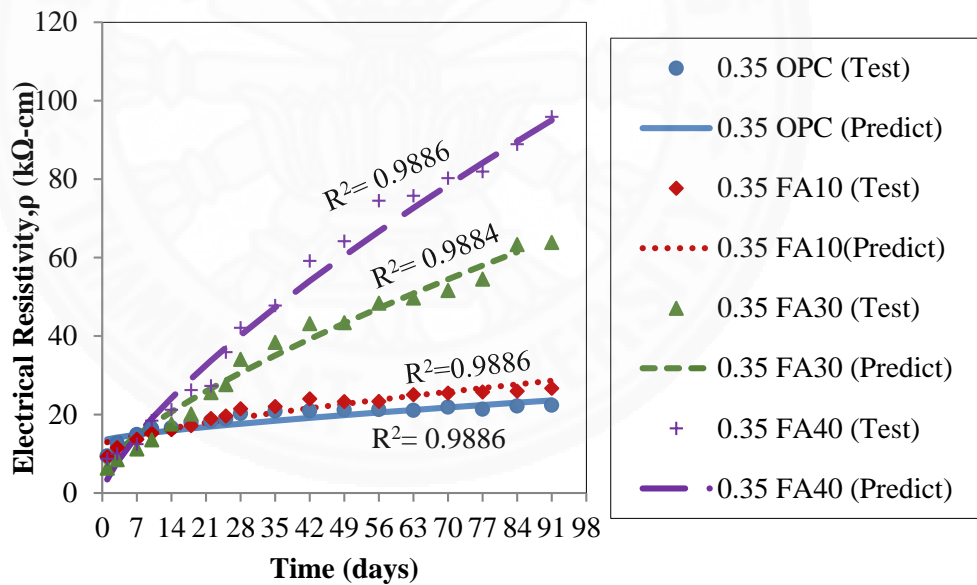


Fig 4.30 Comparison between predicted and tested results of electrical resistivity based on mix proportions (different fly ash content with w/b 0.35)

#### 4.4.2 Prediction Model of Electrical Resistivity based on mix proportions and hydration degree

In Equation (4.4), water to binder ratio, different fly ash content, cement paste content and hydration degree are used as parameters. To calculate hydration degree, the parameters such as concrete mix proportion and time are required. The proposed model can be used in case of curing problem. The hydration degree was predicted from previous study carried out by Saengsoy and Tangtermsirikul (2003). It is seen from Fig. 4.31 that some electrical resistivity values are not well predicted but the overall prediction for electrical resistivity of concrete can be satisfied with  $R^2= 0.9621$  and a possible error of  $\pm 20\%$ .

The comparison between tested and predicted results is shown in Fig. 4.32. As shown in Fig. 4.32, electrical resistivity of concrete increases with hydration degree. Predicted and tested results have satisfactory correlation. Through the prediction using degree of hydration instead of age is quite accurate, the equation is not quite predicted for being used since the degree of hydration remains the information on mix proportion, age and temperature history.

$$\rho = \left\{ 7.379 + \frac{[1.579 + \exp(fa * 0.143)]}{[1848.136 * (\frac{w}{b * 6.521}) * (\gamma * 1848.137)]} \right\} * [-964.208 + \exp(Hy_{deg} * 0.115)] \quad (4.4)$$

Where,  $\rho$  is electrical resistivity of concrete ( $k\Omega\text{-cm}$ ),  $fa$  is fly ash content (%),  $Hy_{deg}$  is hydration degree (%),  $w/b$  is water to binder ratio, and  $\gamma$  is ratio of paste content of concrete to void content between aggregate.

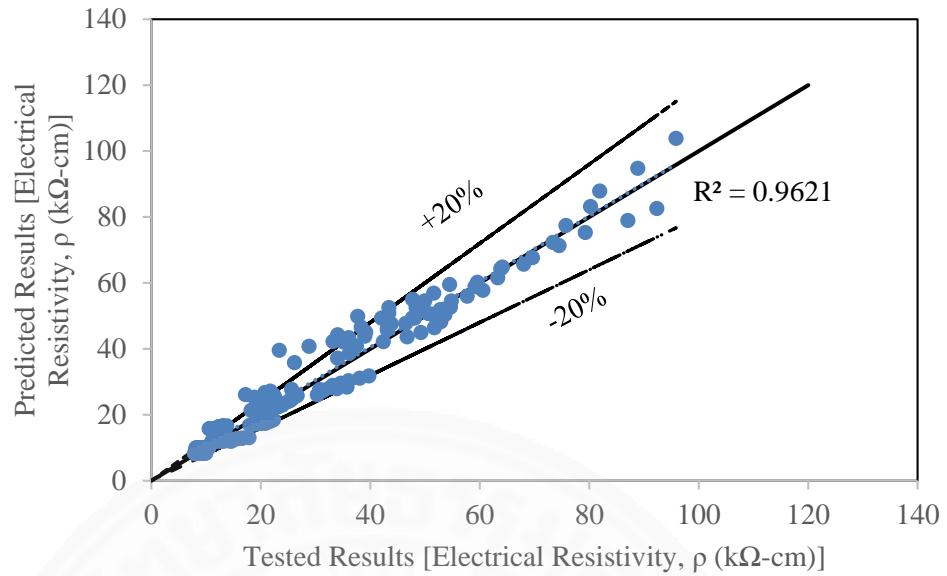


Fig. 4.31 Comparison between predicted and measured results of electrical resistivity of concrete based on mix proportions and hydration degree.

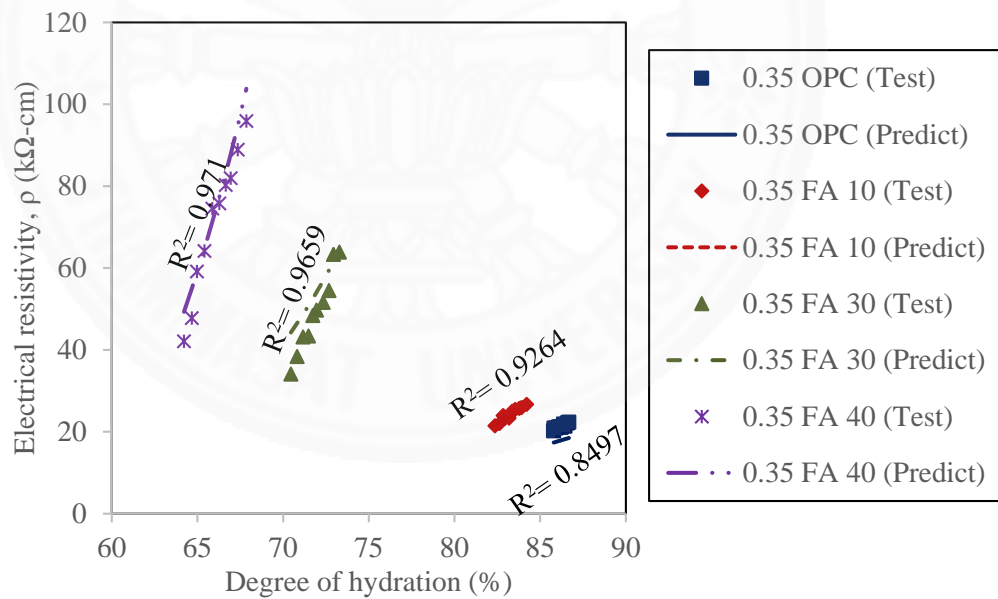


Fig 4.32 Comparison between predicted and tested results of electrical resistivity based on mix proportions and hydration degree (different fly as content with w/b 0.35)

#### 4.4.3 Prediction Model of Electrical Resistivity based on Compressive Strength

In this study, the relationship between electrical resistivity and compressive strength is obtained based on the test results and it is indicated in Equation (4.5). If have compressive strength, the following equation can use to predict electrical resistivity instead of hydration degree. Different fly ash content, cement paste content and age were considered as parameters due to their significantly effects on both properties. A good correlation is obtained between predictions and tested results as shown in Fig. 4.33. The predictions show reasonable accuracy when compared to the test results as shown in Fig. 4.33 and good for in situ evaluation.

It is observed in Fig. 4.34 and Fig. 4.35 that the compressive strength is directly proportional to the electrical resistivity. It is clearly seen that the electrical resistivity increases with the increase of compressive strength. Moreover, specimens with higher replacements of fly ash show exponential increment of electrical resistivity at higher compressive strength values. Therefore, the effect of fly ash content needs to be considered for model formulation.

$$\rho = \{[0.053878 * \exp(fa * 0.065482)] * t\} + [1.886987 * \exp(f'_c * 0.031254)] \quad (4.5)$$

Where,  $\rho$  is electrical resistivity of concrete (k $\Omega$ -cm),  $fa$  is fly ash content (%),  $t$  is age of concrete (days), , and  $f'_c$  is compressive strength.

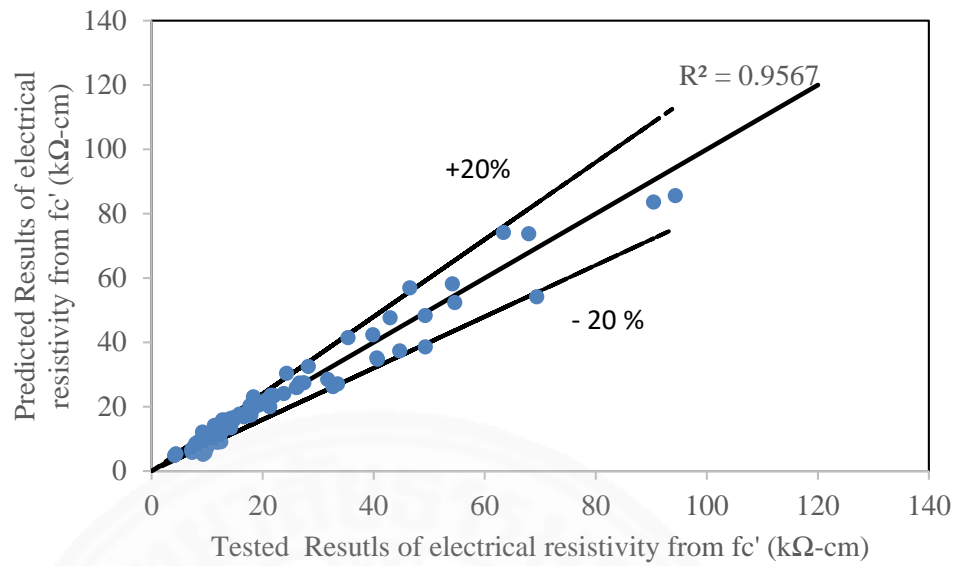


Fig.4.33 Comparison between tested and predicted results of electrical resistivity based on mix proportions and compressive strength

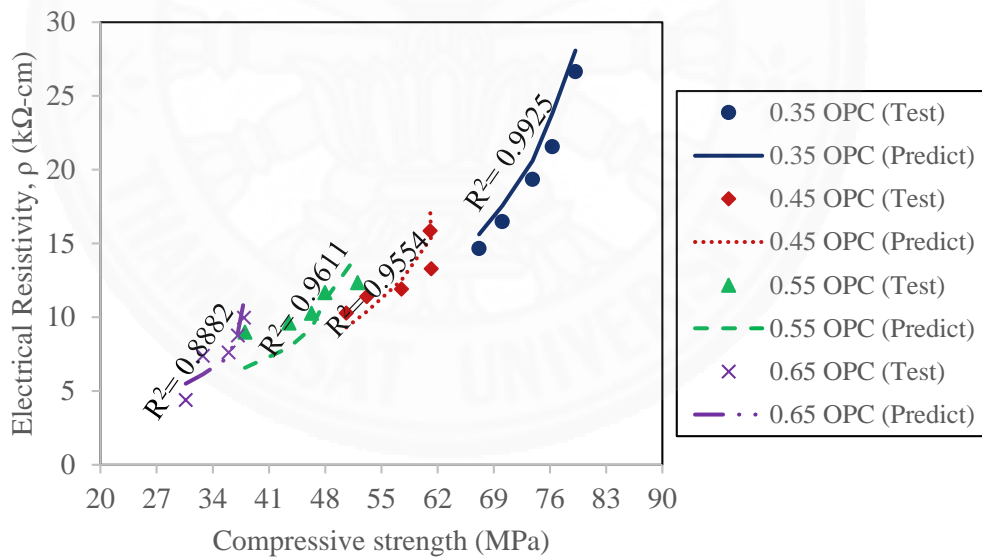


Fig.4.34. Comparison between tested and predicted results of electrical resistivity and compressive strength (different w/b ratios)

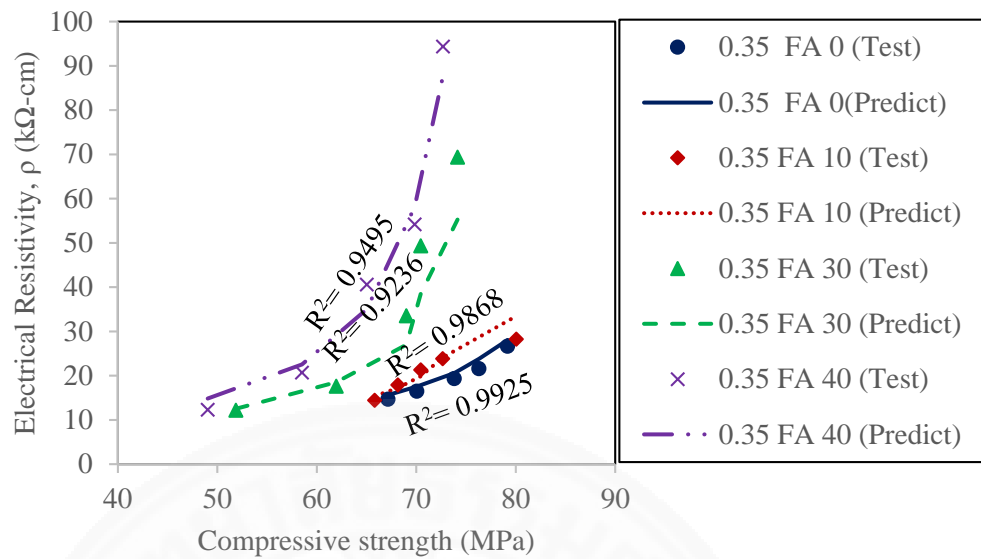


Fig.4.35. Comparison between tested and predicted results of electrical resistivity and compressive strength (different fly ash content at w/b 0.35)

#### 4.4.4 Prediction Model of Rapid Chloride Penetration based on Electrical Resistivity

Equation for Rapid Chloride Penetration based on electrical resistivity is shown in Equation 4.6. A good correlation was obtained with  $R^2=0.9851$  as shown in Fig. 4.36.

$$RCPT = 109335\rho^{-1.087} \quad (4.6)$$

Where RCPT is rapid chloride penetration test (Coulombs),  $\rho$  is electrical resistivity ( $k\Omega\text{-cm}$ ).

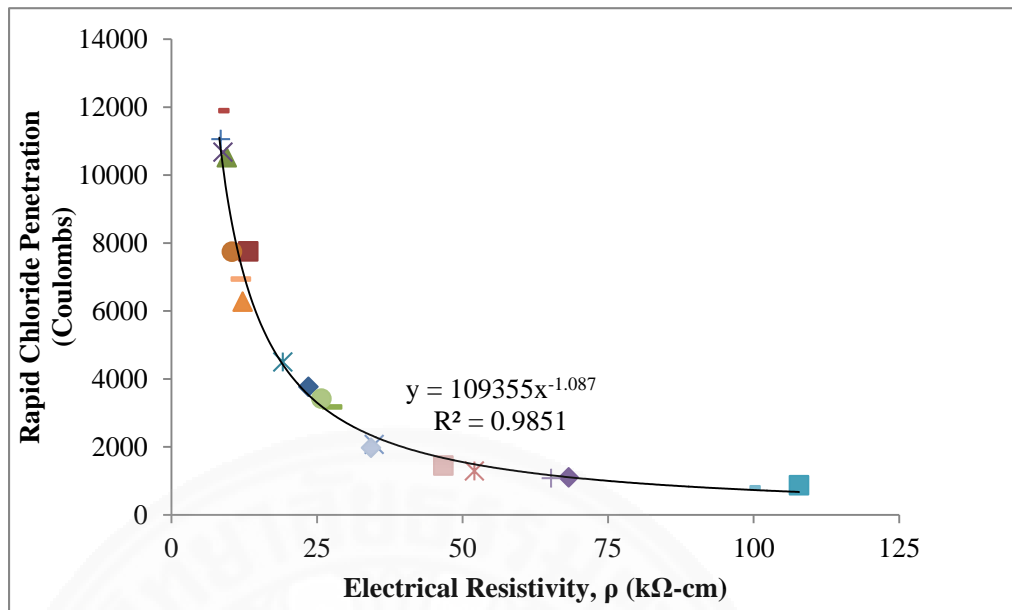


Fig 4.36 Prediction model of Rapid Chloride Penetration based on electrical resistivity.

## Chapter 5

### Conclusions and Recommendations for Future Studies

#### 5.1 Conclusions

The mix proportions of concrete significantly affect the electrical resistivity of concrete. There are good relationship of some concrete properties with electrical resistivity such as compressive strength and rapid chloride penetration test. Equations were proposed to estimate electrical resistivity of concrete based on mix proportions and other concrete properties. Based on the experimental and the predicted results, the formulation and the verification of the electrical resistivity estimations, the following conclusions can be drawn.

1. Electrical resistivity of concrete increases with the decrease of w/b ratios, ratio of paste content of concrete to void content between aggregate and increase in fly ash content. Lower water to binder ratio concrete shows higher electrical resistivity than those with high water to binder ratio (0.55 and 0.65). This is because of amount of interconnected pores decrease as the w/b ratio decreases. However, electrical resistivity did not change when only a small amount of fly ash is used in concrete. When fly ash was used to replace cement at 30% and 40%, the concentration of hydroxyl ions was reduced, and pore size was finer than OPC concrete, so electrical resistivity rate was obviously increased. Increase in aggregate content and reduction in cement paste for a given volume results in higher electrical resistivity values mainly because of the replacing of the porous hardened cement paste with denser aggregates.

2. Specimen geometry also affects on electrical resistivity of concrete. Electrical resistivity values measured from the cubic specimens are higher than those of the cylindrical specimens. Electrical resistivity and area of specimen are directly proportional to each other. In this study, sectional area of cubic specimen is larger than cylindrical specimen. That may be the main reason that the measured electrical resistivity of cubic specimen is higher than that of the cylindrical specimen.

3. Environmental factors also affect electrical resistivity of concrete. Air-cured concrete has higher electrical resistivity than the water cured ones. When specimens are cured in water, they have better electrical connection and therefore result in lower concrete resistivity values. And also the resistivity values of air is higher than water. Higher moisture content causes easier electrical flow and hence, the electrical resistivity reduces.

4. Electrical resistivity and properties of concrete such as compressive strength, rapid chloride permeability and carbonation depth test have good correlations.

5. Electrical resistivity increases with the increase of compressive strength. Both electrical resistivity and compressive strength are influenced by the concrete porosity. A good correlation was obtained electrical resistivity and compressive strength. The relations were not linear because the surface resistivity is more influenced by the factors of pore system and moisture content than compressive strength. Based on the results, 40% fly ash replacement increased the compressive strength by 20% where the electrical resistivity increased up to 85% at 91 days. For fly ash concrete, strength at early ages is generally lower than that of the cement only concrete but higher in long term. Therefore, the relation with age in fly ash concrete is different from that of the OPC concrete.

6. A good relationship between electrical resistivity and rapid chloride permeability of concrete was obtained when electrical resistivity increases, charge passed is significantly reduced. The amount of charge passed is mainly controlled by pore structure, similarly to the electrical resistivity. Electrical resistivity test is easy to use, fast and an accurately repeatable test of which a strong correlation with rapid chloride permeability can be obtained.

7. Electrical resistivity and carbonation depth of concrete also have a relation. Electrical resistivity increases with an increase of carbonation time due to decrease of porosity and sorptivity of carbonated concrete.

8. The prediction of electrical resistivity of concrete was modelled as a function of concrete mix proportions such as w/b ratio, fly ash content, ratio of cement paste content to void content between aggregate based on the test results. Electrical resistivity of concrete increases with age. In early age, resistivity of fly ash concrete is very small compared to OPC concrete because pozzolanic reaction is very slow. When replacement of fly ash is increased, electrical resistivity of concrete is also increased. Water to binder ratio and paste content are inversely proportional to the electrical resistivity of concrete. The model simulations showed sufficient accuracy in predicting the test results of concrete specimens with different water to binder ratios, fly ash content, cement paste content, and age of concrete.

9. A good correlation is obtained between predicted and tested results of electrical resistivity and compressive strength. Different fly ash content, cement paste content and age were considered as parameters due to their significantly effects on both results. It is observed that the compressive strength is directly proportional to the electrical resistivity. The model predictions showed reasonable accuracy when compared to the test results.

10. A good correlation was obtained from the predicted results of electrical resistivity based on concrete mix proportions and hydration degree. The electrical resistivity of concrete increases with age that reflects decreasing of pore space and increasing of hydration products.

## 5.2 Recommendations for Future Study

1. The proposed electrical resistivity simulation model is predicted within the limits of fly ash replacement from 10 to 30%, water to binder ratio from 0.35 to 0.65, and ratio of paste content of concrete to void content between aggregate from 1.3 to 1.4 and water cured condition. The prediction range of these parameters can be further enhanced.

2. The model need to consider other factors such as aggregate type and size, and other environmental factors such as reinforcing steel, coating, temperature and surface moisture conditions.

3. Moreover, the proposed model is necessary to apply to in-situ measurement to compare and check with the tested results in the laboratory in this study.

4. The verification of the proposed electrical resistivity simulation model was proved to be satisfactory. This prediction model can be applied to design sacrificial anode protection system in the further.

## References

- AASHTO TP95-11, (2011). Standard Test Method for Surface Resistivity of Concrete's Ability to Resist Chloride Ion Penetration.
- Addis, B., (2008). Fundamentals of concrete. Midrand: Cement and Concrete Institute, p.58.
- Ahmad, S. (2003). Reinforcement corrosion in concrete structures, its monitoring and service life prediction - A review. *Cement and Concrete Composites*, 25(4–5 SPEC), 459–471. [https://doi.org/10.1016/S0958-9465\(02\)00086-0](https://doi.org/10.1016/S0958-9465(02)00086-0)
- Andrade, C., & Andrea, R. (2010). Electrical resistivity as microstructural parameter for modelling of service life of reinforced concrete structures. *2nd International Symposium on Service Life Design for Infrastructure, Delft, Netherlands*, (October), 379–388.
- ASTM C1202. (2012). Standard Test Method for Electrical Indication of Concrete's Ability to Resist Chloride Ion Penetration. *American Society for Testing and Materials.*, (C), 1–8. <https://doi.org/10.1520/C1202-12.2>
- Basheer, P. A. M., Rankin, G. I. B., Long, A. E., & Russell, D. (2001). Effect of relative humidity and air permeability on prediction of the rate of carbonation of concrete. *Proceedings of the ICE - Structures and Buildings*, 146(3), 319–326. <https://doi.org/10.1680/stbu.2001.146.3.319>
- Bertolini, L., Elsener, B., Pedferri, P., & Polder, R. P. (2004). Properties of Cementitious Materials.
- Broomfield, J. P. (2006). *Corrosion of Steel in Concrete: Understanding, Investigation and Repair, Second Edition*. <https://doi.org/10.4324/9780203414606>
- Cabrera, J. G., & Claisse, P. a. (1990). Measurement of Chloride Penetration into Silica Fume Concrete. *Cement and Concrete Composites*, 12(3), 157–161. [https://doi.org/10.1016/0958-9465\(90\)90016-Q](https://doi.org/10.1016/0958-9465(90)90016-Q)
- Claisse, P. A., El-Sayad, H., & Shaaban, I. G. (1999). Permeability and pore volume of carbonated concrete. *ACI Materials Journal*, 96(3), 378–381. <https://doi.org/10.14359/636>
- Diamond, S. (1981). Effects of two Danish flyashes on alkali contents of pore solutions of cement-flyash pastes. *Cement and Concrete Research*, 11(3), 383–

394. [https://doi.org/10.1016/0008-8846\(81\)90110-1](https://doi.org/10.1016/0008-8846(81)90110-1)
- DURACRETE. (1999). Probabilistic Performance Based Durability Design of Concrete Structures, 86p.
- FDOT. (2004). Florida method of test for concrete resistivity as an electrical indicator of its permeability. *Florida Department of Transportation*, 4–7.
- Ghosh, P., & Tran, Q. (2015). Correlation Between Bulk and Surface Resistivity of Concrete. *International Journal of Concrete Structures and Materials*, 9(1), 119–132. <https://doi.org/10.1007/s40069-014-0094-z>
- González, J. A., Miranda, J. M., & Feliu, S. (2004). Considerations on reproducibility of potential and corrosion rate measurements in reinforced concrete. *Corrosion Science*, 46(10), 2467–2485. <https://doi.org/10.1016/j.corsci.2004.02.003>
- Gowers, K. R., & Millard, S. G. (1999). Measurement of concrete resistivity for assessment of corrosion severity of steel using wenner technique. *ACI Materials Journal*, 96(5), 536–541. <https://doi.org/10.14359/655>
- Gulikers, J., & Raupach, M. (2006). Modelling of reinforcement corrosion in concrete. *Materials and Corrosion*, 57(8), 603–604. <https://doi.org/10.1002/maco.200603899>
- Haque, M. N., & Kayyali, O. A. (1995). Free and water soluble chloride in concrete. *Cement and Concrete Research*, 25(3), 531–542. [https://doi.org/10.1016/0008-8846\(95\)00042-B](https://doi.org/10.1016/0008-8846(95)00042-B)
- Hope, B. B., Ip, A. K., & Manning, D. G. (1985). Corrosion and electrical impedance in concrete. *Cement and Concrete Research*, 15(3), 525–534. [https://doi.org/10.1016/0008-8846\(85\)90127-9](https://doi.org/10.1016/0008-8846(85)90127-9)
- Hornbostel, K., Larsen, C. K., & Geiker, M. R. (2013). Relationship between concrete resistivity and corrosion rate - A literature review. *Cement and Concrete Composites*, 39, 60–72. <https://doi.org/10.1016/j.cemconcomp.2013.03.019>
- Hunkeler, F. (1996). The resistivity of pore water solution - A decisive parameter of rebar corrosion and repair methods. *Construction and Building Materials*, 10(5 SPEC. ISS.), 381–389. [https://doi.org/10.1016/0950-0618\(95\)00029-1](https://doi.org/10.1016/0950-0618(95)00029-1)
- Kessler, R., Powers, R., Vivas, E., Paredes, M. a., & Virmani, Y. P. (2008). Surface resistivity as an indicator of concrete chloride penetration resistance. *Concrete Bridge ...*, 1–18. Retrieved from <http://concreteresistivity.com/Surface>

Resistivity.pdf

- Kobayashi, K., & Takewaka, K. (1984). Experimental studies on epoxy coated reinforcing steel for corrosion protection. *International Journal of Cement Composites and Lightweight Concrete*, 6(2), 99–116.  
[https://doi.org/10.1016/0262-5075\(84\)90039-3](https://doi.org/10.1016/0262-5075(84)90039-3)
- Liang, M. T., Wang, K. L., & Liang, C. H. (1999). Service life prediction of reinforced concrete structures. *Cement and Concrete Research*, 29(9), 1411–1418. [https://doi.org/10.1016/S0008-8846\(99\)00109-X](https://doi.org/10.1016/S0008-8846(99)00109-X)
- McCarter, W. J., Ezirim, H., & Emerson, M. (1992). Absorption of water and chloride into concrete. *Magazine of Concrete Research*, 44(158), 31–37.  
<https://doi.org/10.1680/mac.1992.44.158.31>
- McCarter, W. J., Ezirim, H., & Emerson, M. (1996). Properties of concrete in the cover zone: water penetration, sorptivity and ionic ingress. *Magazine of Concrete Research*, 48(176), 149–156.
- McNeil, J. D. (1980). Electrical conductivity of soils and rocks.
- Monfore, G. (1900). The electrical resistivity of concrete. *Concrete Structures*, 10(2), 61–64. Retrieved from <http://trid.trb.org/view.aspx?id=102173>
- Morris, W., Moreno, E. I., & Sagüés, A. A. (1996). Practical evaluation of resistivity of concrete in test cylinders using a Wenner array probe. *Cement and Concrete Research*, 26(12), 1779–1787. [https://doi.org/10.1016/S0008-8846\(96\)00175-5](https://doi.org/10.1016/S0008-8846(96)00175-5)
- Neville, A. M. (2011). *Properties of Concrete*.  
<https://doi.org/10.4135/9781412975704.n88>
- Osterminski, K., Schießl, P., Volkwein, A., & Mayer, T. F. (2006). Modelling reinforcement corrosion - Usability of a factorial approach for modelling resistivity of concrete. *Materials and Corrosion*, 57(12), 926–931.  
<https://doi.org/10.1002/mac.200604017>
- Polder, R. B. (2001). Test methods for on site measurement of resistivity of concrete - a RILEM TC-154 technical recommendation. *Construction and Building Materials*, 15(2–3), 125–131. [https://doi.org/10.1016/S0950-0618\(00\)00061-1](https://doi.org/10.1016/S0950-0618(00)00061-1)
- Powers, T. C. (1958). Structure and Physical Properties of Hardened Portland Cement Paste. *Journal of the American Ceramic Society*, 41(1), 1–6.  
<https://doi.org/10.1111/j.1151-2916.1958.tb13494.x>

- Resipod. (2016). The world's most accurate concrete surface resistivity meter.  
Retrieved from  
[https://www.proceq.com/uploads/tx\\_proceqproductcms/import\\_data/files/Resipod\\_Sales\\_Flyer\\_English\\_high.pdf](https://www.proceq.com/uploads/tx_proceqproductcms/import_data/files/Resipod_Sales_Flyer_English_high.pdf)
- Rupnow, T., & Icenogle, P. (2012). Surface Resistivity Measurements Evaluated as Alternative to Rapid Chloride Permeability Test for Quality Assurance and Acceptance. *Transportation Research Record: Journal of the Transportation Research Board*, 2290, 30–37. <https://doi.org/10.3141/2290-04>
- R.W., H. B. P. B. (1985). New technique for determining the electrical resistivity of concrete. *Magazine of Concrete Research*, 37, 243–248.
- Saleem, M., Shameem, M., Hussain, S. E., & Maslehuddin, M. (1996). Effect of moisture, chloride and sulphate contamination on the electrical resistivity of Portland cement concrete. *Construction and Building Materials*, 10(3), 209–214. [https://doi.org/10.1016/0950-0618\(95\)00078-X](https://doi.org/10.1016/0950-0618(95)00078-X)
- Seleem, H. E. D. H., Rashad, A. M., & El-Sabbagh, B. A. (2010). Durability and strength evaluation of high-performance concrete in marine structures. *Construction and Building Materials*, 24(6), 878–884. <https://doi.org/10.1016/j.conbuildmat.2010.01.013>
- Sengul, O., & Gjrv, O. E. (2009). Electrical Resistivity Measurements for Quality Control During Concrete Construction. *ACI Materials Journal*, (105), 541–547. <https://doi.org/10.14359/20195>
- Silva, N. (2013). *Chloride Induced Corrosion of Reinforcement Steel in Concrete: Threshold Values and Ion Distributions at the Concrete-Steel Interface* Department of Civil and Environmental Engineering Chloride Induced Corrosion of Reinforcement Steel in Concrete.
- Silva, P. C., Ferreira, R. M., & Figueiras, H. (2011). Electrical Resistivity as a Means of Quality Control of Concrete – Influence of Test Procedure. *XII DBMC International Conference on Durability of Building Materials and Components*, 1–8.
- Tang, L. (2005). Guideline for practical use of methods for testing the resistance of concrete to chloride ingress, CHLORTEST - EU funded research project “Resistance of concrete to chloride ingress - from laboratory tests to in-field

- performance” G6RD-CT-2002-00855. *Deliverable D23*, (December).
- Weyers, R. E., Pyc, W., Zemajtis, J., Liu, Y., Mokarem, D., & Sprinkel, M. M. (1997). Field Investigation of Corrosion-Protection Performance of Bridge Decks Constructed With Epoxy-Coated Reinforcing Steel in Virginia, (970486), 82–90. Retrieved from <http://dx.doi.org/10.3141/1597-11>
- Whiting, D. A., & Nagi, M. A. (2003). Electrical Resistivity of Concrete - A Literature Review. *Portland Cement Association*, 57.
- Whiting, D., Todres, A., Nagi, M., Yu, T., Peshkin, D., Darter, M., ... Geiker, M. (1993). *Synthesis of Current and Projected Concrete Highway Technology*.





## **Appendices**

## Appendix A

Table A1 Comparison between Electrical Resistivity and RCPT of  
Concrete

Designation	w/b	Y	RCPT (Coulombs)	resistivity $\rho$ (k $\Omega$ -cm)
0.35OPC	0.35	1.3	3771	23.525
0.35FA10	0.35	1.3	3171	27.575
0.35FA30	0.35	1.3	1102.5	68.225
0.35FA40	0.35	1.3	873	107.8
0.45OPC	0.45	1.3	7755	13.175
0.55OPC	0.55	1.3	10527	9.5
0.55FA10	0.55	1.3	6276	12.225
0.55FA30	0.55	1.3	2076	34.825
0.55FA40	0.55	1.3	1293	52.025
0.65OPC	0.65	1.3	10677	8.825
0.35OPC	0.35	1.4	4503	19.1
0.35FA10	0.35	1.4	3420	25.75
0.35FA30	0.35	1.4	1080	65.2
0.35FA40	0.35	1.4	792	99.45
0.45OPC	0.45	1.4	7749	10.375
0.55OPC	0.55	1.4	11058	8.45
0.55FA10	0.55	1.4	6936	11.9
0.55FA30	0.55	1.4	1977	34.275
0.55FA40	0.55	1.4	1455	46.7
0.65OPC	0.55	1.4	11895	8.2

## Appendix B

Table B1 Comparison between Electrical Resistivity and Carbonation

Depth of Concrete

Designation	Y	120 days carbonation depth (mm)	148 days carbonation depth (mm)	91 days	120 days resistivity	148 days resistivity
0.35OPC	1.3	0.0	0.000	23.0	37.98	42.575
0.35FA10		0.0	4.000	27.9	49.00	54.425
0.35FA30		4.8	7.500	70.5	94.60	113.45
0.35FA40		5.0	7.667	105.8	169.55	174.95
0.45OPC		0.0	3.500	11.3	27.40	40.975
0.55OPC		4.0	7.000	9.0	25.50	39.225
0.55FA10		5.0	8.500	12.8	35.90	46.55
0.55FA30		9.4	15.200	35.0	63.28	94.275
0.55FA40		10.6	17.333	52.2	75.40	122.05
0.65OPC		5.0	8.500	8.9	24.30	27.85
0.35OPC		1.4	0.0	0.000	18.4	31.75
0.35FA10	0.0		3.000	25.4	40.63	44.225
0.35FA30	3.0		5.500	65.8	89.30	99.475
0.35FA40	5.0		7.500	94.1	114.40	157.3
0.45OPC	0.0		2.500	10.8	22.25	34.375
0.55OPC	3.5		6.200	8.6	21.15	26.075
0.55FA10	5.7		8.400	11.8	35.28	46.45
0.55FA30	9.8		14.000	34.3	60.83	77.675
0.55FA40	8.7		15.500	48.7	69.20	118.25
0.65OPC	4.7		7.167	8.4	20.47	25.775

## Appendix C

Table C1 Electrical Resistivity of different Specimen Dimension

specimen dimension	Time (days)											
	1	3	7	10	14	18	22	25	28	35	42	49
	Electrical resistivity of concrete, $\rho$ (k $\Omega$ -cm)											
10 x 10 x 10	9.4	12.7	14.9	16.4	16.6	18.0	18.3	18.9	20.2	20.8	20.9	21.2
15 x 15 x 15	6.3	9.0	9.8	10.0	10.2	10.5	10.7	10.9	11.4	12.0	11.5	12.0
20 x 15 x 15	5.5	8.2	9.1	9.4	9.7	10.0	10.3	10.5	10.8	11.2	10.4	10.8
30 x 15 x 15	5.4	8.3	9.0	9.2	9.5	9.7	10.0	10.4	10.7	11.2	10.8	11.0

Table C2 Electrical Resistivity of different Specimen Thickness

Mix Design	Electrical Resistivity, $\rho$ (k $\Omega$ -cm)						
	length (cm)						
	10	9	8	7	6	5	4
0.35 OPC	24.86	24.14	23.26	24.48	24.6	32.9	63.8
0.35 FA 10	36.32	28.94	26.06	28.98	31.08	40.3	66.06
0.35 FA 30	115.6	86.08	79.72	74.08	84.68	135.34	231.8
0.55 FA 10	23.34	19.06	16.46	16.58	18.86	22.58	37.96
0.55 FA 30	68.44	46.84	43.86	41.62	44.24	54.82	103.7
0.55 FA 40	78.86	71.22	69.94	66.2	70.58	80.1	121.66
0.65 OPC	17.1	14.88	14.76	14.6	16.64	18.34	37.66